NASA CONTRACTOR REPORT

NASA CR-2817

THE MOISTURE BUDGET IN RELATION TO CONVECTION

Robert W. Scott and James R. Scoggins

Prepared by
TEXAS A&M UNIVERSITY
College Station, Tex. 77843
for George C. Marshall Space Flight Center

NATIONAL AERONAUTICS AND SPACE ADMINISTRATION • WASHINGTON, D. C. • MARCH 1977

1. REPORT NO.	2. GOVERNMENT ACCESSION NO.	3. REC
NASA CR-2817		

4. TITLE AND SUBTITLE	5. REPORT DATE
The Moisture Budget in Relation to Convection	March 1977
	6. PERFORMING ORGANIZATION CODE

7. AUTHOR(S)	8. PERFORMING ORGANIZATION REPORT #
Robert W. Scott and James R. Scoggins	M-216

9. PERFORMING ORGANIZATION NAME AND ADDRESS	10. WORK UNIT NO.
Center for Applied Geosciences College of Geosciences Texas A&M University College Station, Texas 77843	11. CONTRACT OR GRANT NO. NAS8-31773
	13. TYPE OF REPORT & PERIOD COVERED Contractor
12. SPONSORING AGENCY NAME AND ADDRESS National Aeronautics and Space Administration Washington, D. C. 20546	14. SPONSORING AGENCY CODE

15. SUPPLEMENTARY NOTES

Texas A&M

16. ABSTRACT

An evaluation of the moisture budget in the environment of convective storms is presented by using the unique 3- to 6-h rawinsonde data from the National Aeronautics and Space Administration's fourth Atmospheric Variability Experiment (AVE IV) conducted over the eastern two-thirds of the United States on 24 and 25 April 1975.

Net horizontal and vertical boundary fluxes accounted for most of the large amounts of moisture which were concentrated into convective regions associated with two squall lines that moved through the AVE area during the experiment. The largest values of moisture accumulations were located slightly downwind of the most intense convective activity. Relationships between computed moisture quantities of the moisture budget and radar-observed convection improved when lagging the radar data by 3 h. The residual of moisture which represents all sources and sinks of moisture in the budget equation was largely accounted for by measurements of precipitation.

17. KEY WORDS	18. DISTRIBUTION STATEMENT
	47

19. SECURITY CLASSIF. (of this report)	20. SECURITY CLASSIF. (of this page)	21. NO. OF PAGES	22. PRICE
Unclassified	Unclassified	96	$5.00

* For sale by the National Technical Information Service, Springfield, Virginia 22161

FOREWORD

This report is one of several to be published from research conducted under NASA Contract NAS8-31773 entitled, "Relationships Between Severe Storms and Their Environment." This effort is sponsored by the NASA Office of Applications under the direction of Marshall Space Flight Center's Aerospace Environment Division. The results presented in this report represent only a portion of the total research effort. Data used in the report were taken from the AVE IV Experiment conducted during the period beginning at 0000 GMT on 24 April 1975 and ending at 1200 GMT on 25 April 1975.

AUTHORS' ACKNOWLEDGEMENTS

The authors express their appreciation to Prof. Walter K. Henry, Dr. Oliver G. Aberth, and Dr. Kenneth C. Brundidge for their review of the manuscript, to Katy Capt, Carolyn Johnson, and Libby Pearson for typing the manuscript, to Ginny Smith for drafting many of the figures, and to Mr. Kelly Hill of NASA for his encouragement and advice.

The authors gratefully acknowledge support provided under NASA Contract No. NAS8-31773. This contract is under the auspices of the Aerospace Environment Division, Space Sciences Laboratory, National Aeronautics and Space Administration, Marshall Space Flight Center, Alabama.

TABLE OF CONTENTS

TABLE OF CONTENTS (Continued)

LIST OF TABLES

LIST OF FIGURES

LIST OF FIGURES (Continued)

THE MOISTURE BUDGET IN RELATION TO CONVECTION

by Robert W. Scott[1] and James R. Scoggins[2]

Center for Applied Geosciences, Texas A&M University

1. INTRODUCTION

a. Statement of problem

The distribution of moisture throughout the atmosphere is important due to the controlling factor it exerts on daily atmospheric events. Its influence on other meteorological parameters becomes quite substantial in areas where large concentrations of moisture exist. This is readily observed, for example, by the effect water vapor has on the propagation of solar and terrestrial radiation. Similarly, clouds and precipitation are visible signs of the existence of water vapor.

It is known that concentrations of moisture in the general area of convective rainfall are quite large. Synoptic-scale distributions of moisture and horizontal and vertical motions have been related directly to storm development. However, important temporal and spatial changes in meteorological parameters often are not indicated by these data. This is because the operational 12-h synoptic-scale rawinsonde data are unable to resolve accurately the interrelationships between the convective- and synoptic-scale systems. This is due in part to the fact that the life cycle of convective systems often occur entirely within the interval between successive rawinsonde soundings. Nevertheless, these systems have a considerable effect on the local weather. Heavy rainfall, strong winds, and large thermal changes often occur with their passage. Therefore, knowledge of the variations in the distribution of moisture at intervals shorter than 12 h is necessary to understand more completely the effect that moisture has on convection.

b. Objective

The main objective of this research is to examine the moisture balance of the atmosphere in areas of convective storm activity from 3-h rawinsonde data.

---

[1]Graduate Assistant

[2]Professor of Meteorology

Specific objectives include:

(1) Evaluate the moisture budget equation and determine the relative magnitude of each term from 3-h rawinsonde data.

(2) Identify relations of individual terms in the equation to radar-observed convection.

(3) Examine the relationships between computed moisture quantities and radar-observed convection 3 h previous to storms.

(4) Explain regions of sources and sinks of moisture.

c. Previous studies

The moisture budget includes the local rate-of-change of moisture, boundary fluxes (consisting of moisture divergence and advection), evaporation, condensation, and precipitation. Many past researchers have analyzed the moisture budget in particular weather systems. However, due to inadequacies in the data that were available or special characteristics of the systems being investigated, simplified moisture equations were used.

Spar (1953) equated the moisture convergence of a region to the maximum possible increase in precipitable water, assuming any excess to represent quantitative rainfall. This assumes, however, that the entire vertical column must be saturated before precipitation can occur which, in the absence of other errors, gives an underestimate of the precipitation. Nevertheless, he determined that the method would yield some success in locating regions of large quantities of expected rainfall although actual forecasted amounts failed to verify.

Bradbury (1957) conducted a similar experiment in three different types of storms, one of which contained much convective activity. She improved on Spar's evaluation of the time change in the total water vapor by consideration of the local rate-of-change term from sounding data taken at 6-h intervals. Her results showed fair agreement between observed and computed rainfall totals.

Palmén and Holopainen (1962) used a simplified equation to analyze a well-developed extratropical cyclone over the central

United States. They found that the horizontal moisture divergence accounted for 95% of the observed rainfall, indicating a strong dominance by the term. However, very little convection occurred in the area and due to the uniformity of the system, the local change term and evaporation were ignored.

Fankhauser (1965) and Ninomiya (1971) further showed the importance of large-scale moisture divergence in the environment of convective storms. In studies of two different thunderstorm situations over the eastern United States, they found that this term was large below 800 mb and smaller above. Earlier work by Ninomiya (1968) showed similar results. In evaluating the moisture budget of the subcloud layer in convective cloud systems over the Sea of Japan, he found large negative values of horizontal moisture divergence. The net vertical boundary flux of moisture in the same layer nearly equaled the horizontally-converged water vapor.

The importance of large-scale divergence on the moisture field has been shown numerically, also. In work by Chang and Orville (1973), large-scale horizontal convergence-divergence patterns were superimposed on a numerical cloud model. It resulted in broader, more active cloud cells than in the case when no divergence field was superimposed.

In analyses geared more toward the study of thunderstorm activity than general precipitation systems, works by Hudson (1971) and Fritsch (1975) revealed good correlations between horizontal moisture divergence and strong cumulus convection as shown by radar. Even better results were found when the radar data lagged the moisture divergence by 3 h.

Research using data collected from a mesoscale network has indicated that small-scale circulations also can be an important factor in the moisture budget of the atmosphere. Kreitzberg and Brown (1970) found that the effects of the mesoscale systems within the synoptic-scale circulations were important in the banding of precipitation. They discovered that bands of radar echoes were closely related to narrow tongues of warm moist air that feed into

the warm frontal stable layers of mature extratropical cyclones. Rainfall of a convective nature often occurred in these precipitation bands.

In work by Lewis et al. (1974), a squall line passing through the mesoscale rawinsonde network of the National Severe Storms Laboratory was analyzed. By evaluating the substantial derivative of the specific humidity and potential temperature, they concluded that condensation was an important factor in the residual of the moisture budget equation.

In research cited previously, Ninomiya suggested that small-scale convective eddies could sometimes be quite substantial in the moisture budget of the subcloud layer over the Sea of Japan in the presence of strong horizontal moisture convergence. He concluded that this is why active cumulus groups often exist only over the mesoscale convergence zones.

2. DATA

a. Atmospheric Variability Experiment

The data for this research were collected during the Atmospheric Variability Experiment IV (AVE IV) conducted by the National Aeronautics and Space Administration (Fucik and Turner, 1975) . The experiment began at 0000 GMT on 24 April 1975 and ended at 1200 GMT on 25 April. Rawinsonde soundings were taken at 6-h intervals with an extensive period during the middle 12 h of the experiment when soundings were 3 h apart. Forty-two rawinsonde stations in the United States, east of 105° W. longitude, participated in the experiment and are shown in Fig. 1.*

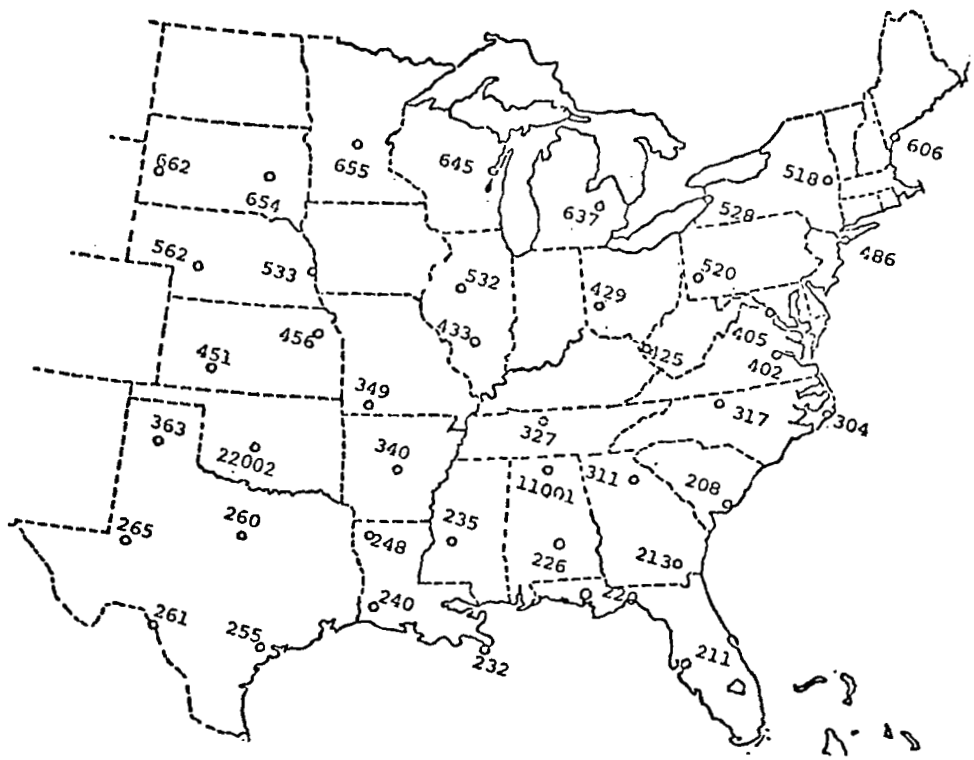

Fig. 1. Rawinsonde stations participating in the AVE IV experiment.

* Station names are given in Appendix I.

An extensive data reduction program was devised by Fuelberg (1974) to obtain the highest possible accuracy from the rawinsonde data. Winds were calculated at 30-s intervals and thermodynamic data were obtained at each pressure contact. Error analysis of the data has been well investigated by Lenhard (1973) and Fuelberg (1974). Estimates of the RMS errors for the different thermodynamic parameters are as follows.

Parameter	Approximate RMS Error
Temperature	0.2°
Pressure	1.5 mb
Humidity	10 per cent

RMS errors in wind speed for the AVE IV data are as follows.

Level	Elevation Angle	
	40°	10°
700 mb	0.5 m s^{-1}	2.5 m s^{-1}
500 mb	0.8 m s^{-1}	4.5 m s^{-1}
300 mb	1.0 m s^{-1}	7.8 m s^{-1}

b. Manually Digitized Radar

The location and intensity of radar-observed convection during the AVE IV experiment were obtained from Manually Digitized Radar data, acquired through the Techniques Development Laboratory of the National Oceanic and Atmospheric Administration (NOAA). The MDR grid network is shown in Fig. 2. The size of each MDR block is approximately 83 km on a side. The MDR coded values represent areal coverage and echo intensity within each block. Table I summarizes the explanation of the MDR code (Foster and Reap, 1973).

Three-hour composites of radar data, centered on each sounding time, were created in order to made comparisons with selected computed quantities. The composite value was the highest MDR coded value that appeared in each block during the 3-h period. Distinction

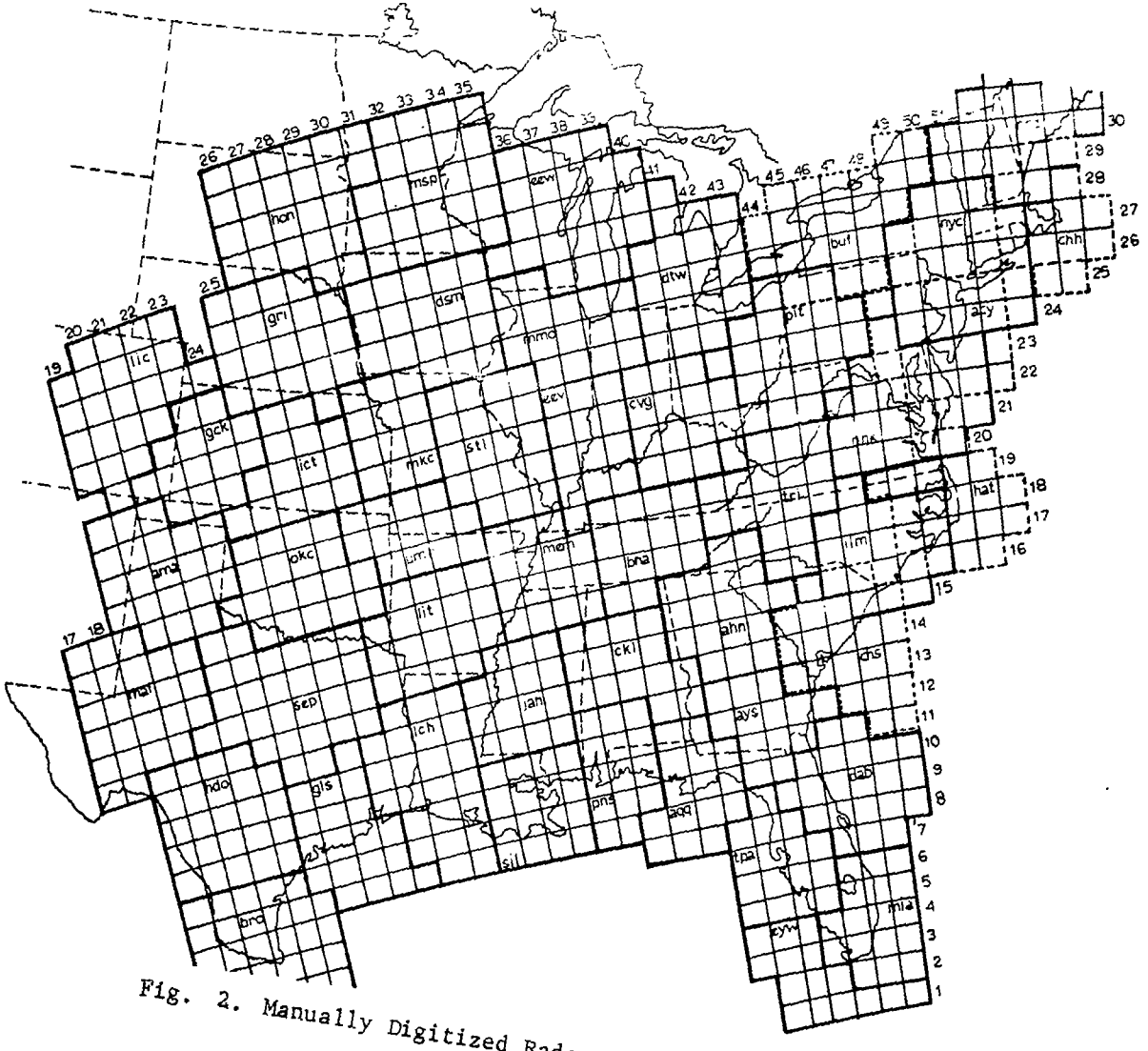

Fig. 2. Manually Digitized Radar (MDR) grid network.

was made between different rainfall intensities. Five categories of MDR were selected for comparisons to computed moisture quantities. They are all MDR points, MDR $\leq$ 1, MDR $\geq$ 2, MDR $\geq$ 4, and MDR $\geq$ 8.

Table I. Explanation of the Manually Digitized Radar code.

Code No.	Maximum Observed VIP[1] Values	Coverage In Box	Maximum Rainfall Rate (in./hr)	Intensity Category
0	No Echoes			
1	1	Any VIP	<.1	Weak
2	2	$\leq$ 50% of VIP2	.1-.5	Moderate
3	2	> 50% of VIP2	.5-1.0	Moderate
4	3	$\leq$ 50% of VIP3	1.0-2.0	Strong
5	3	> 50% of VIP3	1.0-2.0	Strong
6	4	$\leq$ 50% of VIP3 and 4	1.0-2.0	Very Strong
7	4	> 50% of VIP3 and 4	1.0-2.0	Very Strong
8	5 or 6	$\leq$ 50% of VIP3, 4, 5 and 6	>2.0	Intense or Extreme
9	5 or 6	> 50% of VIP3, 4, 5 and 6	>2.0	Intense or Extreme

[1]Video Integrator Processor

c. Precipitation

Hourly precipitation data were obtained from the National Climatic Center of the Environmental Data Service of NOAA. An area smaller than the entire AVE IV area consisting of around 1050 stations was chosen for analysis purposes. Precipitation in the areas not included in the analysis was either light or nonexistent.

3. SYNOPTIC CONDITIONS

Analyses of the surface and 700-mb level at 0600 GMT on 24 and 25 April 1975, appear in Figs. 3 and 4, respectively. The analyses were taken, without modification, from the data summary report by Fucik and Turner (1975) and show the synoptic conditions 6 h after the start and prior to the end of the AVE IV experiment. Frontal positions and areas of precipitation are located on each chart.

The synoptic situation in AVE IV was characterized by a mass of cold polar air moving slowly across the northern United States from Iowa to New England. A surface cyclone, located over Lake Huron at the beginning of the experiment, tracked east-northeastward to the Gulf of St. Lawrence while a secondary low moved eastward from southern Kansas to Kentucky. A warm front stretched eastward from the primary low across the central Appalachians to the mid-Atlantic coast and moved northeastward ahead of a large mass of warm moist Gulf air flowing through the eastern United States.

The contrasting air masses were separated by a cold front which linked the low pressure areas and then trailed southwestward into west Texas. The southern portion of the front was relatively inactive and remained nearly stationary throughout the experiment. In contrast, the northern segment became quite active, generating two lines of instability during the period. The first was in existence at the start of the experiment and stretched from central Illinois into northeastern Kansas. The line moved in an easterly direction ahead of the front reaching maximum thunderstorm activity around 0600 GMT on the 24th (the same time as shown in Fig. 3) and then dissipated over southeastern Missouri about 6 h later. Maximum tops were in excess of 17 km (55,000 ft). Scattered thunderstorms continued in the system for the next 12 h as it moved through the Ohio Valley. Although some regeneration occurred in central Kentucky around 1800 GMT, all thunderstorm activity had ended in this system by 0000 GMT on 25 April.

The second squall line formed just after 2100 GMT on the 24th and stretched from northwestern Arkansas into central Oklahoma.

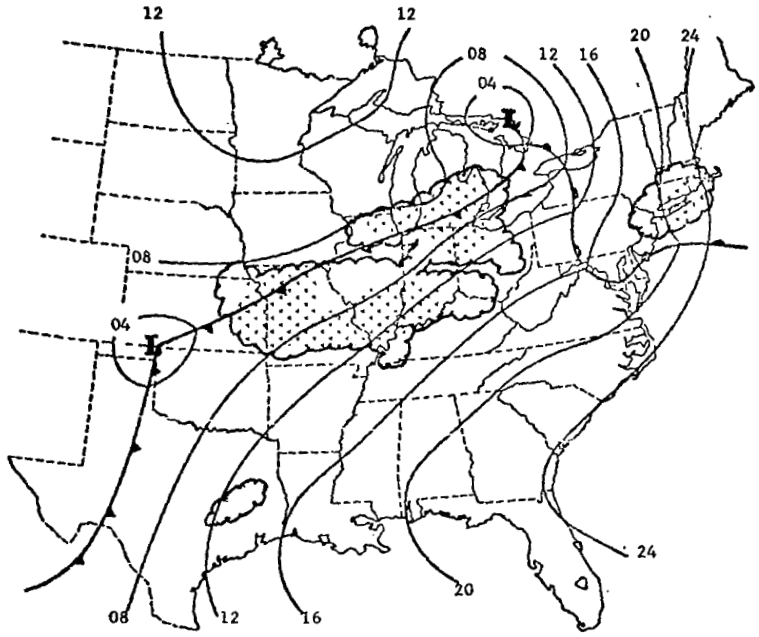

(a) Surface

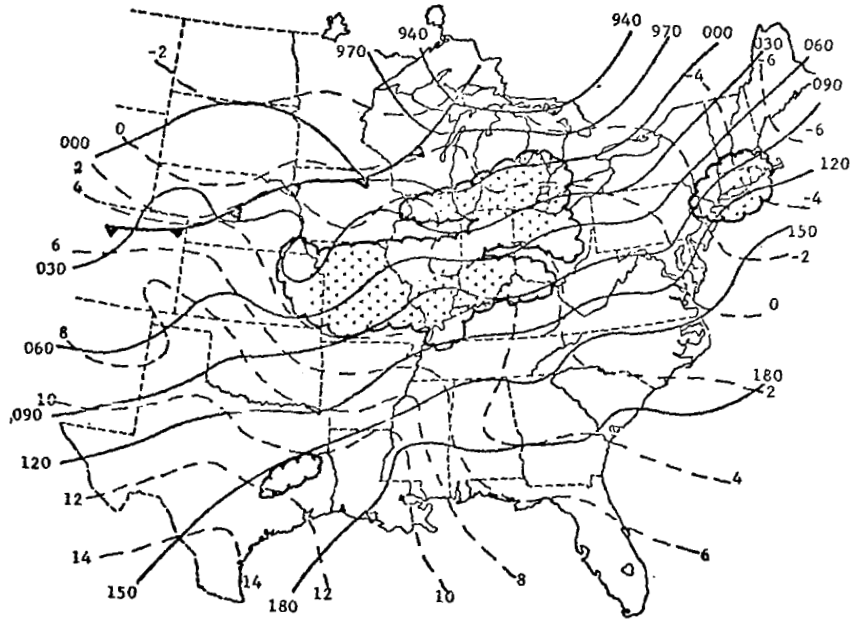

(b) 700 mb

Fig. 3. Synoptic charts for 0600 GMT on 24 April 1975.

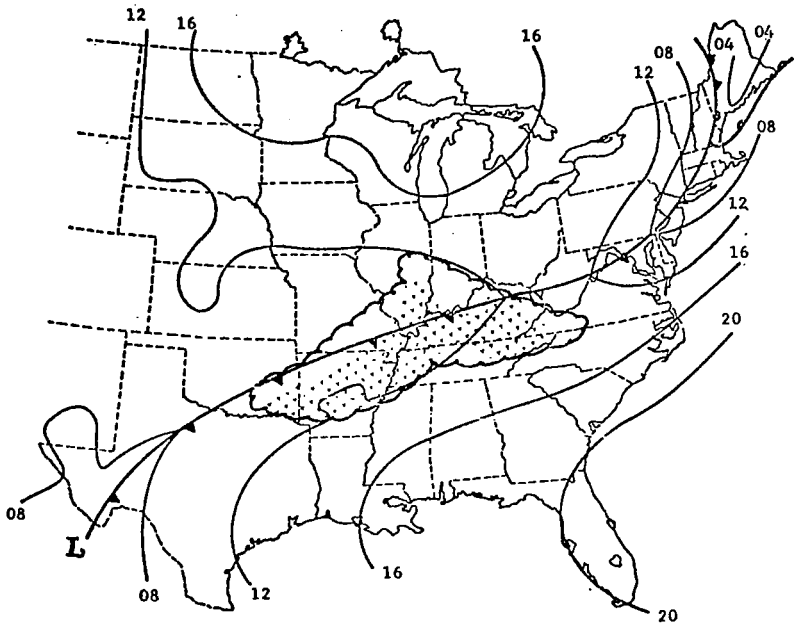

(a) Surface

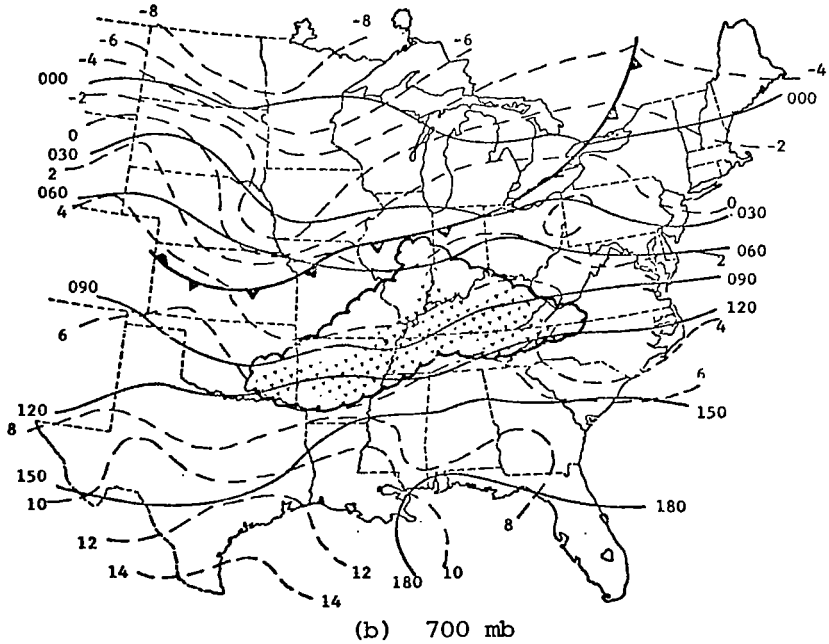

(b) 700 mb

Fig. 4. Synoptic charts for 0600 GMT on 25 April 1975.

Development continued to the northeast of the initial formation until the time of maximum storm development, about 0600 GMT on 25 April (see Fig. 4). At this time the squall line extended from western Kentucky into central Arkansas. The eastern part of the line was the most active with several tops exceeding 15 km (50,000 ft). The line was still strong at 1200 GMT (the end of the experiment); however, thunderstorm activity had lessened. It stretched from eastern Kentucky across Tennessee into northern Mississippi and southeast Arkansas. Tops were generally less than 14 km (45,000 ft).

Rainfall of a stratiform nature covered much of the central Appalachians and northeastern states during the experiment. It fell in association with the northeastward movement of the warm front during the initial hours of the experiment and persisted as the remains of the two squall lines passed through the area during their dissipation stages.

4. THE MOISTURE BUDGET EQUATION

The moisture budget equation for the atmosphere has been derived by several authors (Spar, 1953; Palmén and Newton, 1969; Haltiner, 1971). A combination of the methods of Haltiner and Palmén and Newton is reproduced here.

Haltiner began with the continuity equation for water vapor in the atmosphere which is given as

$$\frac{\partial \rho_v}{\partial t} + \vec{\nabla} \cdot (\rho_v \vec{V}) = S, \tag{1}$$

where ρ_v is the density of water vapor in the air and $\vec{\nabla}$ and $\vec{V}$ are the three-dimensional del operator and velocity in pressure coordinates. The term S represents sources or sinks of moisture in mass per unit volume per unit time.

The density of water vapor is defined as $\rho_v \equiv \rho q$, where ρ and q are the density and specific humidity of the air, respectively. If this definition is exchanged with ρ_v in Eq. 1 and an expansion is made of the resulting terms, one has

$$q \frac{\partial \rho}{\partial t} + \rho \frac{\partial q}{\partial t} + \rho q \vec{\nabla} \cdot \vec{V} + \rho \vec{V} \cdot \vec{\nabla} q + q \vec{V} \cdot \vec{\nabla} \rho = S. \tag{2}$$

Now by assuming an incompressible fluid (i.e., $\frac{d\rho}{dt} = 0$), Eq. 2 can be written

$$\rho \frac{\partial q}{\partial t} + \rho \vec{\nabla} \cdot (q \vec{V}) = S. \tag{3}$$

The rest of the derivation follows that by Palmén and Newton in a slightly expanded form. By integrating Eq. 3 over a vertical column, assuming hydrostatic equilibrium, one has

$$\frac{1}{g} \int_{p_2}^{p_1} \frac{\partial q}{\partial t} \, dp + \frac{1}{g} \int_{p_2}^{p_1} \vec{\nabla}_2 \cdot (q \vec{V}_2) \, dp + \frac{1}{g} \int_{p_2}^{p_1} \frac{\partial (q\omega)}{\partial p} \, dp = R, \tag{4}$$

where the second term on the left-hand side (LHS) has been expanded into its horizontal and vertical components. The right-hand side (RHS) of Eq. 4, R, results from the integration of S and represents the effects of evaporation, precipitation, and condensation.

Integration of the third term on the LHS of Eq. 4 gives

$$\frac{1}{g}\int_{p_2}^{p_1}\frac{\partial q}{\partial t}\,dp + \frac{1}{g}\int_{p_2}^{p_1}\vec{\nabla}_2\cdot(q\vec{V}_2)\,dp + \frac{1}{g}\left[(q\omega)_{p_1} - (q\omega)_{p_2}\right] = R. \qquad (5)$$

which is the moisture budget equation for a unit column over each grid point. It was believed, however, that a moisture balance cannot be obtained at each grid point. Therefore, the equation was integrated over an area, A, of three grid distances square. Previous researchers had used a similar routine except that averages were taken over much larger regions, enclosing entire cyclones and its associated weather. Since convective systems are subsynoptic phenomena, a smaller area was chosen in order to show the moisture budget in the region immediately surrounding storms. Upon integration, Eq. 5 becomes

$$\frac{1}{gA}\iint_A\int_{p_2}^{p_1}\frac{\partial q}{\partial t}\,dp\,dA + \frac{1}{gA}\iint_A\int_{p_2}^{p_1}\vec{\nabla}_2\cdot(q\vec{V}_2)\,dp\,dA$$

$$+ \frac{1}{gA}\int_A\left[(q\omega)_{p_1} - (q\omega)_{p_2}\right]dA = \frac{1}{A}\int_A R\,dA, \qquad (6)$$

where each term was divided by A, resulting in g $cm^{-2}s^{-1}$ as the final units.

The terms on the LHS of Eq. 6 are the local rate-of-change of moisture, the horizontal moisture divergence, and the net vertical boundary flux of moisture, respectively. By application of the divergence theorem, Eq. 6 becomes

$$\frac{1}{gA}\iint_A\int_{p_2}^{p_1}\frac{\partial q}{\partial t}\,dp\,dA + \frac{1}{gA}\oint_L\int_{p_2}^{p_1}qV_n\,dp\,dL$$

$$+ \frac{1}{gA}\int_A\left[(q\omega)_{p_1} - (q\omega)_{p_2}\right]dA = \frac{1}{A}\int_A R\,dA, \qquad (7)$$

where V_n is defined by convention as positive outward and L is the length of the boundary around area A. Equation 7 is the final form of the moisture budget equation used in this research. For convenience, q is replaced in Eq. 7 by the mixing ratio which introduces only a small error.

5. METHODS OF EVALUATION OF TERMS IN THE MOISTURE EQUATION

a. Gridding of basic data fields

Values of wind and mixing ratio were interpolated to a numerical grid by a Fourier analysis scheme developed by Barnes (1964). The grid, shown in Fig. 5, consists of an 18 x 18 grid point array placed on a conformal conic projection which is true at 30° and 60° N. latitude. The map factor here is small and was neglected. A spacing of approximately 158 km exist between grid points. It is believed that this grid provides the best possible horizontal resolution based on existing rawinsonde station spacing (Barr et al., 1971).

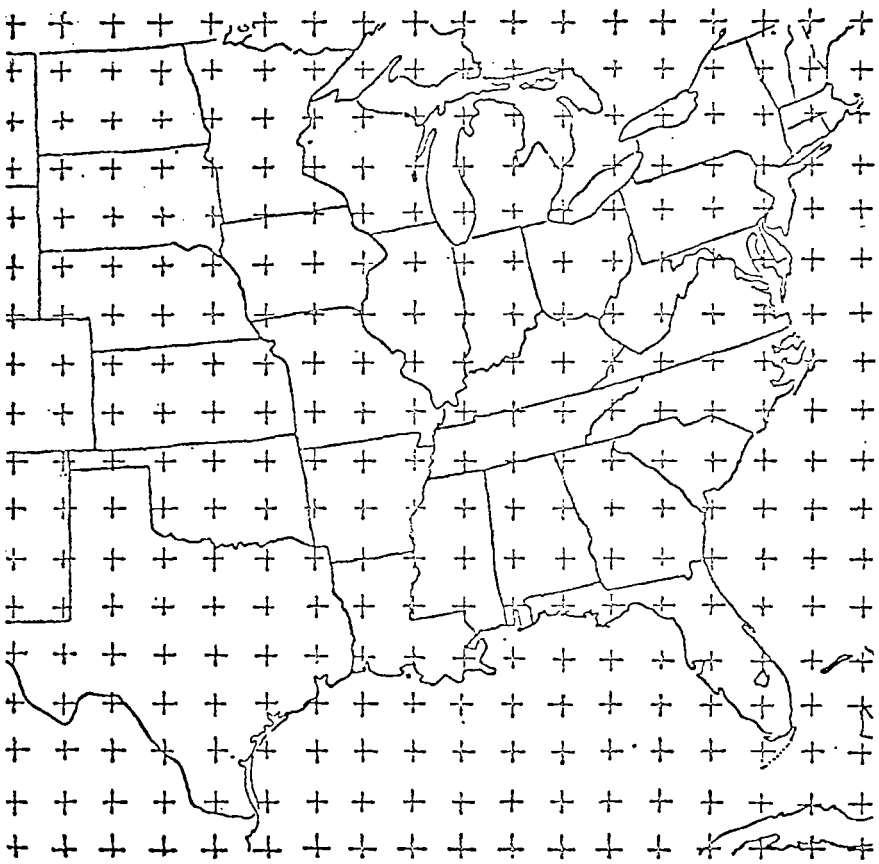

Fig. 5. Grid used for numerical computations.

A radius of influence of three grid distances from each rawinsonde station was used in order to include major subsynoptic-scale systems in the analysis. Noise in the computations was kept minimal by allowing only four iterations of the Barnes technique. The resulting fields were smoothed by a process developed by Shuman (1957) to prevent spurious amplification of high frequency meteorological phenomena created by the iterative process. The values of the interpolated fields were averaged over a depth of 50 mb and computed at 50-mb intervals from 900-350 mb.

b. Local changes

The local rate-of-change of moisture is represented by the first term on the LHS of Eq. 7. The evaluation of $\frac{\partial q}{\partial t}$ was performed at each grid point and level by use of a centered finite difference using values of mixing ratio at times immediately adjacent to the one being considered. This operation was performed at each time except for the first and last time periods of the experiment when a forward difference and backward difference scheme was used, respectively.

The values found at each grid point were integrated with respect to pressure over an interval of 50 mb, utilizing a first order integration approximation. The method used was the trapezoidal rule which has the form $(f_1 + f_2)\frac{h}{2}$ where the f's represent the values of $\frac{\partial q}{\partial t}$ at the adjacent pressure levels and h = 50 mb. For two values, this amounts to simple averaging. This process was continued for each layer and resulted in pressure-integrated values of the local change of moisture for 50-mb layers from 900-350 mb.

As stated previously, the area integral was evaluated over an area of three grid distances square, centered at each grid point. This was done by summing the eight adjacent grid point values with the point they surround. This value was multiplied by one grid distance square, d^2, which was the area over which the value at each grid point was assumed to be representative. The resultant amount was divided by the total area, $A = (3d)^2$, of the nine points and

placed at the central grid point. Division by gravity completed the evaluation of the term.

c. Vertical Changes

Vertical motion in this research was computed using the kinematic scheme developed by O'Brien (1970). The product of mixing ratio and vertical motion at each grid point was calculated for every 50-mb level. The net vertical boundary flux was found by subtracting the upper-level value from that of the next level below. The nine-point area-averaging routine that was described in the previous section was utilized here. Division by A and gravity completed the evaluation of this term.

d. Horizontal changes

The initial step in evaluating the net horizontal boundary flux of moisture was to compute fields of q times the u component of velocity, and q times the v component of velocity at each grid point and level. Each of these fields was integrated separately with respect to pressure by the method described in the section concerning local changes. Using these pressure integrated fields, the horizontal boundary flux into the area over which the local and vertical changes had been averaged was computed. This area is represented by the solid line in the schematic diagram below. Each side of the area was segmented (as shown by the dashed lines) and the flux was

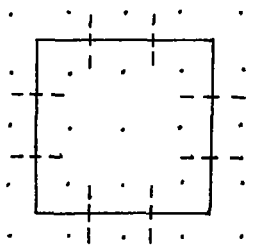

calculated individually across each segment. This was done by averaging the two points on opposite sides of each segment. Each average was multiplied by the length of the segment, d, along which

it was assumed constant. Care was taken in the averaging process to insure that the pressure-integrated values containing the east-west velocity component and those containing the north-south velocity component were used on their respective sides of the area boundary.

Since the net horizontal boundary flux of moisture was defined by convention as positive outward, the signs of the averaged values on the west and south sides were taken into consideration. The averages were then summed and the resultant placed at the central grid point. Evaluation of the term was completed by dividing this final value by A and gravity.

As stated previously, by use of the divergence theorem the net horizontal boundary flux can be replaced by the moisture divergence. This quantity can be expanded into two separate components, the moisture concentration due to velocity divergence of the wind. ($q\vec{\nabla}\cdot\vec{v}$) and horizontal moisture advection ($\vec{v}\cdot\vec{\nabla}q$). Calculations of these two terms were made for purposes of comparison with the evaluation of the net horizontal boundary flux.

The initial step in the evaluation of $q\vec{\nabla}\cdot\vec{v}$ was to calculate a field of divergence, using centered finite differences at every grid point. These values were multiplied by the value of q at that point. The rest of the evaluation followed the pressure and area integration method described in the section concerning local changes. Division by gravity and A completed the calculation.

Moisture advection was evaluated by first computing values of the components of $\vec{\nabla}q$, using centered finite differences at each grid point. Values of $u\frac{\partial q}{\partial x}$ and $v\frac{\partial q}{\partial y}$ were summed for each grid point. Integrations with respect to pressure and area were performed as was described previously and division by gravity and A completed the evaluation.

e. Combination of terms (residual)

Three-hour composites of hourly precipitation data were tabulated and plotted in order to be analyzed manually. Values were assigned to each grid point according to the analysis. Integration

with respect to area and division by A, discussed in previous sections, completed the evaluation.

6. RESULTS

a. Relationships between MDR values and terms in the moisture budget equation

The computed values of the individual terms of the moisture budget equation often became quite large in the convective regions. Direct comparisons of the computed moisture quantities to storms was made by use of the MDR data. These data were placed on the numerical grid manually in four categories of MDR described previously (MDR $\leq$ 1, MDR $\geq$ 2, MDR $\geq$ 4, MDR $\geq$ 8). Averages of the terms in the equation were made corresponding to the individual categories of MDR. From these, vertical profiles were constructed to determine the relative magnitude of each term in each 50-mb layer from 900-350 mb. These profiles are shown throughout the discussion that follows.

In order to define major trends more clearly, values of the moisture quantities in the 50-mb layers were combined into deeper layers. The layers chosen were 900-750 mb, 750-500 mb, and 500-350 mb which best defined the different regions where individual terms showed relative importance. In the following sections, analyses of the moisture quantities in most of these layers are presented at 0600 GMT on 24 and 25 April 1975. These analyses were at the time of maximum thunderstorm activity in each squall line occurring in the AVE IV experiment and are representative of all other sounding times unless stated otherwise. Surface frontal positions and radar-observed convection are shown on each chart. All precipitation of MDR $\geq$ 2 is enclosed by a heavy scalloped line with thunderstorm areas (MDR $\geq$ 4) indicated by shading. Frequently, reference is made in this section toward the most intense thunderstorm regions (MDR $\geq$ 8). Location of these areas can be found in Appendix II.

1) Local changes

Vertical profiles of the local rate-of-change of moisture are shown in Fig. 6. Below 750 mb, the atmosphere was characterized by moderate losses of moisture locally. The greater losses were found in the regions of the more intense convection as indicated by MDR. This means that in the environment of storms, the atmosphere was

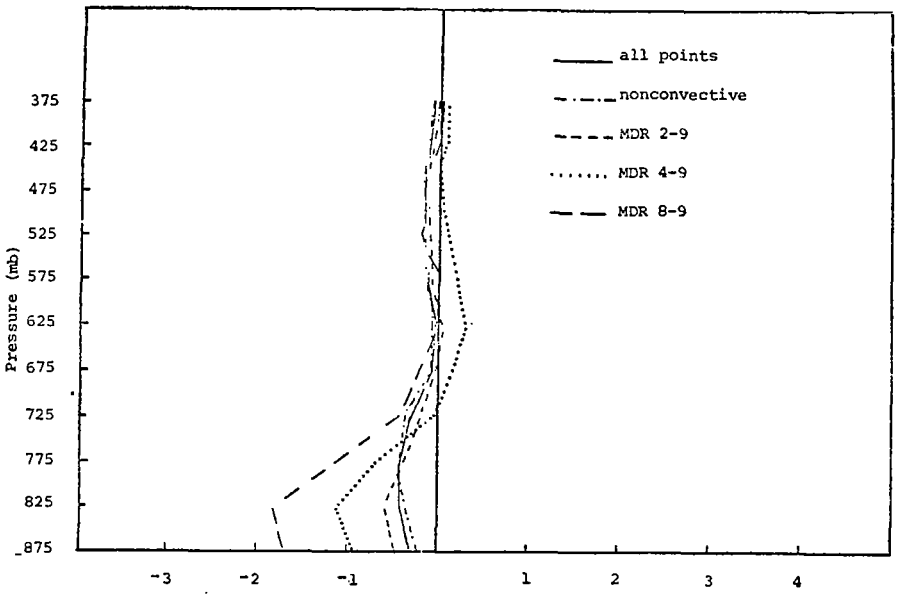

Fig. 6. Vertical profiles of the local rate-of-change of moisture related to MDR. (Units: $x10^{-6}$ g $cm^{-2}s^{-1}$).

drier 3 to 6 h after convective activity than it was 3 to 6 h before the storms.

Above 750 mb, the change in the amount of moisture with time was much smaller. Values generally stayed slightly negative but showed little change regardless of storm intensity.

Analyses of the local rate-of-change of moisture at 0600 GMT on 24 April and 0600 GMT on 25 April appear in Figs. 7 and 8. Surface fronts and precipitation observed from radar are shown in each chart with the convective areas shaded.

Figure 7 shows that generally a wide area of moisture loss was present locally in the 900-750 mb layer around the convective regions. The centers of negative values were found some distance from the area of strong convection. The general pattern obtained by a study of analyses at all times in the experiment indicate small positive areas ahead of the squall lines and slightly larger negative areas to the rear. The convection was usually located in the negative regions but downwind from the center of maximum loss.

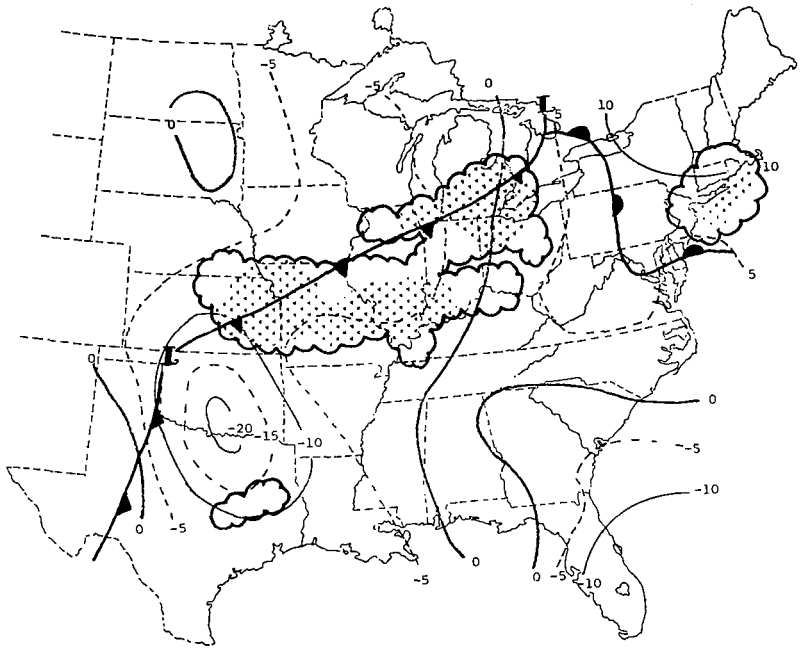

(a) 0600 GMT, 24 April 1975.

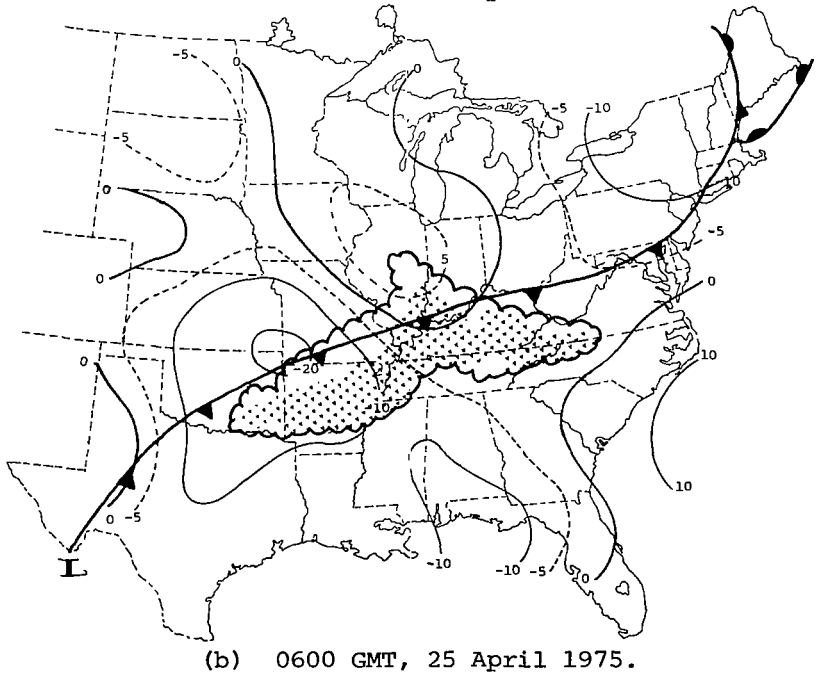

(b) 0600 GMT, 25 April 1975.

Fig. 7. Analyses of the local rate-of-change of moisture in the layer from 900-750 mb. (Superimposed are surface frontal positions and radar-observed convection. Units: $x10^{-6}g\ cm^{-2}s^{-1}$).

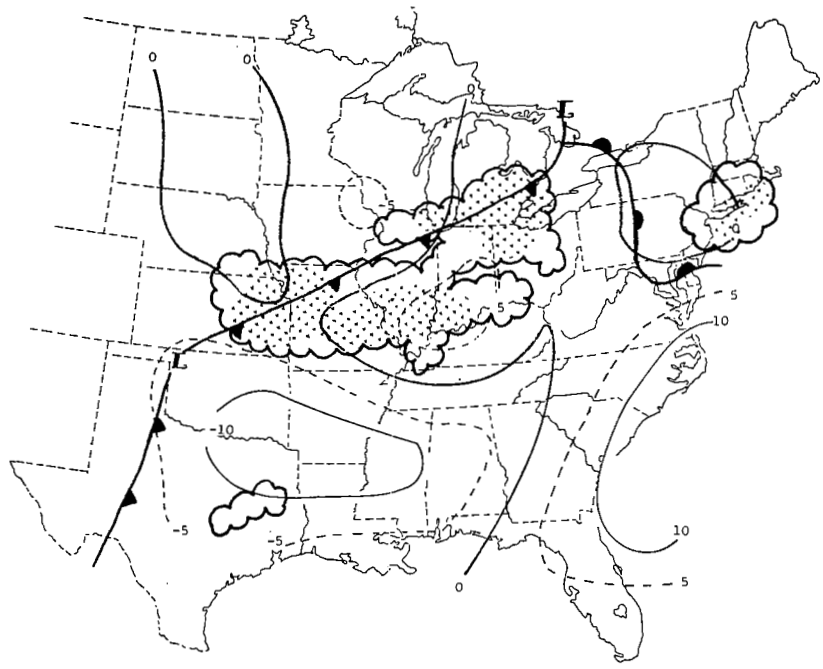

(a) 0600 GMT, 24 April 1975.

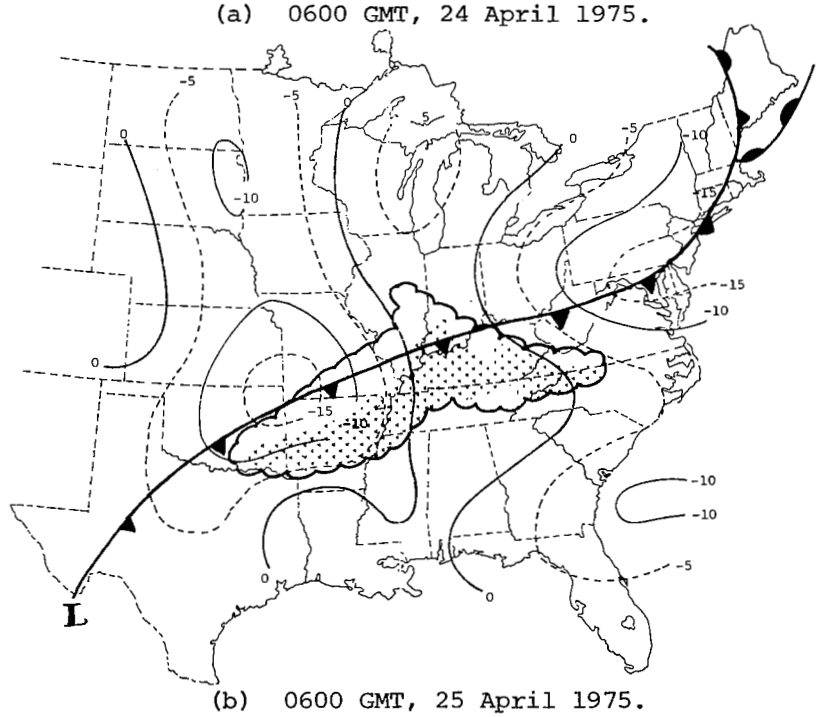

(b) 0600 GMT, 25 April 1975.

Fig. 8. Analyses of the local rate-of-change of moisture in the layer from 750-500 mb. (Superimposed are surface frontal positions and radar-observed convection. Units: $x10^{-6}$ g $cm^{-2}s^{-1}$).

The same general pattern existed above 750 mb that was found below (see Fig. 8). The values were almost half as large as below, but the convection was located more along the dividing line between positive and negative areas which yielded an overall average of near zero. This confirms what was found in the vertical profiles in this layer.

Analyses of the local rate-of-change of moisture in the layer from 500-350 mb (not presented) showed the same patterns as those in Fig. 8. However, since the moisture content was very low, the actual values were an order of magnitude smaller. Thus, the local rate-of-change of water vapor in this layer was quite minimal.

2) Net vertical boundary flux

Past moisture budget studies for the most part have ignored the evaluation of the net vertical boundary flux of moisture. In many previous works, the atmosphere has been considered as a whole, where the vertical flow of moisture is measured only at the top and bottom of the atmosphere. Since the vertical motion is zero at the earth's surface and the moisture content is small at upper levels, this term becomes negligible. This assumption is valid in moisture budgets used for locating areas of precipitation. However, to understand the concentration of moisture in smaller layers of the atmosphere, especially in regions of convection, it is necessary to consider the effect of this term.

Figure 9 shows vertical profiles of the net vertical boundary flux of moisture (vertical moisture divergence) averaged for all times in the different MDR categories. In the lowest layer (900-850 mb), there were large losses of moisture due to the synoptic-scale vertical motion. Losses were the greatest in the most intense convective regions, averaging over 4.0×10^{-6} g cm^{-2} s^{-1}. It will be shown in the next section that these losses occurred in connection with strong horizontal convergence in the same layer.

These results agree with those found in a study by Ninomiya (1968). He detected large positive values of net vertical boundary flux in the subcloud layer of the mesoscale convergence zones over

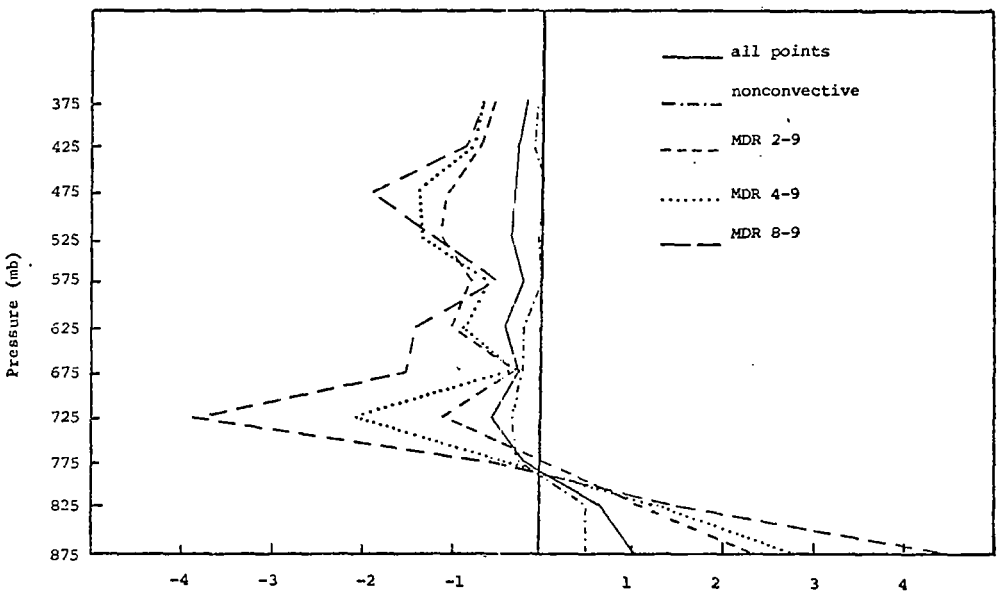

Fig. 9. Vertical profiles of the net vertical boundary flux of moisture related to MDR. (Units: $x10^{-6}$g $cm^{-2}s^{-1}$).

the Sea of Japan. His actual values were larger than those in this study due probably to exceptionally strong horizontal convergence in the area.

The large positive flux divergence decreased quickly with decreasing pressure and by 750 mb had become negative. Strong upward vertical motion was present in all of the convective regions and carried large amounts of moisture out of the surface layer, creating an area of large flux convergence, centered in the 750-700 mb layer. A average of nearly 4.0 x 10^{-6}g $cm^{-2}s^{-1}$ of vertical flux convergence was found in this layer in the areas of strongest thunderstorms. A secondary maximum was found from 500-450 mb which probably was due to the fact that the vertical motion reached its maximum value at the bottom of this layer. In both layers, the areas of intense convection were associated with the largest average vertical flux convergence of moisture.

Vertical profiles of this term, constructed by Fritsch (1975), relate well to the ones produced here. Similar magnitudes of

flux divergence were found in both the positive region near the ground and the negative area higher up. Fritsch found the region of maximum negative flux divergence slightly higher than was found in this research. This probably was due to a deeper moist layer near the surface in his study.

Analyses of the horizontal distribution of the vertical flux divergence of moisture for 0600 GMT on 24 and 25 April 1975, appear in Figs. 10 through 12. Surface fronts and radar-observed precipitation are shown with the convective areas shaded.

A study of Fig. 10 indicates that large amounts of moisture were flowing out of the 900-750 mb layer in areas of convection. The outflow was the strongest slightly to the east of the most intense region of convection (MDR $\geq$ 8) and maintained this relative position during the lifetime of each individual squall line. The fact that the movement of the storms was in the direction of the centers indicates that the net vertical boundary flux of moisture possible aided in the maintenance and continuing development of the storms. The flux divergence was not strong in the lower layer at the time of initial thunderstorm development but it grew rapidly and its magnitude paralleled the intensity of the convective systems soon after their formation.

The convective regions in Fig. 11 were characterized by large values of vertical flux convergence. This is shown especially well at 0600 GMT on 24 April where the accumulation of moisture into this layer exceeded 45 x 10^{-6} g $cm^{-2}s^{-1}$ over central Missouri. It must be remembered that these amounts represent an average of values over an area of three grid distances square. Again, as in the layer below, the center of the large negative values was just east of the most intense convection.

Figure 12 indicates the extent to which moisture was accumulated through vertical motion in the environment of storms. Values exceeding 15 x 10^{-6} g $cm^{-2}s^{-1}$ were found in the 500-350-mb layer over northeastern Arkansas at 0600 GMT on 25 April. Occasionally, large values of vertical moisture divergence were found below 500 mb over the stratiform rainfall areas. However, the inflow of moisture from

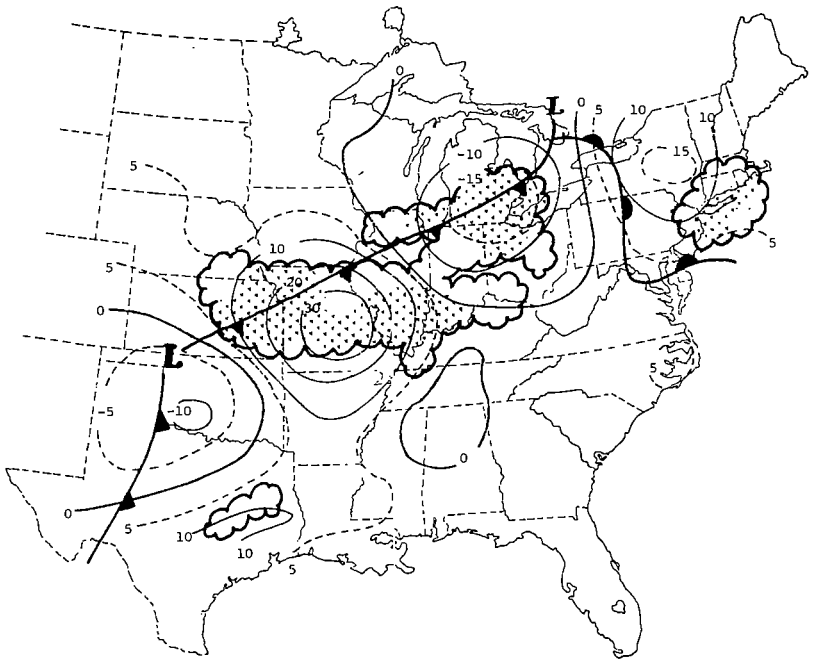

(a) 0600 GMT, 24 April 1975.

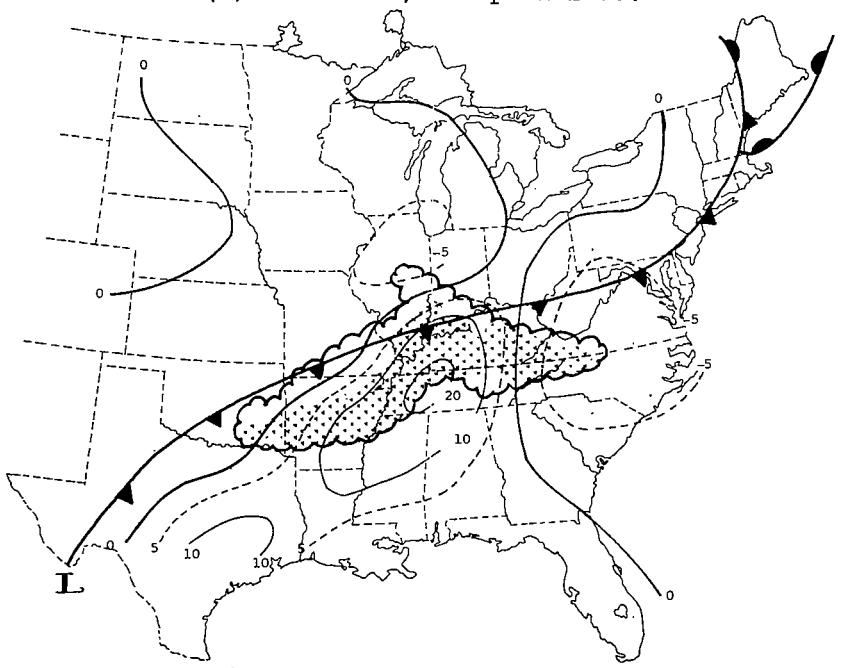

(b) 0600 GMT, 25 April 1975.

Fig. 10. Analyses of the net vertical boundary flux of moisture in the layer from 900-750 mb. (Superimposed are surface frontal positions and radar-observed convection. Units: $x10^{-6}g\ cm^{-2}s^{-1}$).

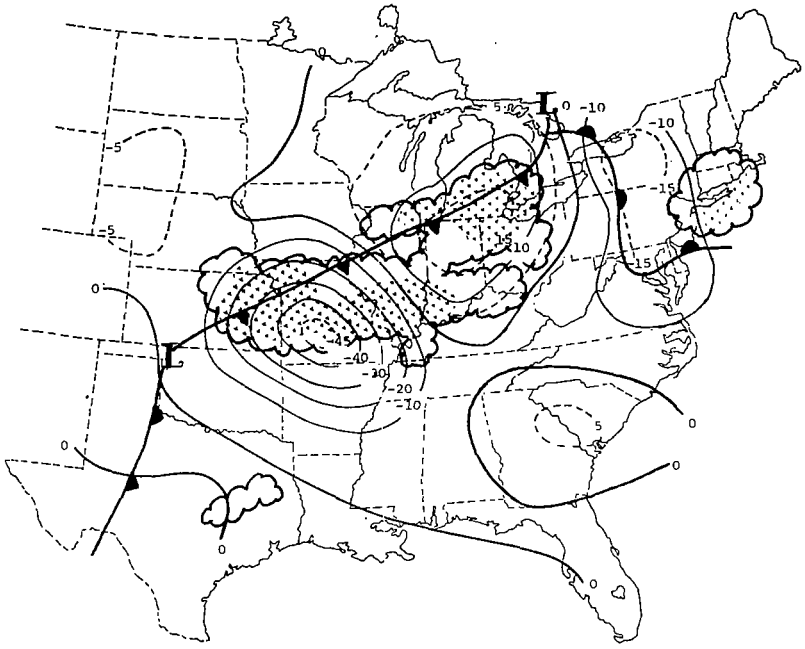

(a) 0600 GMT, 24 April 1975.

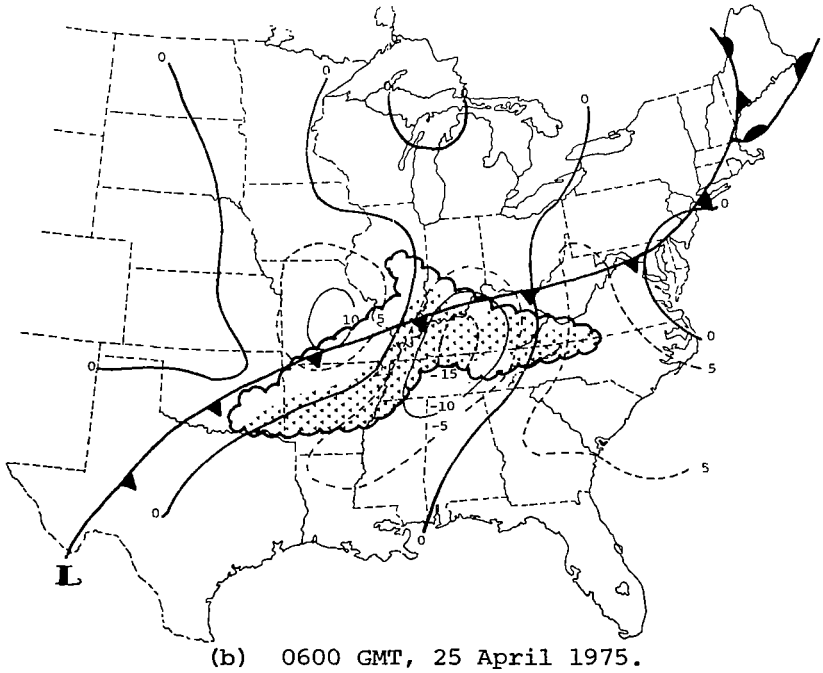

(b) 0600 GMT, 25 April 1975.

Fig. 11. Analyses of the net vertical boundary flux of moisture in the layer from 750-500 mb. (Superimposed are surface frontal positions and radar-observed convection. Units: $x10^{-6}g\ cm^{-2}s^{-1}$).

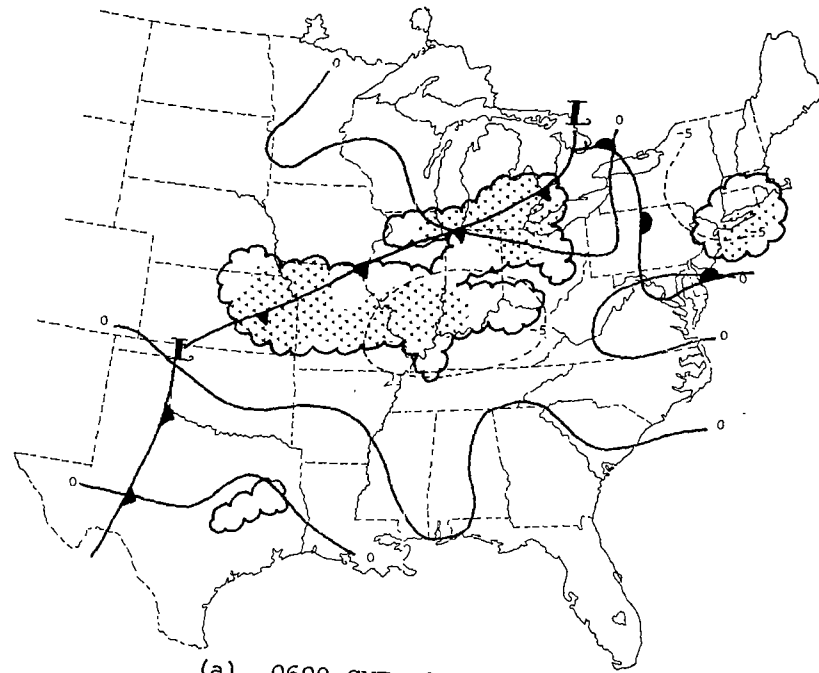

(a) 0600 GMT, 24 April 1975

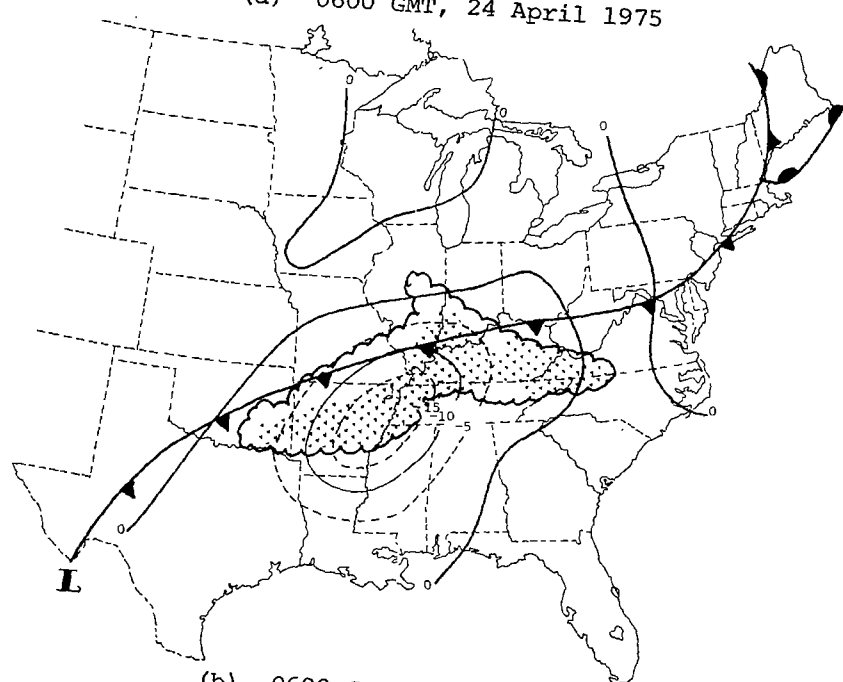

(b) 0600 GMT, 25 April 1975.

Fig. 12. Analyses of the net vertical boundary flux of moisture in the layer from 500-350 mb. (Superimposed are surface frontal positions and radar-observed convection. Units: $x10^{-6}$g $cm^{-2}s^{-1}$).

vertical motion was never strong above 500 mb in these regions which further emphasizes the effect of the net vertical boundary flux in convective areas.

Convection sometimes occurred in a region where it would not be expected by the calculated values of the vertical motion in the area. For example, over southern Michigan at 0600 GMT on 24 April (Fig. 10a), the opposite conditions of those just described occurred. A region of strong downward motion coincided with the leading edge of the first squall line giving an instantaneous picture opposite to that found in the rest of the squall line. The situation did not last long, however, since the downward motion acted as a constraint to the convection. All precipitation had ended in the area 3 h later (see Appendix II for the MDR composite at 0900 GMT on 24 April).

3) Divergence

Vertical profiles of the concentration of moisture due to the horizontal divergence of the wind ($q\vec{\nabla}\cdot\vec{V}$) are shown in Fig. 13. The

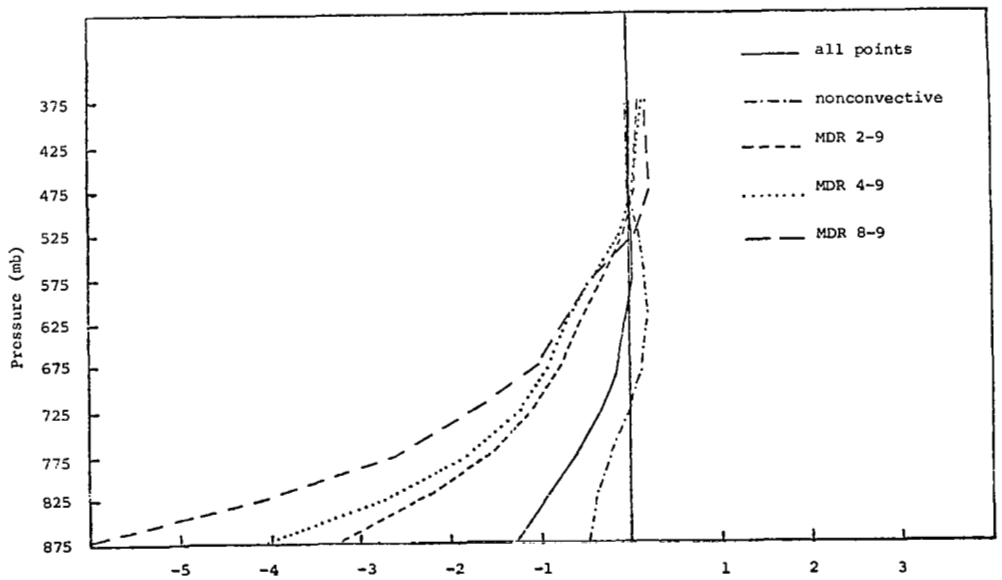

Fig. 13. Vertical profiles of the moisture concentration due to wind divergence related to MDR. (Units: $x10^{-6}$g $cm^{-2}s^{-1}$).

profiles show that large quantities of moisture converged horizontally into the areas covered by precipitation. Vertically, this zone of convergence extended from 900 mb to almost 500 mb. The increase of moisture in the 900-850-mb layer exceeded 6.0 x 10^{-6} g $cm^{-2}s^{-1}$ in the areas covered by the most severe storms (MDR $\geq$ 8) but decreased rapidly with decreasing pressure. Computed values were generally larger in all layers in the more intense regions of convection shown by the MDR data.

Ninomiya also found this term to be large close to the ground. He observed very strong horizontal convergence of the wind in the subcloud layer over the Sea of Japan. This was probably why he found larger values of $q\vec{\nabla}\cdot\vec{V}$ than was revealed in this research.

Analyses of $q\vec{\nabla}\cdot\vec{V}$ at 0600 GMT on 24 April and 0600 GMT on 25 April for the 900-750-mb and 750-500-mb layers appear in Fig. 14 and 15. Surface fronts and precipitation have been superimposed as before.

Indeed, areas of large increases in moisture from the evaluation of $q\vec{\nabla}\cdot\vec{V}$ were found in the convective regions from 900-500 mb. Area-averaged values at 0600 GMT on 24 April in central Missouri approached 50 x 10^{-6} g $cm^{-2}s^{-1}$ in the 900-750-mb layer along. Highest values in the 750-500-mb layer reached almost 25 x 10^{-6} g cm^{-2} s^{-1} at the same time. This indicates that horizontal convergence of the wind occurred throughout a deep layer of the atmosphere in the convective regions.

Generally, the highest MDR values were located slightly to the west or northwest of these maximum central values. This indicates that large amounts of moisture converged into the storm areas just ahead of the squall lines, thus contributing toward their maintenance. Similar results were found by Hudson (1971) and Fritsch (1975).

Above 500 mb, values of $q\vec{\nabla}\cdot\vec{V}$ were quite small. Although the moisture was very low here, the level of nondivergence was found near 500 mb which greatly reduced the values in this layer.

It was shown earlier that the vertical flux divergence of moisture did not become well-developed until some time after the

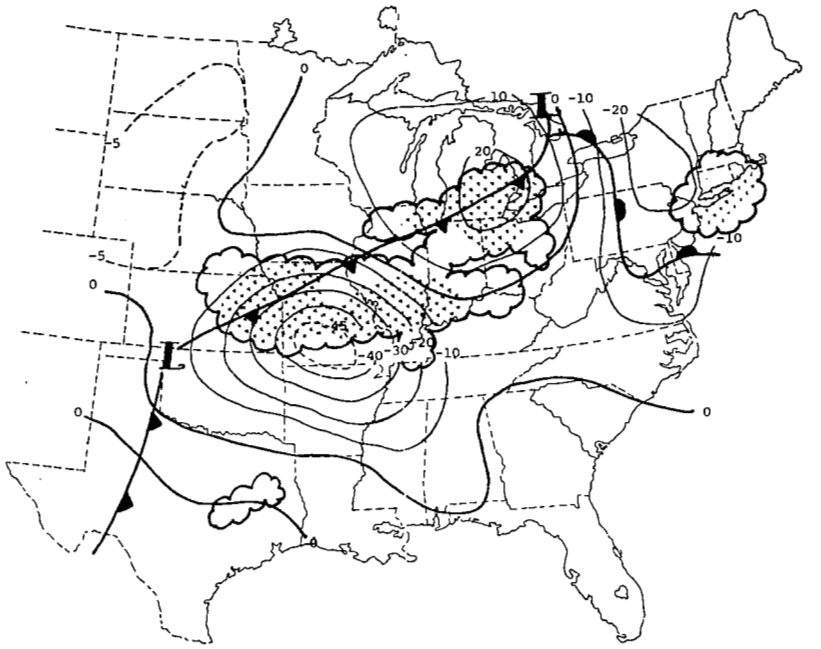

(a) 0600 GMT, 24 April 1975.

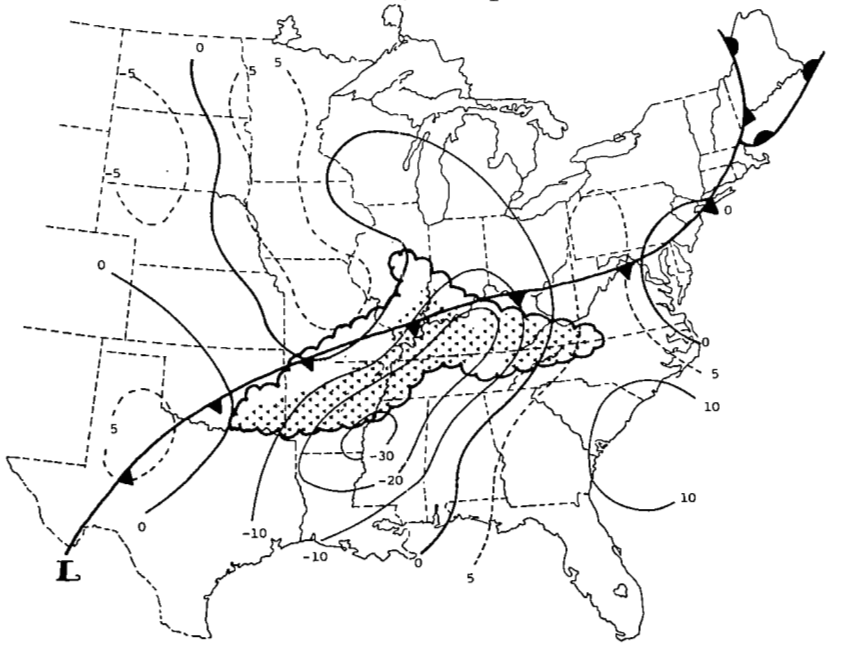

(b) 0600 GMT, 25 April 1975.

Fig. 14. Analyses of the moisture concentration due to wind divergence in the layer from 900-750 mb. (Superimposed are surface frontal positions and radar-observed convection. Units: $x10^{-6}$g $cm^{-2}s^{-1}$).

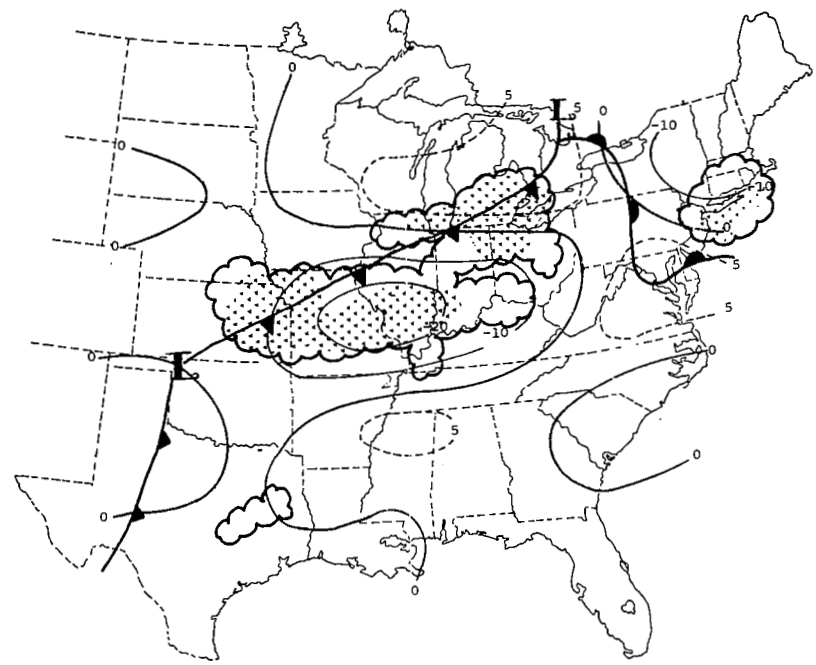

(a) 0600 GMT, 24 April 1975.

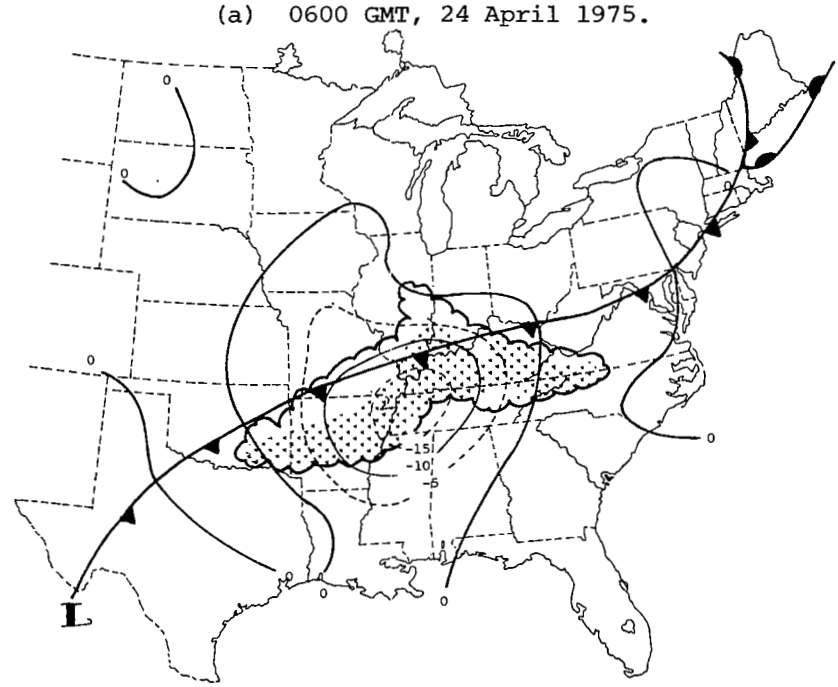

(b) 0600 GMT, 25 April 1975.

Fig. 15. Analyses of the moisture concentration due to wind divergence in the layer from 750-500 mb. (Superimposed are surface frontal positions and radar-observed convection. Units: $x10^{-6}g\ cm^{-2}s^{-1}$).

initial development of the convective systems. A study of the analyses of $q\vec{\nabla}\cdot\vec{V}$ in the 900-750-mb layer at 0000 GMT on both days showed that, unlike the vertical flux divergence, a well-defined center of $q\vec{\nabla}\cdot\vec{V}$ was associated with the early stages of both squall lines.

Similar to the vertical flux divergence, there were times when the calculated values of $q\vec{\nabla}\cdot\vec{V}$ in convective areas were opposite in sign to what was expected. The same situation used in the previous section is discussed here. A review of the 0000 GMT analysis on 24 April showed a large area of moisture loss due to horizontal divergence over Wisconsin. By 0600 GMT this area had moved to southern Michigan and met the leading edge of the first squall line (see Fig. 14). Although convection occurred in the strongly positive area of $q\vec{\nabla}\cdot\vec{V}$, the MDR data 3 h later (0900 GMT) indicated no precipitation in the area. Therefore, even existing convection diminished quickly when it encountered positive values of the divergence of moisture.

4) Advection

Vertical profiles of the horizontal moisture advection are shown in Fig. 16. It is seen readily that the contribution of this

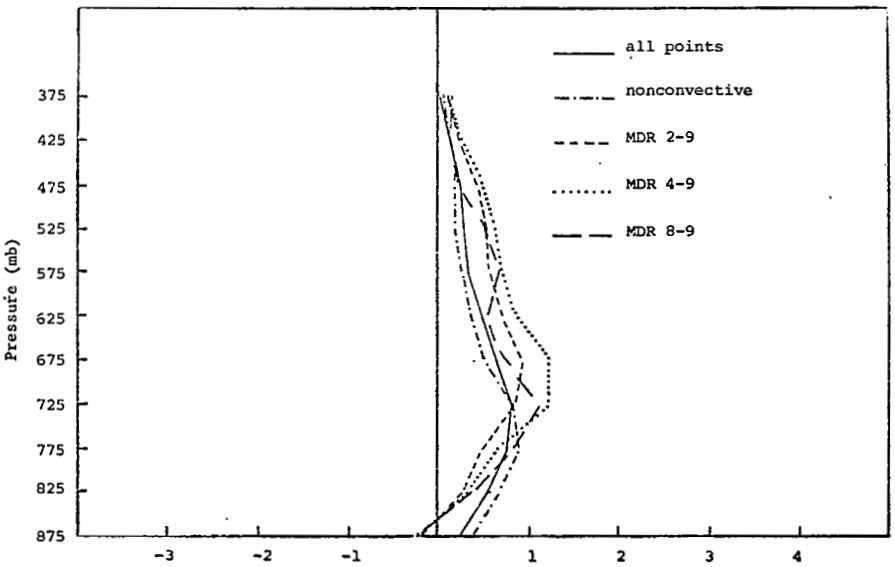

Fig. 16. Vertical profiles of the moisture advection related to MDR. (Units: $x10^{-6}g\ cm^{-2}s^{-1}$).

term was very small in the lower layers of the atmosphere compared to $q\vec{\nabla}\cdot\vec{v}$. This reflects the fact that the moisture content close to the ground was nearly constant over the convective areas. Unlike the terms discussed previously, the intensities of thunderstorms did not affect the magnitude of this term (i.e. profiles of moisture advection in convective regions were not distinctly different from the one for nonconvective areas). The largest contribution was made in the middle layers where positive moisture advection occurred in association with all regions of precipitation.

Analyses of the moisture advection at 0600 GMT on 24 April and 0600 GMT on 25 April in the 900-750- and 750-500-mb layers appear in Figs. 17 and 18. Surface fronts and precipitation are shown as before.

The small values of moisture advection indicated at low levels by the profiles were confirmed here. There was a general tendency throughout the atmosphere for negative values of advection ahead of the storms and positive values in the rear with the squall line located between them. For the most part, the moisture advection in the lower layers at the times shown was rather weak although larger values occurred occasionally at other times of the experiment. However, even then, the convection was positioned between the positive and negative areas of advection which still resulted in small averaged values in the individual MDR categories.

In the 700-500-mb layer, the centers of moisture advection were more well-defined and the quantity was slightly larger in absolute value. The regions of precipitation were located more in the positive areas which accounted for the relative maximum of the term in the vertical profiles.

Above 500 mb (no figure shown), the term was again small in actual value but gave the largest horizontal contribution. The patterns of moisture advection were the same as were found in lower layers.

5) Combination of terms

i. Net horizontal flux. The combination of the moisture concentration due to horizontal velocity divergence and the moisture

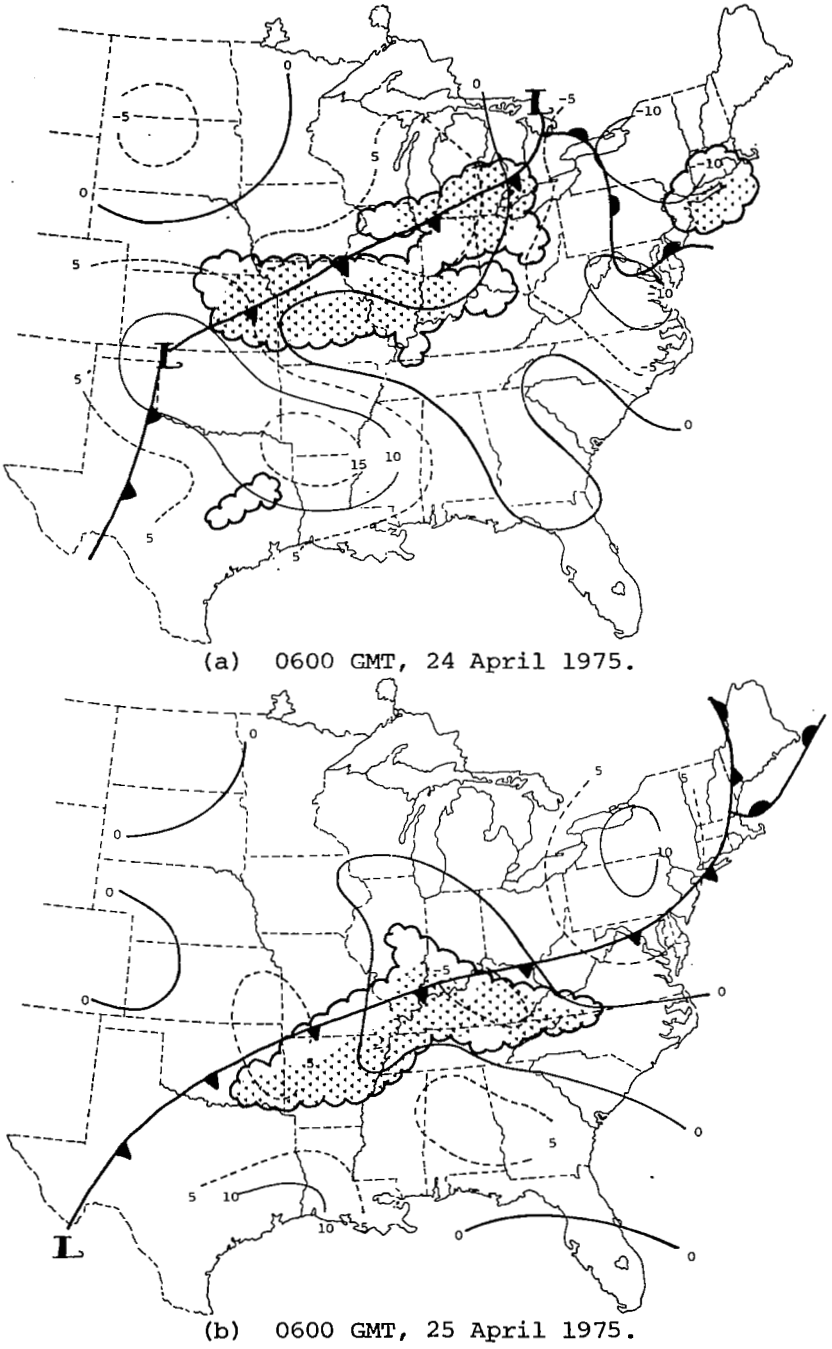

Fig. 17. Analyses of the moisture advection in the layer from 900-750 mb. (Superimposed are surface frontal positions and radar-observed convection. Units: $x10^{-6}g\ cm^{-2}s^{-1}$).

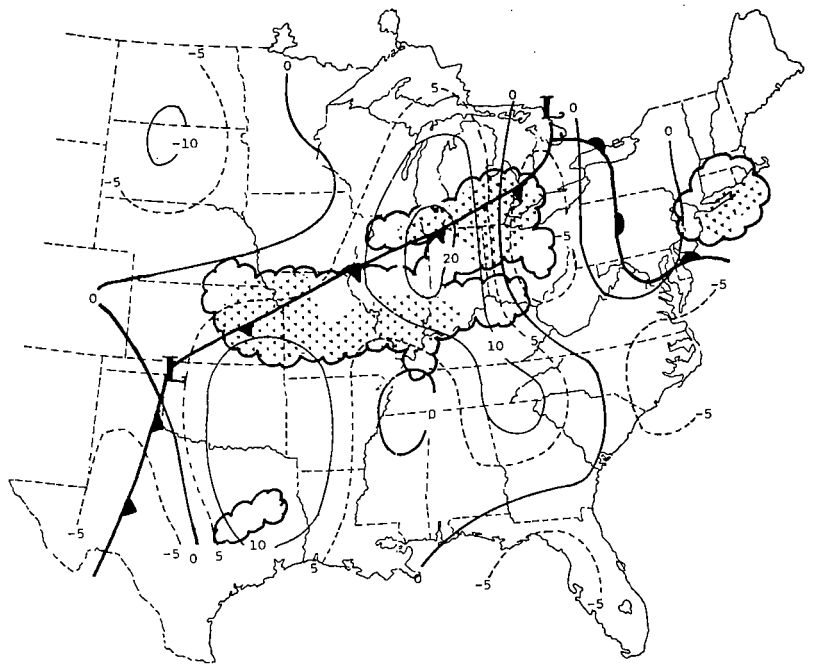

(a) 0600 GMT, 24 April 1975.

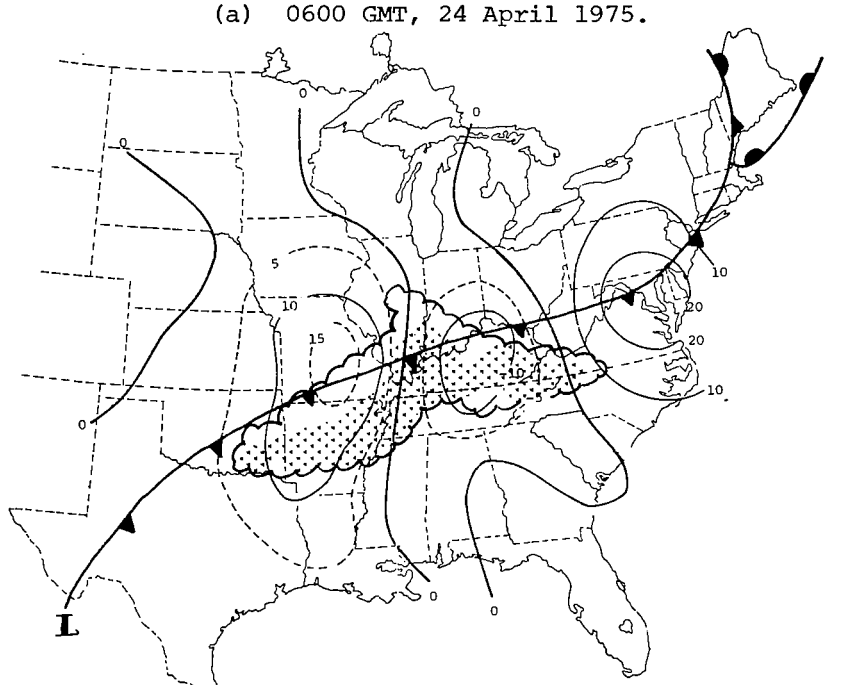

(b) 0600 GMT, 25 April 1975.

Fig. 18. Analyses of the moisture advection in the layer from 750-500 mb. (Superimposed are surface frontal positions and radar-observed convection. Units: $x10^{-6}g\ cm^{-2}s^{-1}$).

advection yields the horizontal moisture divergence. As shown in Eq. 7, this is equal to the net horizontal boundary flux of moisture. These two names are used interchangeably in the following discussion.

Vertical profiles of the term appear in Fig. 19. A large amount of convergence occurred in the lower layers of the atmosphere. This region of convergence extended vertically to about 700 mb and was the strongest in the areas where convection was most intense. Above about 700 mb the quantity was slightly positive up to 350 mb. Fankhauser (1965), Ninomiya (1971), and Fritsch (1975) showed similar profiles of horizontal moisture divergence at the boundary of thunderstorm regions. Actual values of the term differed somewhat, but this could be explained by differences in the individual systems being studied.

By comparing Fig. 19 with the profiles in Figs. 13 and 16, it was determined that the net horizontal boundary flux was dominated by $q\vec{\nabla}\cdot\vec{V}$ in the lower layer of the atmosphere. Moisture advection became important above about 800 mb and due to the decrease in value of $q\vec{\nabla}\cdot\vec{V}$ caused the quantitv to change sign between 750 and 650 mb.

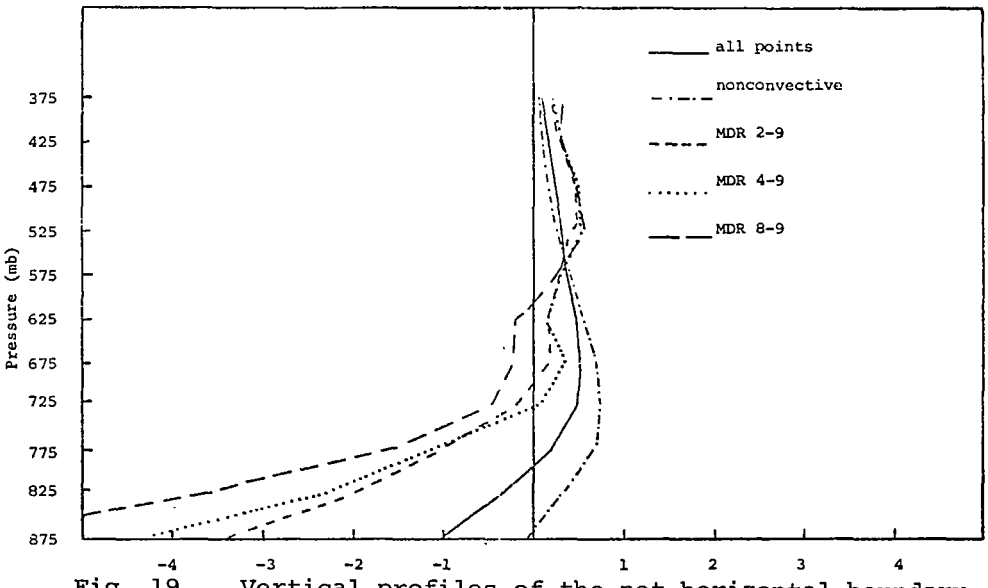

Fig. 19. Vertical profiles of the net horizontal boundary flux of moisture related to MDR. (Units: $x10^{-6}g\ cm^{-2}s^{-1}$).

Analyses of the net horizontal boundary flux at 0600 GMT on 24 April and 0600 GMT on 25 April in the layers from 900-750 mb, and 750-500 mb, appear in Figs. 20 and 21. Surface fronts and precipitation are indicated as before. These charts represent the total contribution by synoptic-scale horizontal motions toward the moisture budget of the atmosphere.

The pattern of net horizontal boundary flux in the layer from 900-750 mb shown in Fig. 20b was the most representative of the patterns found at the other hours of the experiment. The pattern is very similar to that found by the evaluation of $q\vec{\nabla}\cdot\vec{V}$ alone (see Fig. 14b). However, moisture advection was important at 0600 GMT on 24 April. Two separate areas of large positive advection, over Oklahoma and the Midwest (Fig. 17a), aligned with strong convergence in central Missouri (Fig. 14a) and resulted in a very well-defined area of horizontal moisture convergence over central Missouri (Fig. 20a). The central value, 50×10^{-6} g cm^{-2}s^{-1}, was only slightly larger than that found in the evaluation of $q\vec{\nabla}\cdot\vec{V}$, but the moisture advection increased the gradient of the term in the area.

Figure 21 represents the net horizontal boundary flux in the 750-500 mb layer. Generally, the patterns here were very similar to the ones found in the evaluation of moisture advection in the same layer. The analysis in Fig. 21b showed the pattern that was found most often, considering all sounding times. Large negative values were found ahead of the squall line while positive amounts existed in the rear. In the immediate area of convection, $q\vec{\nabla}\cdot\vec{V}$ was still large which gave emphasis to the negative areas.

The analysis at 0600 GMT on 24 April showed a situation when the patterns were not the same as the general case just described. This was due primarily to changes from the usual pattern of moisture advection. The field of $q\vec{\nabla}\cdot\vec{V}$ was strong in the convective areas so the resultant field was quite different from its regular appearance.

The entire analysis of net horizontal flux in the 500-350 mb layer (not shown) was dominated by the advection of moisture. This

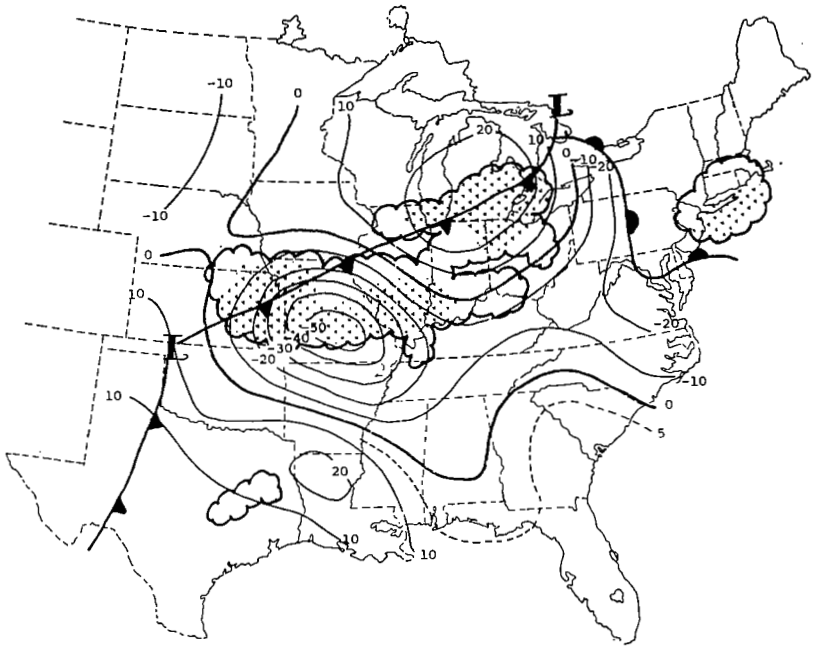

(a) 0600 GMT, 24 April 1975.

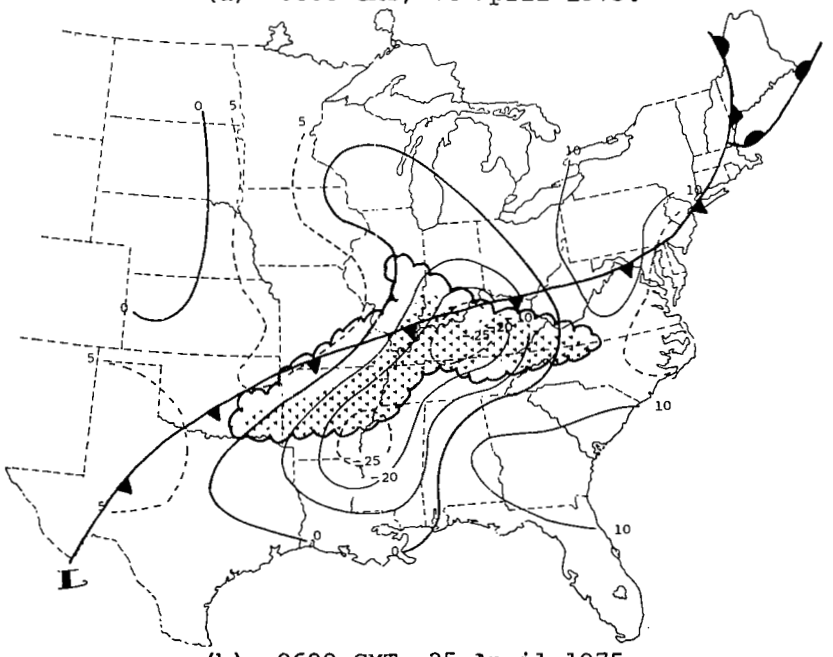

(b) 0600 GMT, 25 April 1975.

Fig. 20. Analyses of the net horizontal boundary flux of moisture in the layer from 900-750 mb. (Superimposed are surface frontal positions and radar-observed convection. Units: $x10^{-6}g\ cm^{-2}s^{-1}$).

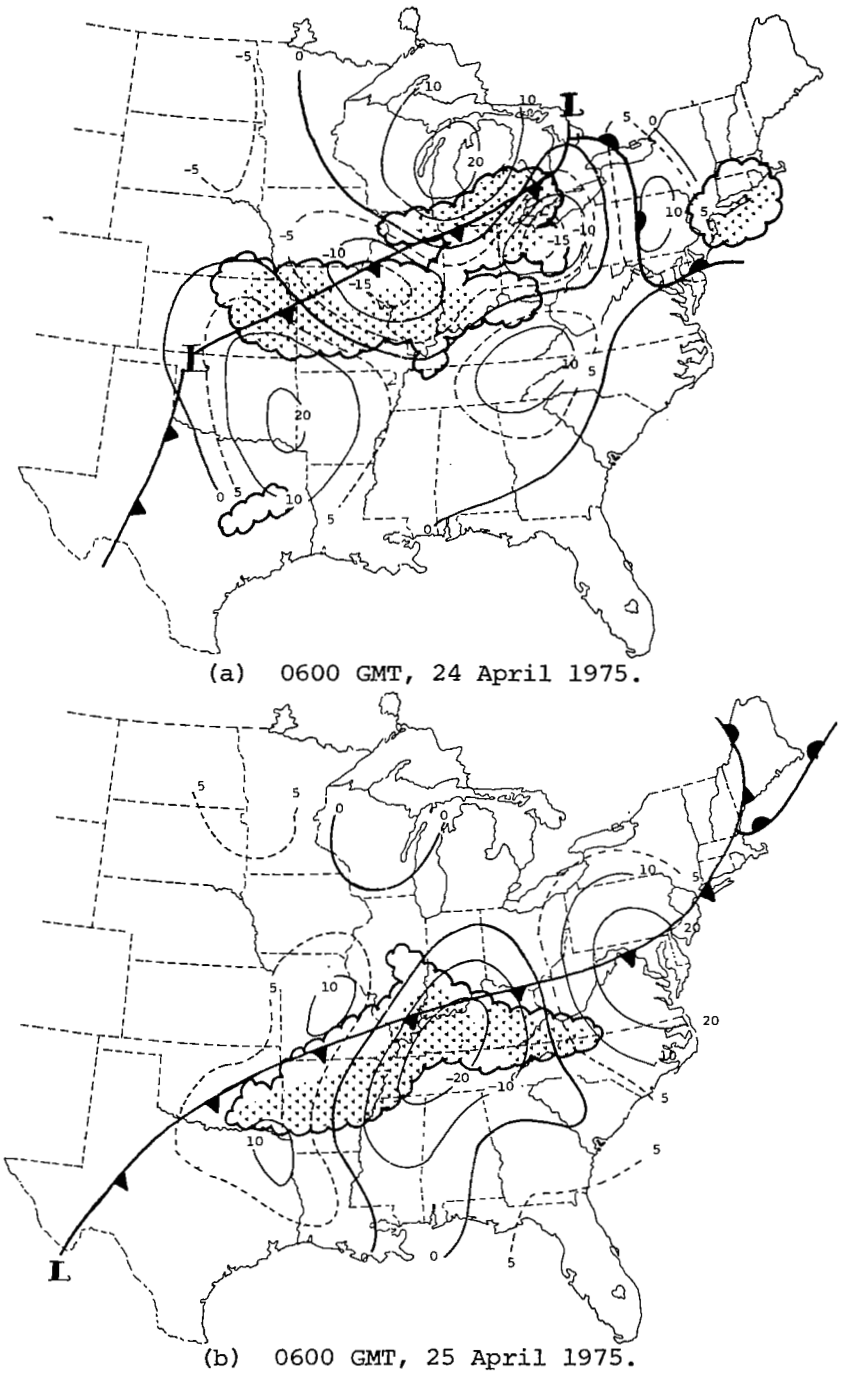

(a) 0600 GMT, 24 April 1975.

(b) 0600 GMT, 25 April 1975.

Fig. 21. Analyses of the net horizontal boundary flux of moisture in the layer 750-500 mb. (Superimposed are surface frontal positions and radar-observed convection. Units: $x10^{-6}g\ cm^{-2}s^{-1}$).

is only obvious since the level of nondivergence was found in this layer, thus, $q\vec{\nabla}\cdot\vec{V}$ was small.

ii. Residual. Subsequent to the complete evaluation of the LHS of Eq. 7, the terms were summed in each 50-mb layer and related to MDR data. Vertical profiles of the resulting residual are shown in Fig. 22.

A large negative residual of moisture occurred in the lower layer of the atmosphere with the regions of more intense convection showing the greatest deficit. In all areas of precipitation (MDR $\geq$ 2), the average residual found in each 50-mb layer for the lower 200 mb was about -1.5×10^{-6} g cm^{-2}sec^{-1}. However, within the region of intense convection (MDR $\geq$ 8), the values averaged over twice as much.

Above 700 mb the residual decreased considerably but generally stayed negative throughout the atmosphere. For the most part, the convective areas continued to possess the largest residual of moisture and a secondary maximum of negative values appeared in these regions from 500-450 mb. Conversely, in the areas where

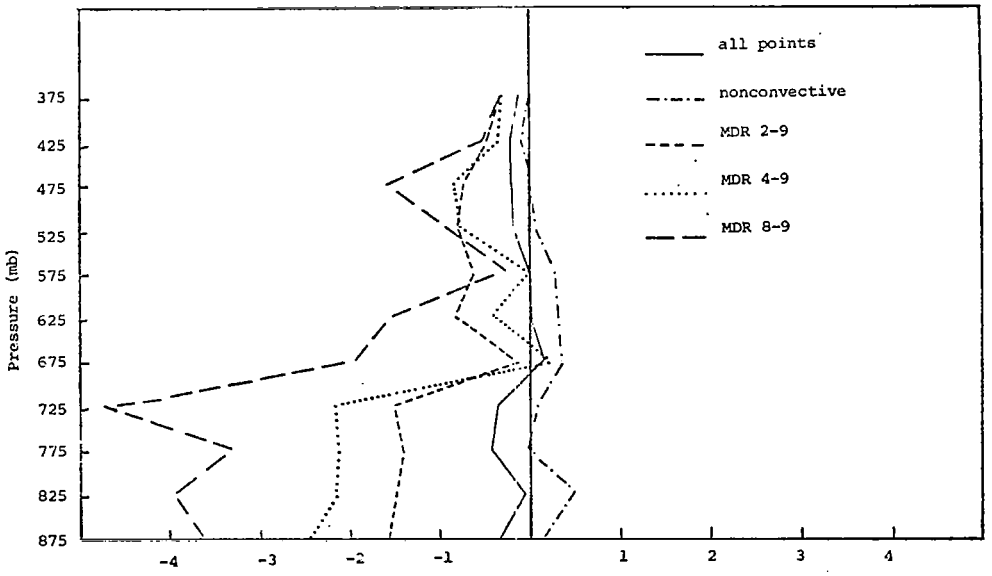

Fig. 22. Vertical profiles of the residual of moisture related to MDR. (Units: $x10^{-6}$g cm^{-2}s^{-1}).

there was little or no precipitation (MDR $\leq$ 1), small gains of moisture were found in every layer below 500 mb.

Analysis of the residual at 0600 GMT on 24 and 25 April in the 900-750-mb, 750-500-mb, and 500-350-mb layers appear in Figs. 23 through 25. Surface fronts and precipitation are shown as before.

Large negative values of the residual term were found in and around the squall lines on both days throughout much of the atmosphere. The 750-500-mb layer showed the largest imbalance with nearly 55 x 10^{-6} g cm^{-2} s^{-1} of moisture loss over central Missouri at 0600 GMT on 24 April (Fig. 24a). However, the 500-350-mb layer also exhibited large losses on the 25th (Fig. 25b), which was due, for the most part, to the large negative vertical flux divergence in the region.

In order to determine the relationship among all the terms, averages of each term were taken for all times in the different MDR categories. The layers shown in the analyses were used since these seemed to isolate strong differences in some of the terms individually. The results are shown in Table II.

In no case could a term be excluded from the moisture budget equation for the entire atmosphere. Each term showed some importance in at least one layer regardless of the intensity of the precipitation in the area. However, there were several situations where a term was not important in a particular layer.

Tables IIa and IIb generally showed the same result; all the terms had some importance in each layer. The only exception was the divergence term which could be neglected from 500-350 mb and was small in the 750-500-mb layer. Conversely, $q\vec{\nabla}\cdot\vec{V}$ was quite strong in the lowest layer, dominating the equation in Table IIa.

In the precipitation areas (Tables IIe, IId, and IIe), the results were quite different. The local rate-of-change could be neglected above 750 mb. Its magnitude was very large in the lowest layer, compared to higher up, but it was still small when compared to the larger terms in the layer. Nevertheless, it was not small enough to neglect its influence on the total balance of moisture in the lowest layer. These results are supported by those of Bradbury

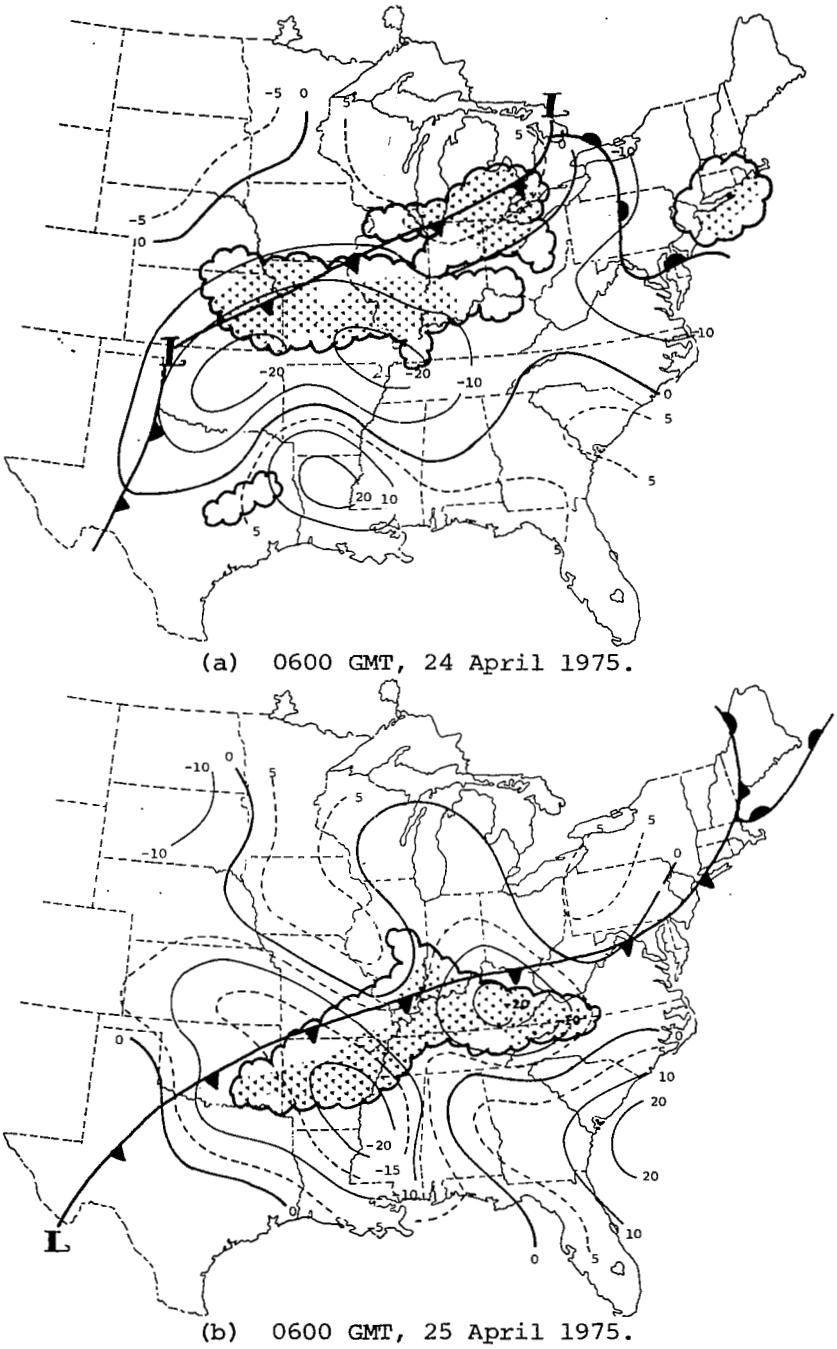

(a) 0600 GMT, 24 April 1975.

(b) 0600 GMT, 25 April 1975.

Fig. 23. Analyses of the residual of moisture in the layer from 900-750 mb. (Superimposed are surface frontal positions and radar-observed convection. Units: $x10^{-6}g\ cm^{-2}s^{-1}$).

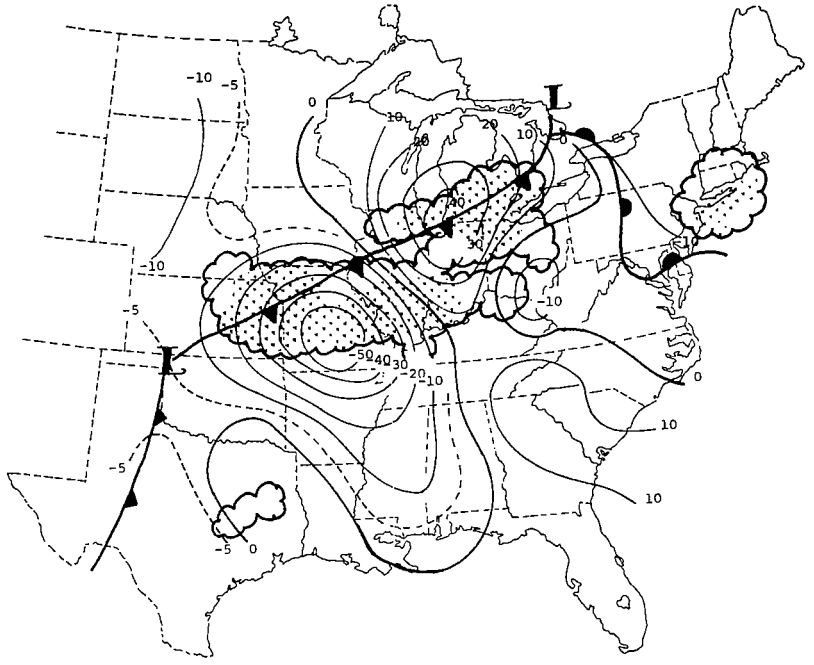

(a) 0600 GMT, 24 April 1975.

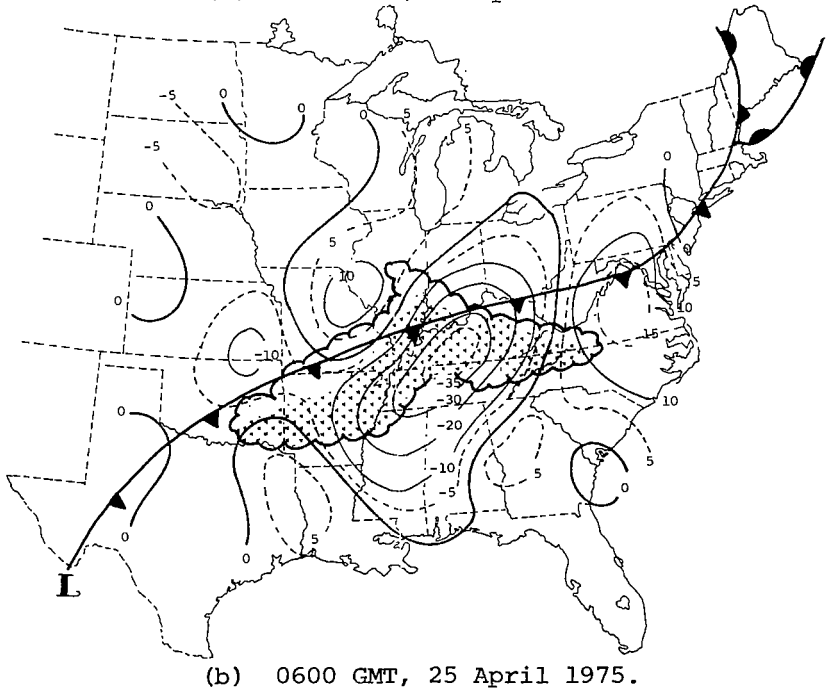

(b) 0600 GMT, 25 April 1975.

Fig. 24. Analyses of the residual of moisture in the layer from 750-500 mb. (Superimposed are surface frontal positions and radar-observed convection. Units: $x10^{-6}$g $cm^{-2}s^{-1}$).

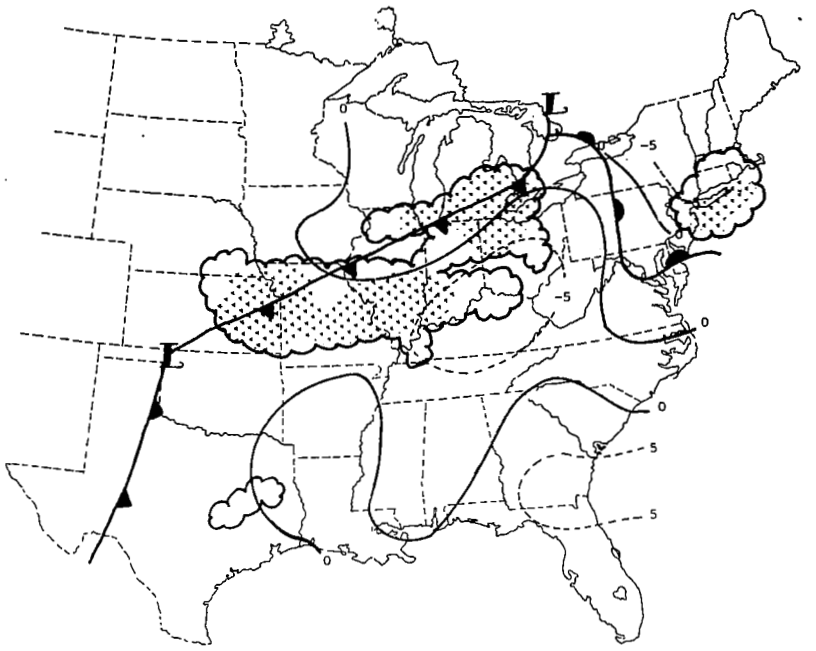

(a) 0600 GMT, 24 April 1975.

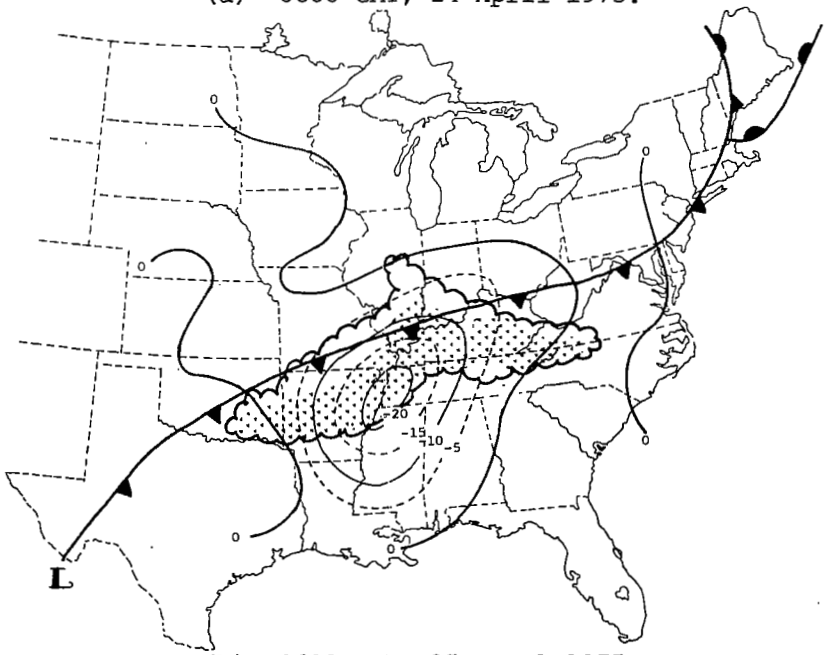

(b) 0600 GMT, 25 April 1975.

Fig. 25. Analyses of the residual of moisture in the layer from 500-350 mb. (Superimposed are surface frontal positions and radar-observed convection. Units: $x10^{-6}$g $cm^{-2}s^{-1}$).

Table II. Averages of each term in the moisture budget equation in the layers indicated related to values of MDR (Units: $x10^{-6}$g $cm^{-2}s^{-1}$).

a. All points

Layer	Local Change	Net Vertical Flux	Net Horizontal Flux	Horizontal Divergence	Horizontal Advection	Residual
500-350	-0.3	-0.7	0.5	0.1	0.5	-0.6
750-500	-0.7	-1.8	2.2	-0.4	2.5	-0.4
900-750	-1.1	1.5	-1.2	-2.8	1.6	-0.9

b. MDR 0-1

500-350	-0.4	-0.1	0.4	0.0	0.3	-0.1
750-500	-0.8	-0.8	2.7	0.6	2.1	1.1
900-750	-1.0	0.7	0.9	-1.1	2.0	0.6

c. MDR 2-9

500-350	-0.2	-2.3	1.0	0.2	0.7	-1.6
750-500	-0.4	-4.4	0.8	-2.8	3.5	-4.0
900-750	-1.4	3.4	-6.4	-7.1	0.6	-4.5

d. MDR 4-9

500-350	0.2	-2.8	1.0	0.3	0.8	-1.6
750-500	0.6	-5.2	1.4	-3.4	4.6	-3.2
900-750	-2.7	3.6	-7.7	-8.6	0.7	-6.8

e. MDR 8-9

500-350	-0.2	-3.4	1.1	0.6	0.5	-2.5
750-500	-0.9	-8.5	0.0	-3.9	3.5	-9.4
900-750	-4.6	5.3	-11.6	-12.9	0.9	-10.9

(1957). She also found that the local rate-of-change of moisture was important but smaller than the net horizontal boundary flux from the ground to 400 mb. The term became much larger however, at the times of strong thunderstorm activity.

Contrary to this, Ninomiya (1968) found the local change of moisture to be negligible in the subcloud layer. He evaluated it as at least an order of magnitude smaller than the horizontal and vertical divergences. However, his work was performed over the Sea of Japan and large values of moisture content would be fairly constant in the subcloud layer. This would tend to keep the local change of moisture from becoming very large.

The net vertical boundary flux of moisture was large in every layer, contributing the most above 750 mb. The increase of this quantity in all layers as the storms became more severe (higher MDR values), is indicated quite well here.

The importance of each of the horizontal terms was different from one layer to the next. Moisture advection could be neglected in the 900-750-mb layer, whereas the divergence term was much larger and dominated the equation. In the middle layer, moisture advection and $q\vec{\nabla}\cdot\vec{V}$ were almost equal in magnitude and individually were as important as the net vertical boundary flux. However, they were always opposite in sign which resulted in a small total horizontal contribution of moisture in this layer. Above 500 mb, the moisture advection was generally larger than $q\vec{\nabla}\cdot\vec{V}$ except in the area of the most intense storms where they were equal. Nevertheless, in the atmosphere as a whole, $q\vec{\nabla}\cdot\vec{V}$ greatly outweighed the importance of moisture advection. This directly agrees with the results found by Palmén and Holopainen (1964).

b. Relationships between terms in the moisture budget equation and MDR values 3 h later

It was indicated in several of the terms discussed previously that large amounts of moisture accumulated slightly to the east of the most intense area of storms (MDR $\geq$ 8; located in Appendix II). Since the movement of both squall lines was eastward, a comparison

was made between the computed fields of moisture and MDR data 3 h later. Due to the fact that some time lag is involved between the initial collection of water vapor in a region and the formation of rain (i.e. storms), it was thought that the lagging process would yield a better relationship between computed quantities of moisture in the atmosphere and the later occurrence of convective activity.

1) Local changes

Vertical profiles of the local rate-of-change of moisture 3 h previous to convection indicated by MDR data appear in Fig. 26. These show that, in general, changes of moisture were small throughout the atmosphere 3 h previous to storm occurrence.

Except for the lower 100 mb, the precipitation areas were represented by a small gain of moisture locally up to 350 mb. The largest values were found from about 800 mb to 600 mb in the area of the most intense convection. This indicates that in the areas of convection that existed 3 h after each sounding, the atmosphere was slightly more moist at the sounding time subsequent to the time

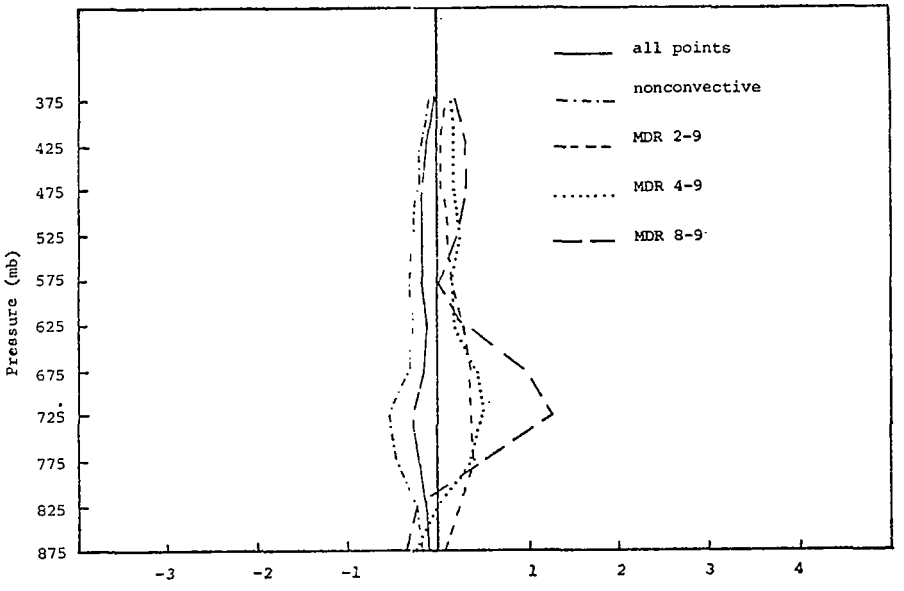

Fig. 26. Vertical profiles of the local rate-of change of moisture related to MDR lagged by 3 h. (Units: $x10^{-6}g\ cm^{-2}s^{-1}$).

of observation than the preceding time. This seems only logical since the comparison here is between the moisture content in the area where convection is present and its value in the same area 6-9 h before.

Analyses of the local rate-of-change of moisture at 0600 GMT on 24 April and 0600 GMT on 25 April appear in Figs. 27 and 28. Superimposed is radar-observed convection lagged by 3h.

The lagging of the MDR data had the effect of moving the convection away from the areas of negative local change toward more positive regions. This happened, generally, throughout the greater part of the atmosphere and was the reason for the change toward positive values on the profiles.

2) Net vertical boundary flux

Vertical profiles of the net vertical boundary flux of moisture appear in Fig. 29. As was true in the case with no time lag of MDR data, a large outflow (positive flux divergence) of moisture occurred in the lower layers of the atmosphere in regions of precipitation. The greatest losses were found in areas where MDR ≥ 4; however, deficits were about the same in all rainfall areas regardless of storm intensity.

Above 800 mb, there was a net gain of moisture due to vertical motion. The increases continued up to 350 mb and were dominated by lower values of MDR than was true when no lag was used. MDR ≥ 8 was associated with the largest values of net vertical boundary flux only from 800-750 mb. Above this layer, lesser values of MDR were found in the largest flux divergence areas.

Analyses of this term at 0600 GMT on 24 April and 0600 GMT on 25 April appear in Figs. 30 through 32 where the precipitation 3 h later has been superimposed. A study of the charts revealed that in all layers the convective systems 3 h later were more closely aligned with the centers of maximum flux divergence than when MDR was not lagged. In earlier results, it was supposed that the centers of the net vertical boundary flux of moisture which were located east of the squall line, might indicate the preferred area for continued storm development. The results shown here support the supposition.

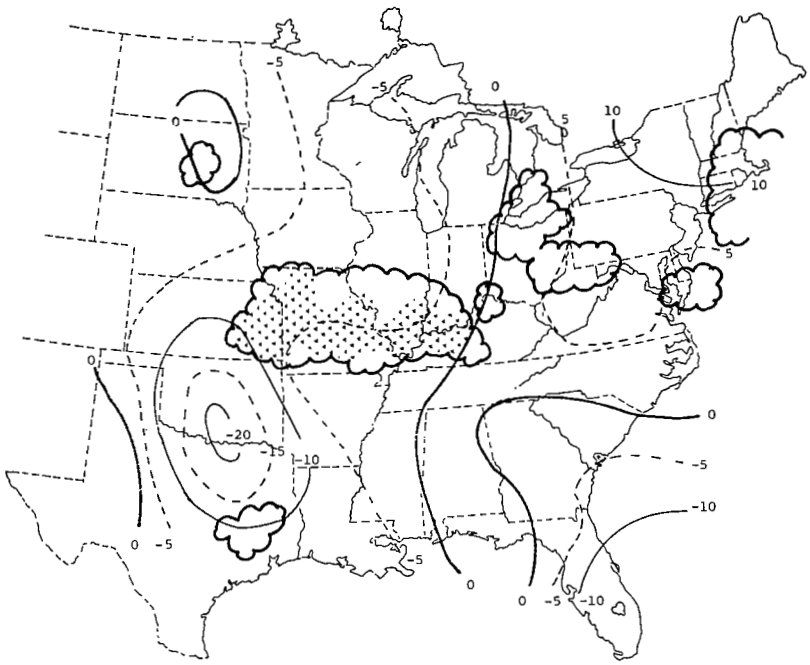

(a) 0600 GMT, 24 April 1975.

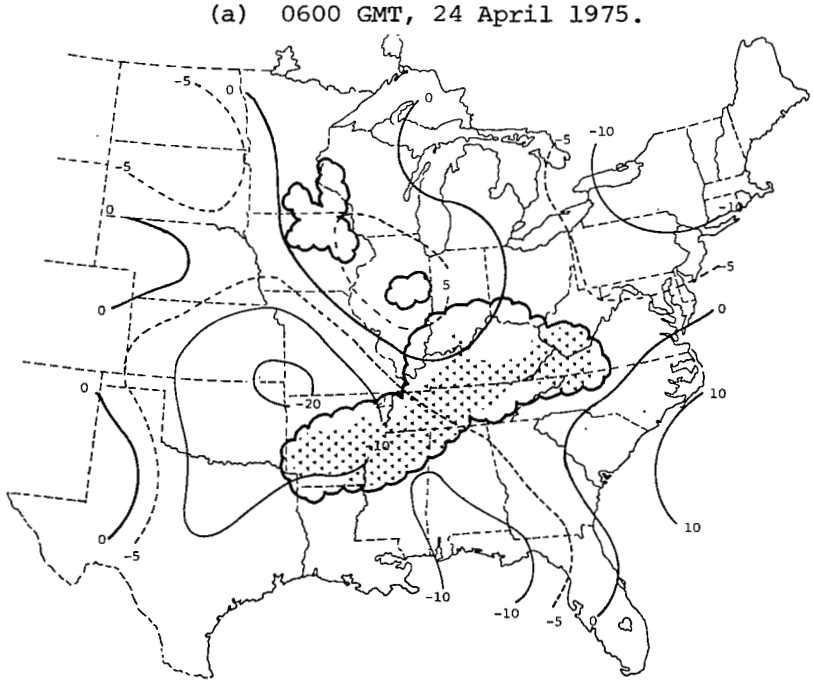

(b) 0600 GMT, 25 April 1975.

Fig. 27. Analyses of the local rate-of change of moisture in the layer from 900-750 mb. (Superimposed is radar-observed convection lagged by 3 h. Units: $x10^{-6}g\ cm^{-2}s^{-1}$).

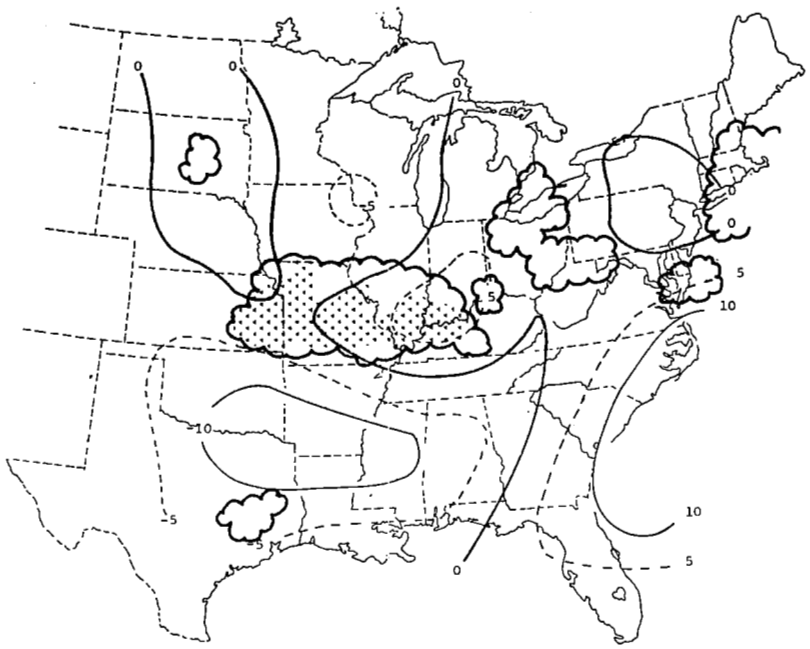

(a) 0600 GMT, 24 April 1975.

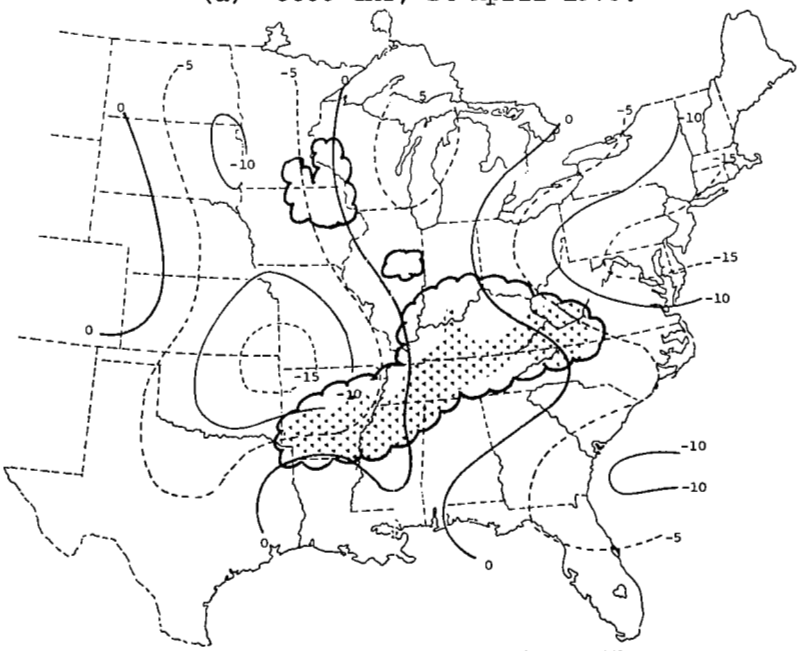

(b) 0600 GMT, 25 April 1975.

Fig. 28. Analyses of the local rate-of-change of moisture in the layer from 750-500 mb. (Superimposed is radar-observed convection lagged by 3 h. Units: $x10^{-6}$g $cm^{-2}s^{-1}$).

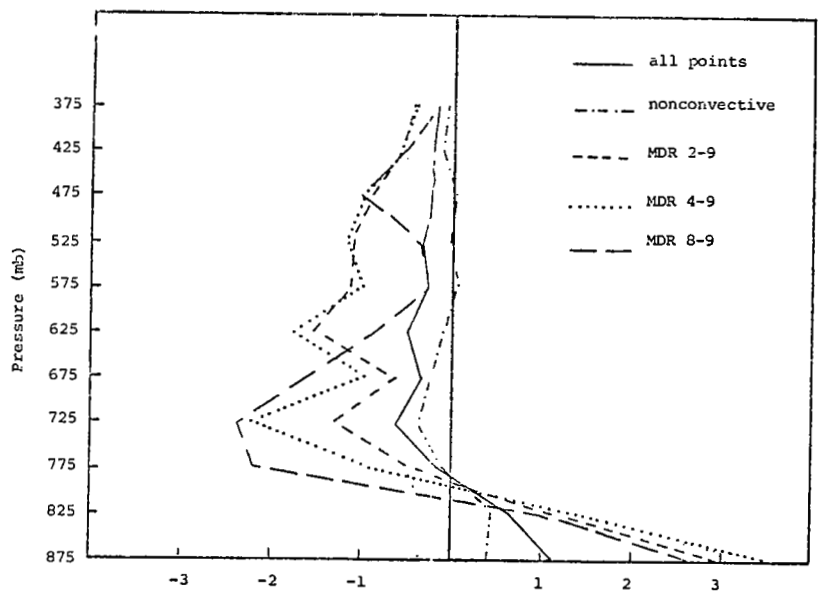

Fig. 29. Vertical profiles of the net vertical boundary flux of moisture related to MDR lagged by 3 h. (Units: $x10^{-6}g\ cm^{-2}s^{-1}$).

In order to indicate this more convincingly, the beginning of the second squall line was examined more closely. It was stated previously that it was some time after the initial development of the squall line that the net vertical boundary flux became large in the layer from 900-750 mb. However, by looking at the flux divergence in the lowest 50-mb layer of the atmosphere measured by this research (900-850 mb), it was observed that favored regions of convection were indicated in the early development stages.

Analyses of the net vertical boundary flux at 2100 GMT on 24 April in the 900-850-mb layer appears in Fig. 33. MDR data at 2100 GMT and 0000 GMT on 25 April have been superimposed. A study of the charts revealed that the squall line which had formed by 0000 GMT on 25 April was related to the computed fields of vertical flux divergence 3 h previously. In the next layer above (850-800 mb), a net gain occurred over the same area. This indicates that the synoptic-scale vertical motion was not developed enough at this time

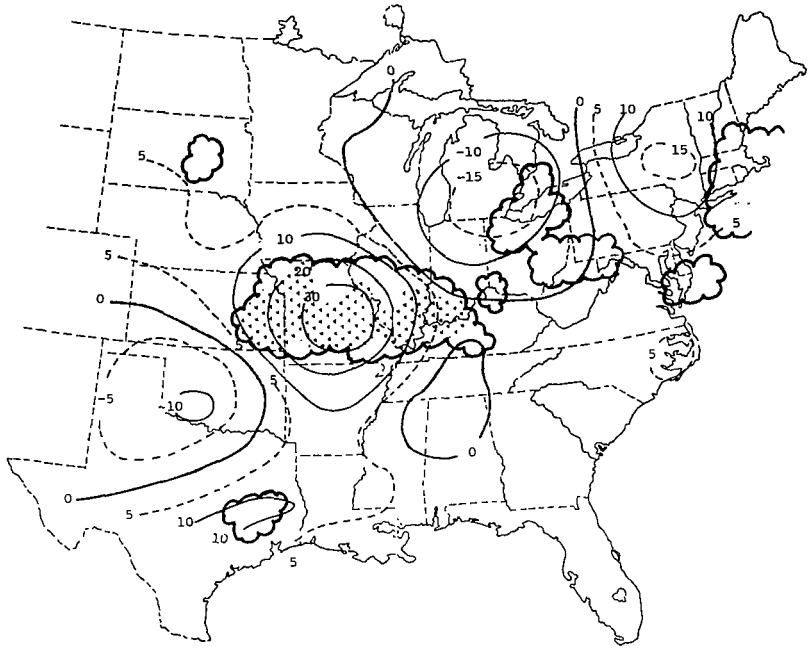

(a) 0600 GMT, 24 April 1975.

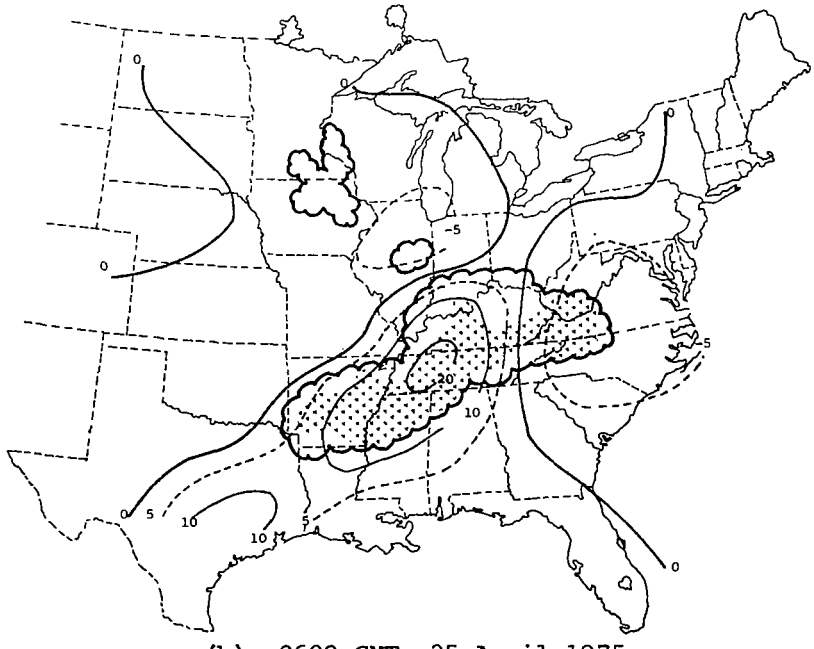

(b) 0600 GMT, 25 April 1975.

Fig. 30. Analyses of the net vertical boundary flux of moisture in the layer from 900-750 mb. (Superimposed is radar-observed convection lagged by 3 h. Units: $x10^{-6}$g $cm^{-2}s^{-1}$).

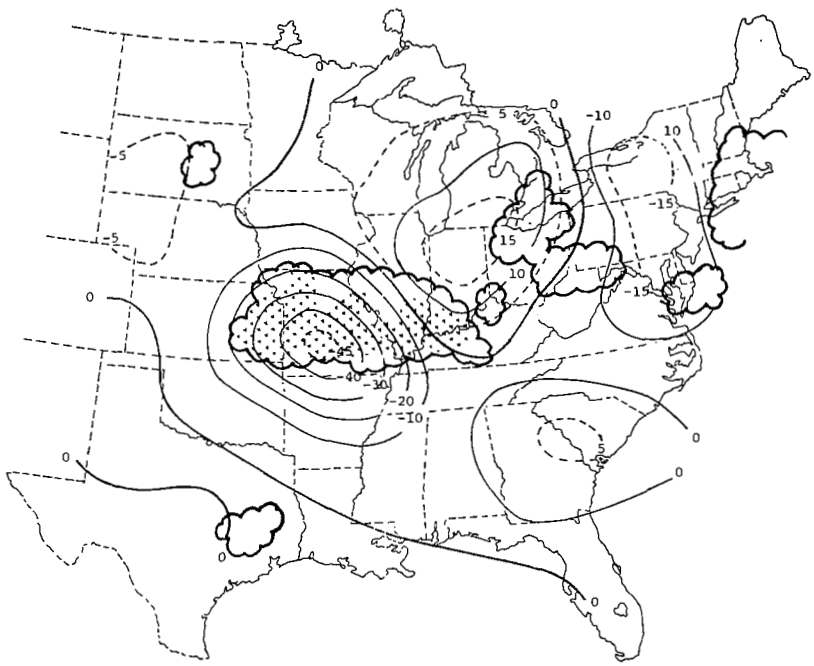

(a) 0600 GMT, 24 April 1975.

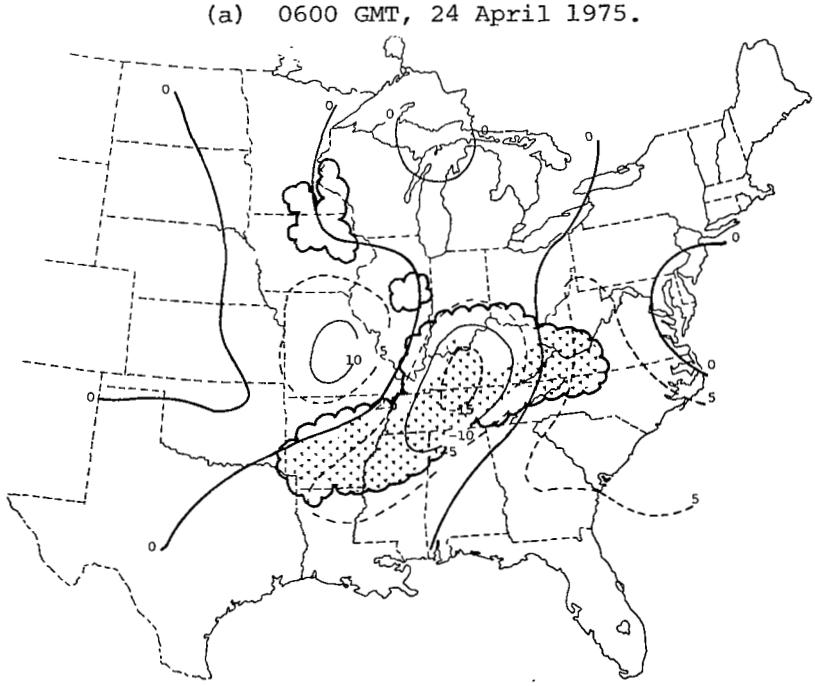

(b) 0600 GMT, 25 April 1975.

Fig. 31. Analyses of the net vertical boundary flux of moisture in the layer from 750-500 mb. (Superimposed is radar-observed convection lagged by 3 h. Units: $x10^{-6}$g $cm^{-2}s^{-1}$).

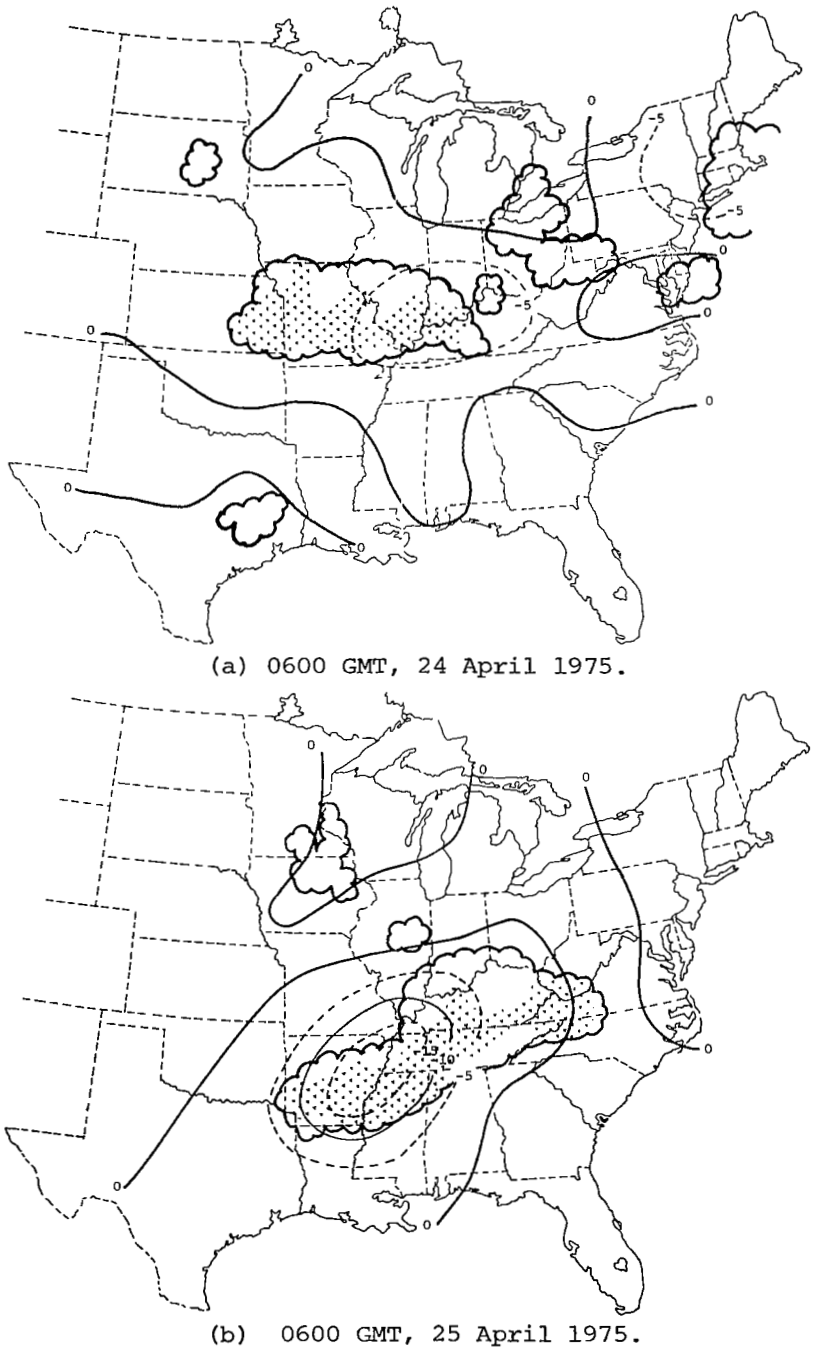

(a) 0600 GMT, 24 April 1975.

(b) 0600 GMT, 25 April 1975.

Fig. 32. Analyses of the net vertical boundary flux of moisture in the layer from 500-350 mb. (Superimposed is radar-observed convection lagged by 3 h. Units: $x10^{-6}$g $cm^{-2}s^{-1}$).

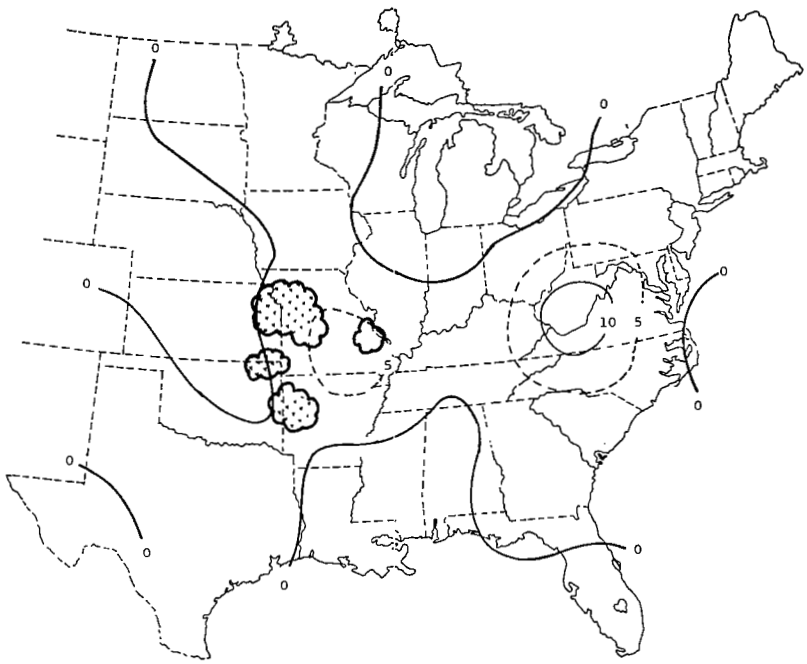

(a) Superimposed is radar-observed convection at 2100 GMT on 24 April 1975.

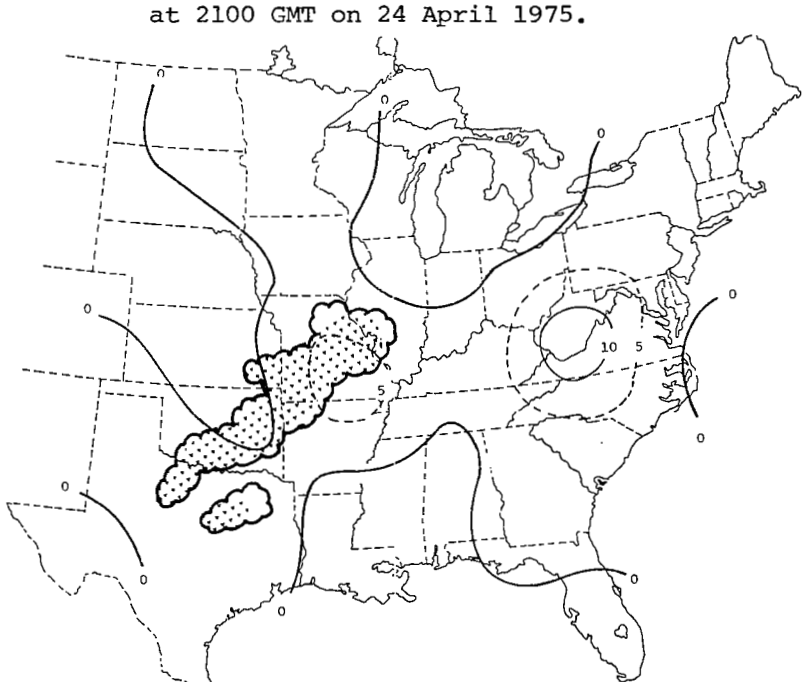

(b) Superimposed is radar-observed convection at 0000 GMT on 25 April 1975.

Fig. 33. Analyses of the net vertical boundary flux of moisture at 2100 GMT on 24 April 1975 in the layer from 900-850 mb. (Units: $x10^{-6}g\ cm^{-2}s^{-1}$).

to transport large amounts of moisture vertically to be used in the formation of the thunderstorm system.

In the vertical profiles, the averages of this quantity in the region of the most intense storms (MDR $\geq$ 8) had dropped from its value 3 h earlier. The reason for this can be found by a close examination of the MDR data. The maximum intensity of each squall line was at 0600 GMT on both days. However, less intense convection continued afterwards for the next six hours. By 0900 GMT, there were fewer MDR $\geq$ 8 but more MDR $\geq$ 4. The less intense convection had simply replaced the intense storms that had weakened from 3 h earlier.

The extent of this was shown strongly by comparison of the vertical profiles in Figs. 9 (p. 26) and 27. The extreme values of MDR $\geq$ 8 dropped substantially when the MDR was lagged. Conversely, the average values of the vertical flux divergence in areas of MDR $\geq$ 4 were larger in absolute value in every 50-mb layer below 550 mb when the radar data were lagged by 3 h than when data were not lagged.

3) Divergence

Vertical profiles of the moisture concentration due to horizontal divergence appear in Fig. 34 where the MDR data lagged the computed fields by 3 h. A large amount of moisture converged horizontally into the precipitation regions in the layers below 600 mb.

Analogous to the results concerning the net vertical boundary flux, the averages of $q\vec{\nabla}\cdot\vec{v}$ in areas where MDR $\geq$ 4 increased when the radar data were lagged 3 h, despite the large reduction of averaged values in areas of MDR $\geq$ 8 from 3 h earlier. The change of the averages in the most intense storm areas represented the most notable difference in the profiles from the ones where there was no lag of radar data. Except in these storm areas, the profiles were essentially unchanged above 750 mb.

Analyses of the concentration of moisture due to horizontal divergence at 0600 GMT on 24 April and 0600 GMT on 25 April are shown in Fig. 35 and 36 where the MDR data at 0900 GMT has been superimposed on the respective days.

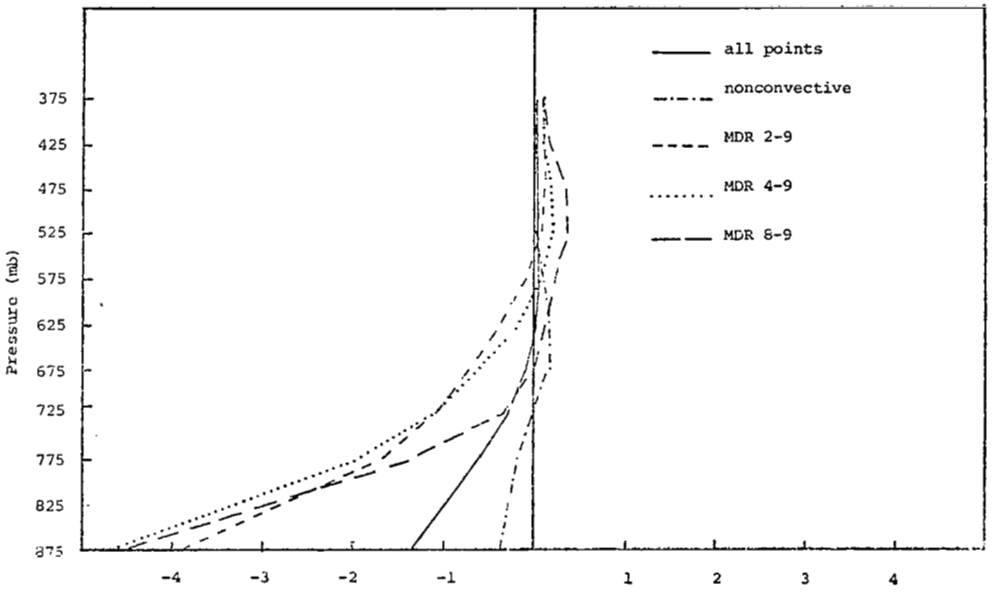

Fig. 34. Vertical profiles of the moisture concentration due to wind divergence related to MDR lagged by 3 h. (Units: $x10^{-6}g\ cm^{-2}s^{-1}$).

Fig. 35 indicates that there was a closer relationship between the computed fields of $q\vec{\nabla}\cdot\vec{v}$ and MDR 3 h later than the radar data at the same time. The relationship on 24 April was only slightly better but it was much improved on 25 April. The values of $q\vec{\nabla}\cdot\vec{v}$ at 0600 GMT on the 25th showed an elongated maximum from central Kentucky to southeastern Arkansas. There was some evidence of a double center, one at each end of the maximum area. There was no indication of this type of structure in the MDR data at 0600 GMT. However, at 0900 GMT, the MDR data show that development had continued in the region where $q\vec{\nabla}\cdot\vec{v}$ was a maximum, over southeastern Arkansas, and had remained strong in central Kentucky. This suggests that, analogous to the net vertical boundary flux of moisture, the areas of the strongest convection in the squall lines were indicated from computed fields of $q\vec{\nabla}\cdot\vec{v}$ 3 h earlier.

Observations of $q\vec{\nabla}\cdot\vec{v}$ at 2100 GMT on 24 April in the 900-850-mb layer showed, similar to that found with the net vertical boundary flux, a favored location for storm development 3 h before a strong squall line was indicated by radar. Figure 37 shows the analysis

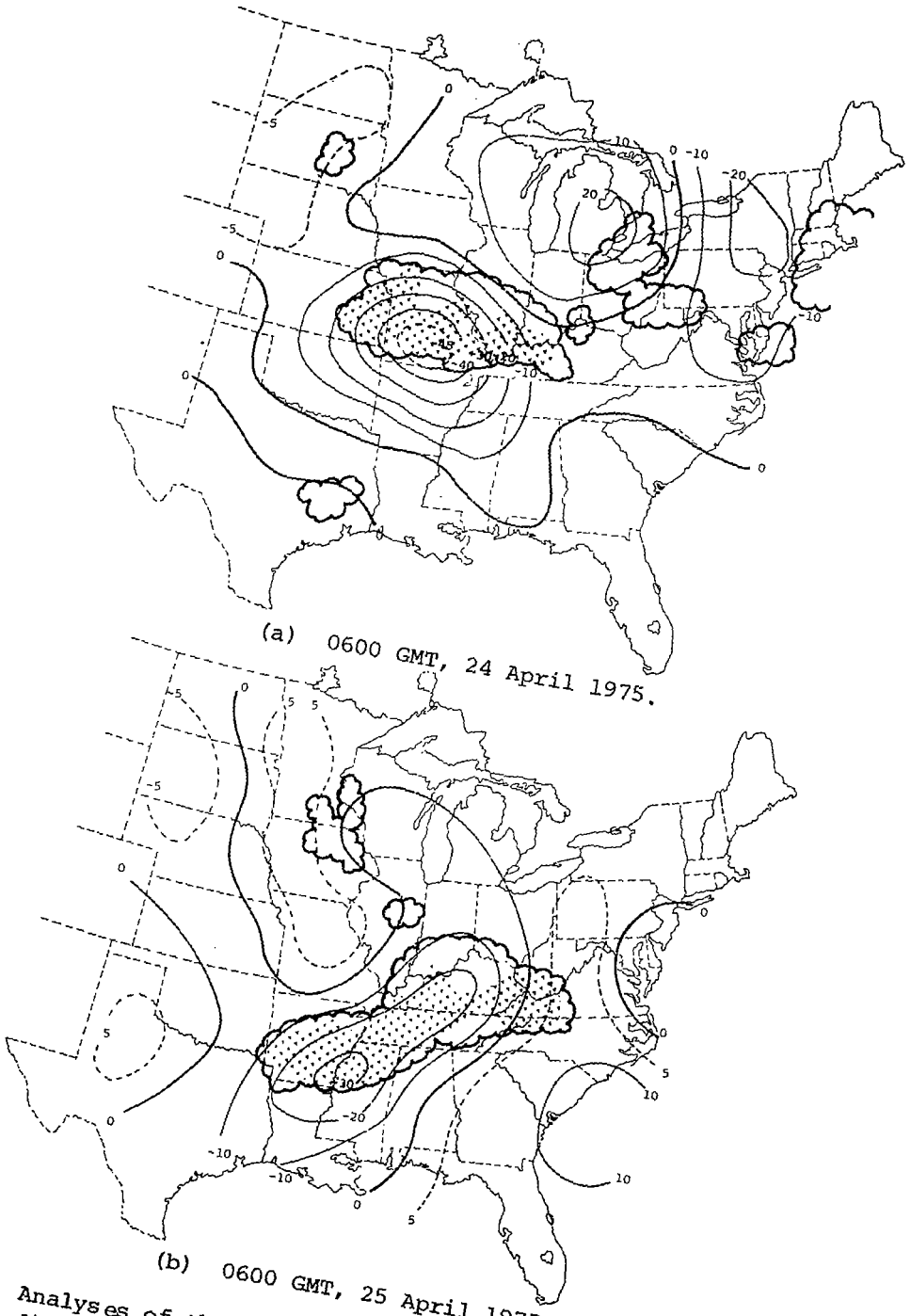

(a) 0600 GMT, 24 April 1975.

(b) 0600 GMT, 25 April 1975.

Fig. 35. Analyses of the moisture concentration due to wind divergence in the layer from 900-750 mb. (Superimposed is radar-observed convection lagged by 3 h. Units: $x10^{-6}$ g $cm^{-2}s^{-1}$).

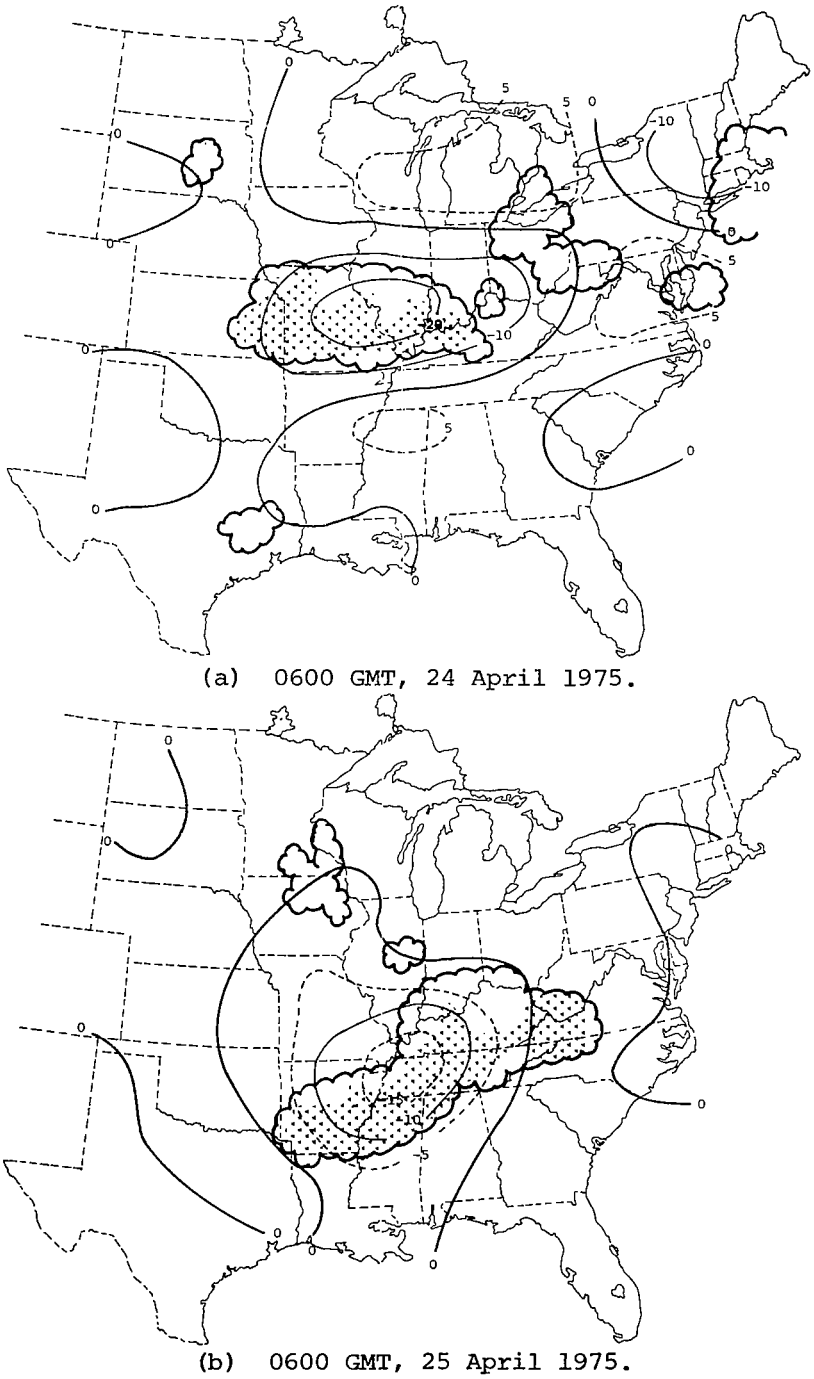

Fig. 36. Analyses of the moisture concentration due to wind divergence in the layer from 750-500 mb. (Superimposed is radar-observed convection lagged by 3 h. Units: $x10^{-6}$g $cm^{-2}s^{-1}$).

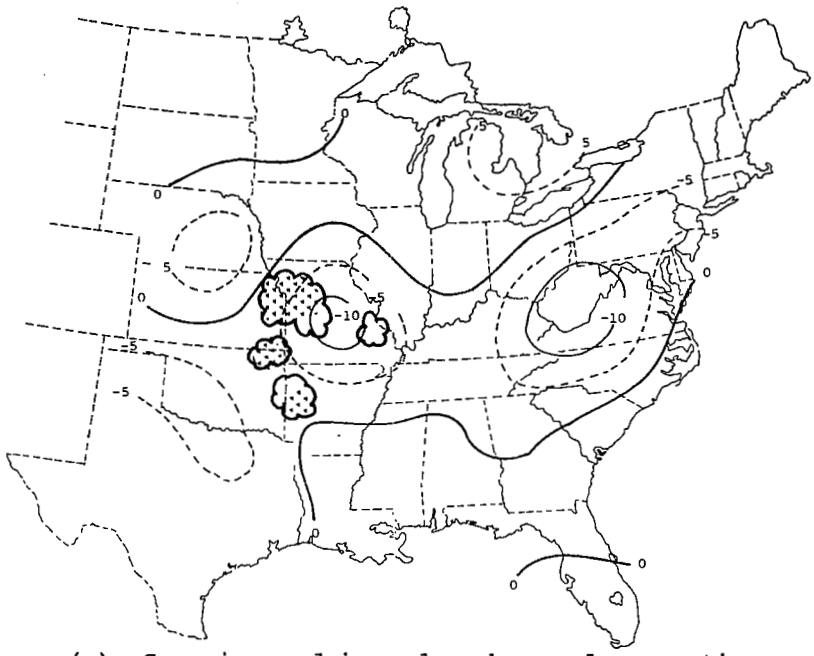

(a) Superimposed is radar-observed convection at 2100 GMT on 24 April 1975.

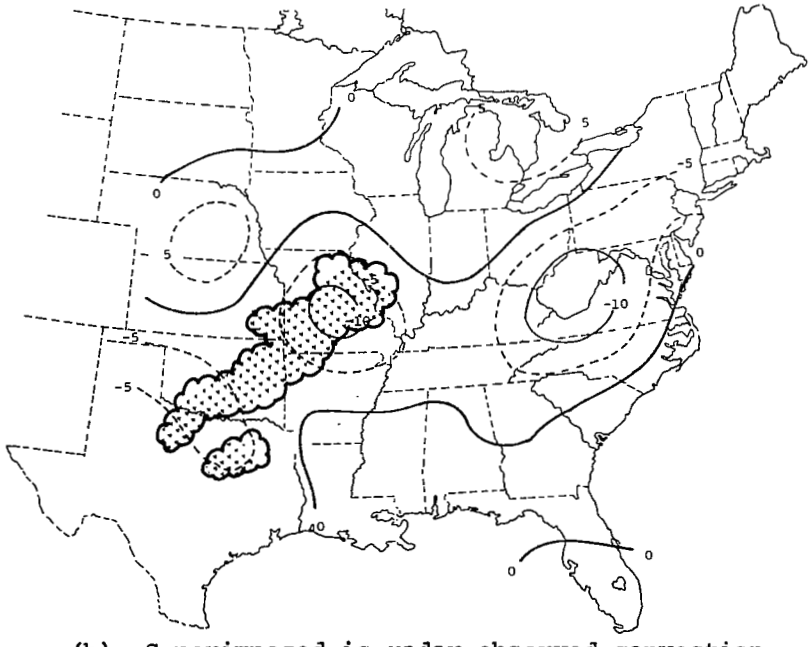

(b) Superimposed is radar-observed convection at 0000 GMT on 25 April 1975.

Fig. 37. Analyses of the moisture concentration due to wind divergence at 2100 GMT on 24 April 1975 in the layer from 900-850 mb. (Units: $x10^{-6}g\ cm^{-2}s^{-1}$).

of this situation where the radar data at 2100 GMT and 0000 GMT on 25 April have been superimposed. Increases in moisture due to $q\vec{\nabla}\cdot\vec{V}$ were present in the next 50-mb layer but were much weaker.

4) Advection

Vertical profiles of the moisture advection 3 h previous to convection as shown by MDR data appear in Fig. 38. The effect of the 3 h lag on this term was to shift all the profiles slightly to more negative values below about 650 mb, staying virtually unchanged above this. All rainfall areas were associated with negative advection from 900 to 800 mb. A region of maximum positive advection occurred between 750 and 650 mb, and then all the profiles except MDR $\geq$ 8 returned slowly to zero near 350 mb. In the areas of the most intense convection, the moisture advection was again negative above about 550 mb.

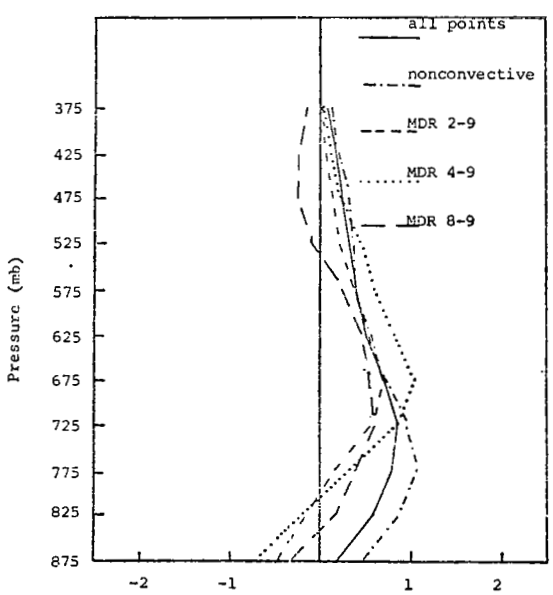

Fig. 38. Vertical profiles of moisture advection related to MDR lagged by 3 h. (Units: $x10^{-6}$g $cm^{-2}s^{-1}$).

Analyses of the moisture advection at 0600 GMT on 24 and 25 April are shown in Figs. 39 and 40. It was stated in the discussion of moisture advection with no lag of MDR that, throughout the atmosphere, negative values were located ahead of the squall lines with positive values in the rear. By lagging the radar data, the convection was positioned further to the east and was associated more with lower positive values or negative advection. This is the reason for the occurrence of more negative values of moisture advection indicated in the profiles.

However, the moisture advection never dominated the horizontal moisture divergence in the convection regions. Although it was usually more important above 700 mb in comparison to $q\vec{\nabla}\cdot\vec{V}$ outside of storm areas, it was often equalled or surpassed in areas where convection was present. Centers of maximum advection, positive or negative, were not as well-defined or as large as values of the net vertical boundary flux and $q\vec{\nabla}\cdot\vec{V}$ in the convective regions. Instead they were rather flat and elongated. Therefore, lagging the MDR data made only a small difference.

5) Combination of terms.

i. Net horizontal flux. Vertical profiles of the net horizontal boundary flux of moisture, compared with MDR data lagged by 3 h, appear in Fig. 41. The total horizontal contribution was only slightly changed by the lag of MDR data. As was true in the case with no lag, the net horizontal boundary flux was dominated by $q\vec{\nabla}\cdot\vec{V}$ in the lower layers with moisture advection becoming important above 750 mb. Increases occurred in the magnitude of the quantity in areas where MDR $\geq$ 4, despite reductions in the net boundary flux where MDR $\geq$ 8.

Analyses of the net horizontal boundary flux of moisture at 0600 GMT on 24 April and 0600 GMT on 25 April are shown in Figs. 42 and 43 where MDR data 3 h later have been superimposed.

Empirically, the relationship between the computed fields and MDR data lagged by 3 h held a better relationship than when the radar data were not lagged. Precipitation was centered more on the

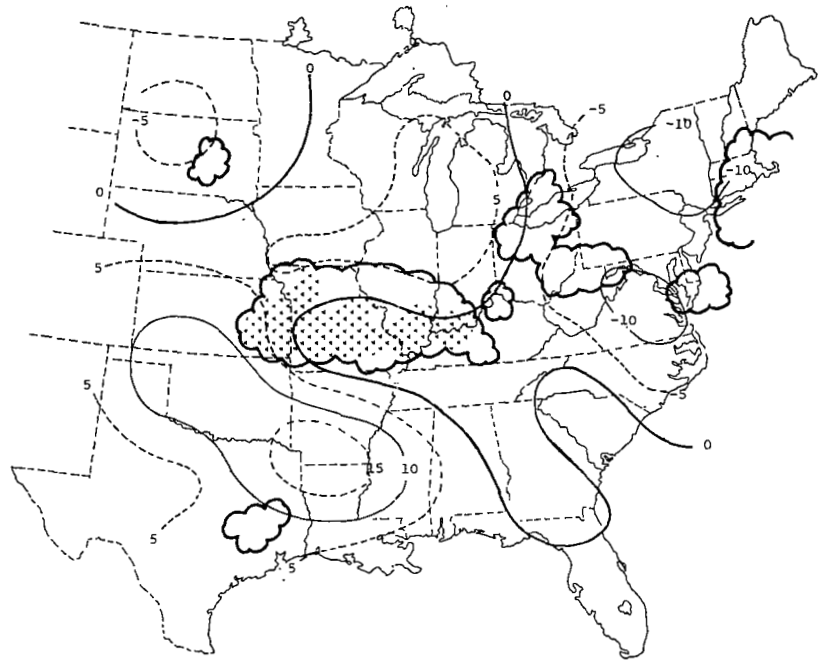

(a) 0600 GMT, 24 April 1975.

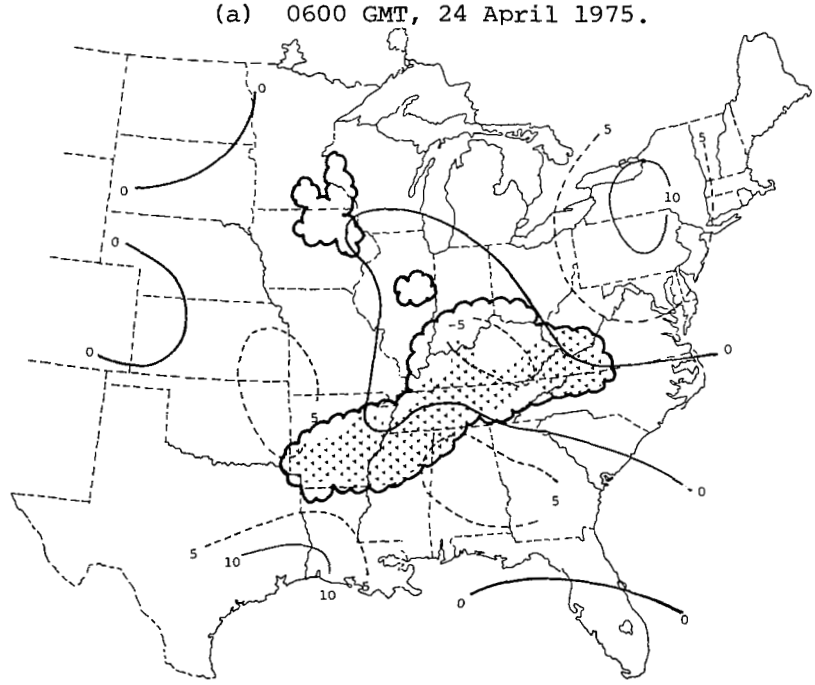

(b) 0600 GMT, 25 April 1975.

Fig. 39. Analyses of the moisture advection in the layer from 900-750 mb. (Superimposed is radar-observed convection lagged by 3 h. Units: $x10^{-6}g\ cm^{-2}s^{-1}$).

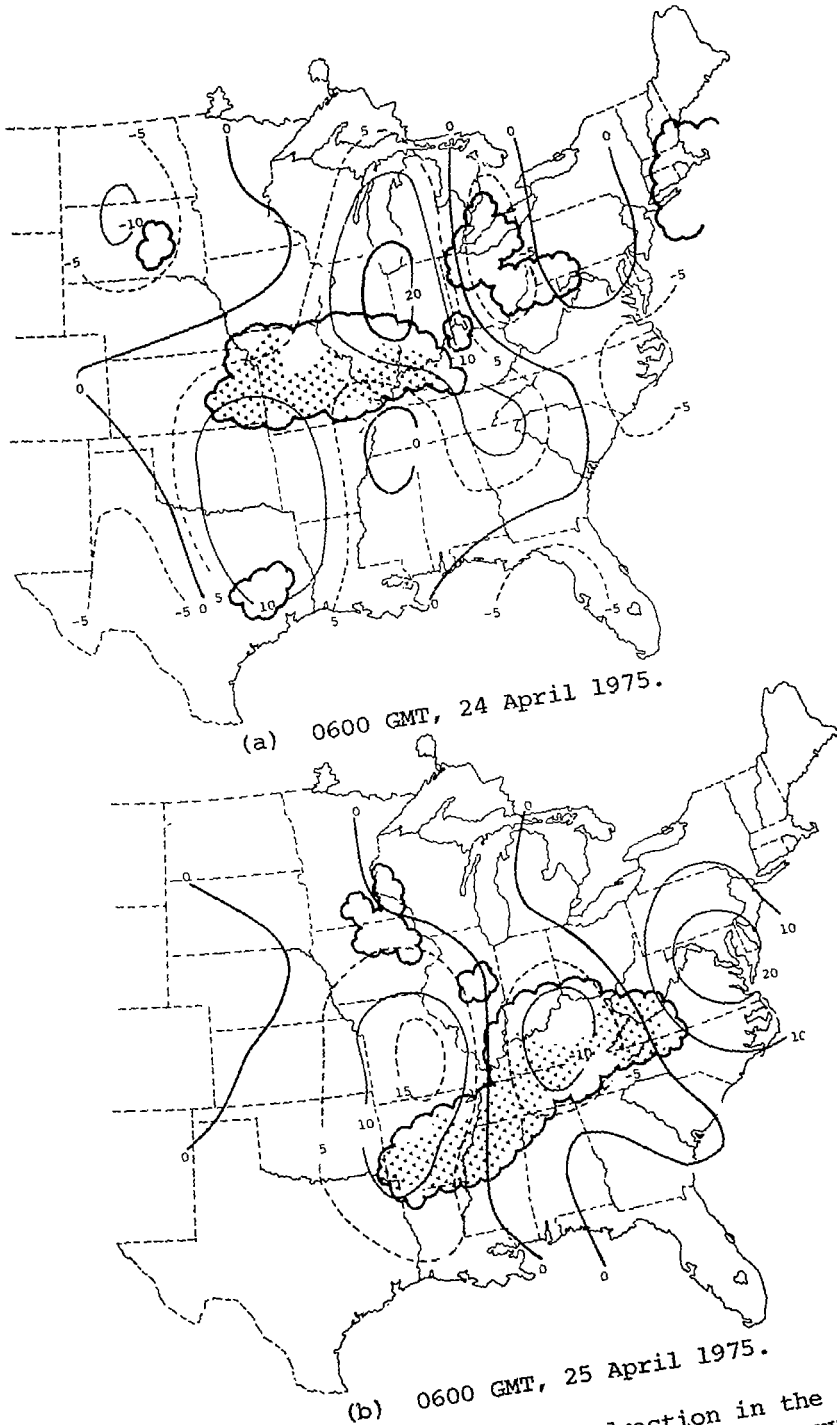

(a) 0600 GMT, 24 April 1975.

(b) 0600 GMT, 25 April 1975.

Analyses of the moisture advection in the layer from
(Superimposed is radar-observed convection
x10^{-6}g cm^{-2}s^{-1}).

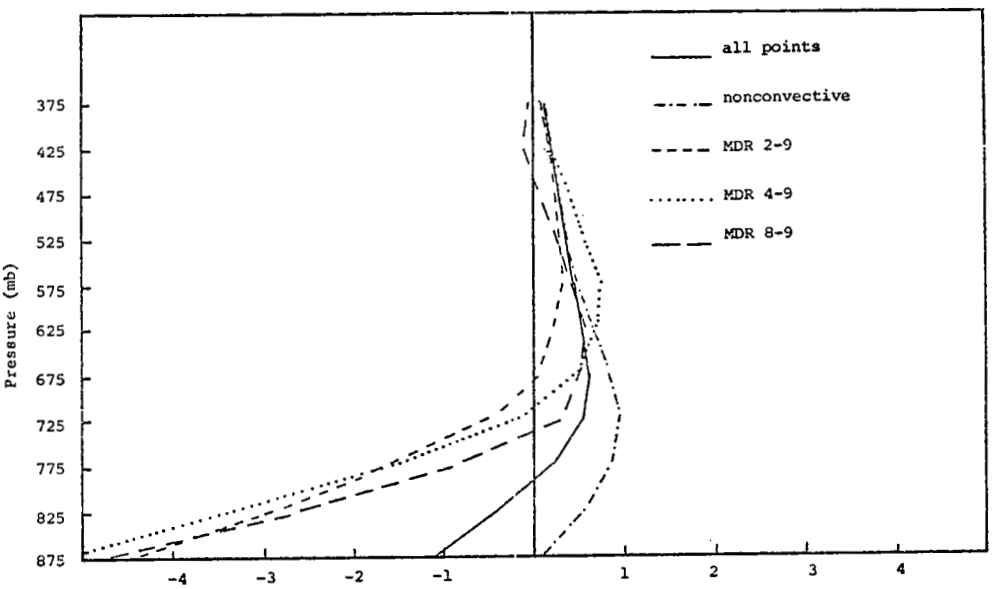

Fig. 41. Vertical profiles of the net horizontal boundary flux of moisture related to MDR lagged by 3 h. (Units: $x10^{-6}$g $cm^{-2}s^{-1}$).

areas of largest negative net boundary flux, giving further support to the suggestions that favored locations of rainfall were indicated at least 3 h ahead of its occurrence.

These results agree well with work by Hudson (1971) and Fritsch (1975). Both authors found good relationships between fields of moisture divergence and precipitation observed by radar 3 h later.

ii. Residual. Vertical profiles of the LHS of Eq. 7 related to MDR data lagged 3 h after the computed quantities, appear in Fig. 44. Large negative residual values were found below 700 mb in all areas of precipation. However, compared to when MDR was not lagged, the amount of outflow of moisture in the most intense convection region (MDR $\geq$ 8) was much smaller. Other changes in the profiles from the "no lag" MDR case were minimal.

Comparisons in the relative magnitude of the terms are presented in Table III. The relationship among the terms themselves showed no significant change from results found when MDR data were not

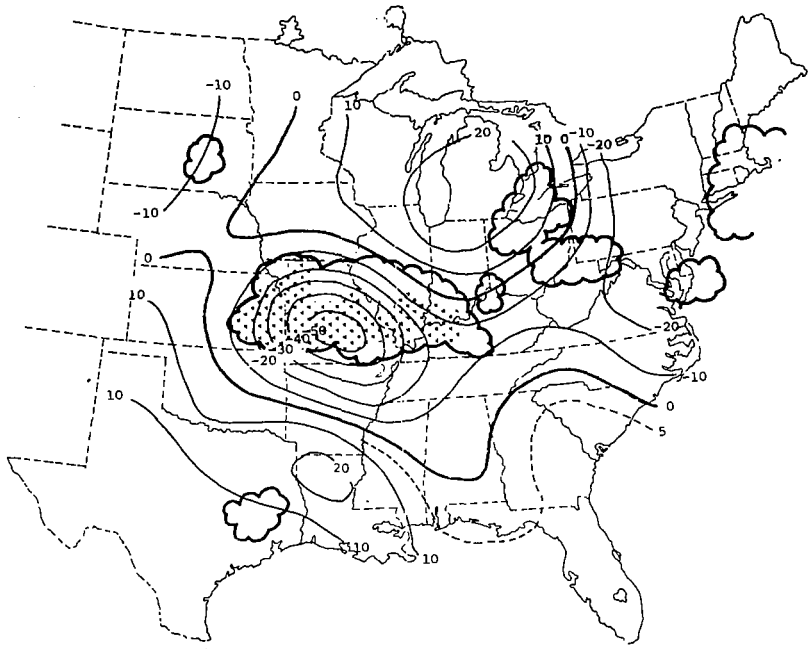

(a) 0600 GMT, 24 April 1975.

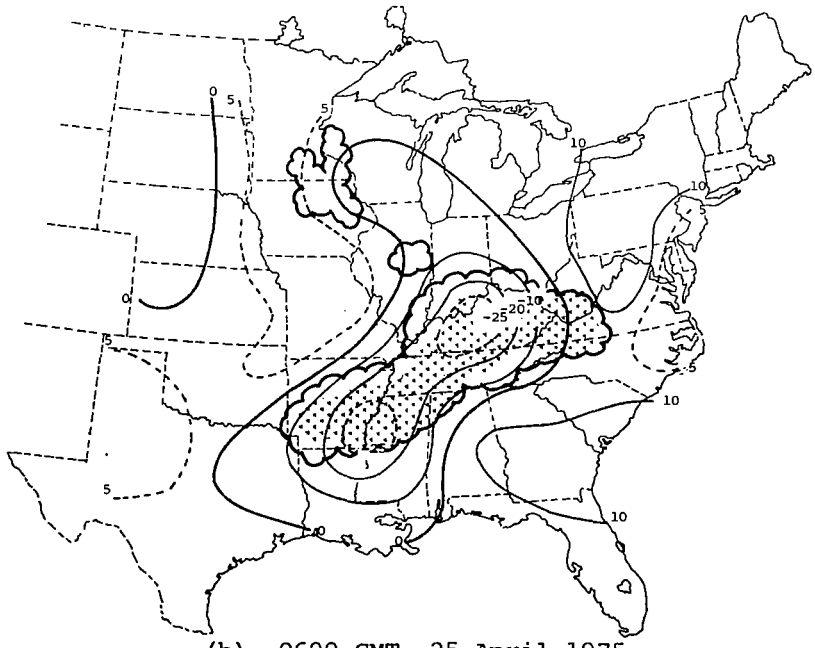

(b) 0600 GMT, 25 April 1975.

Fig. 42. Analyses of the net horizontal boundary flux of moisture in the layer from 900-750 mb. (Superimposed is radar-observed convection lagged by 3 h. Units: $x10^{-6}$g $cm^{-2}s^{-1}$).

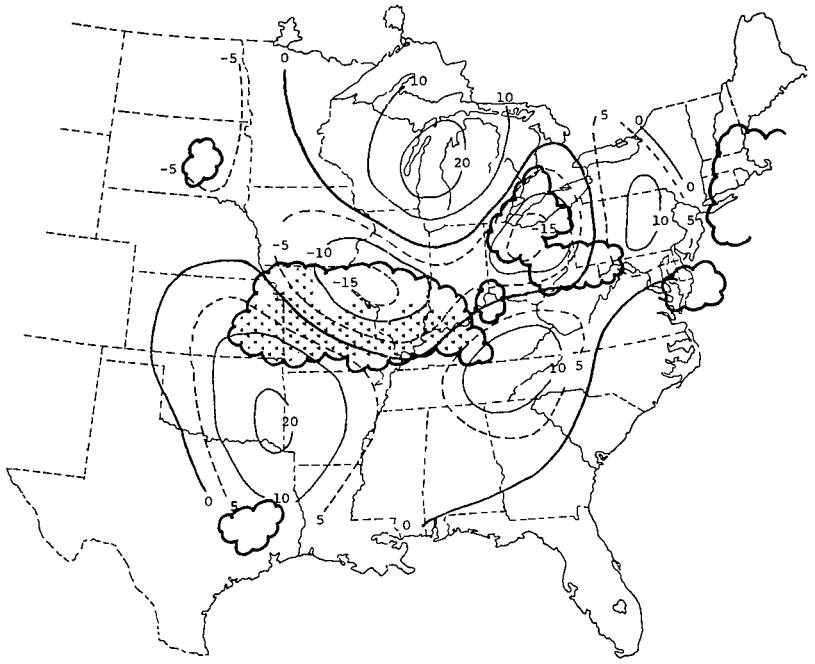

(a) 0600 GMT, 24 April 1975.

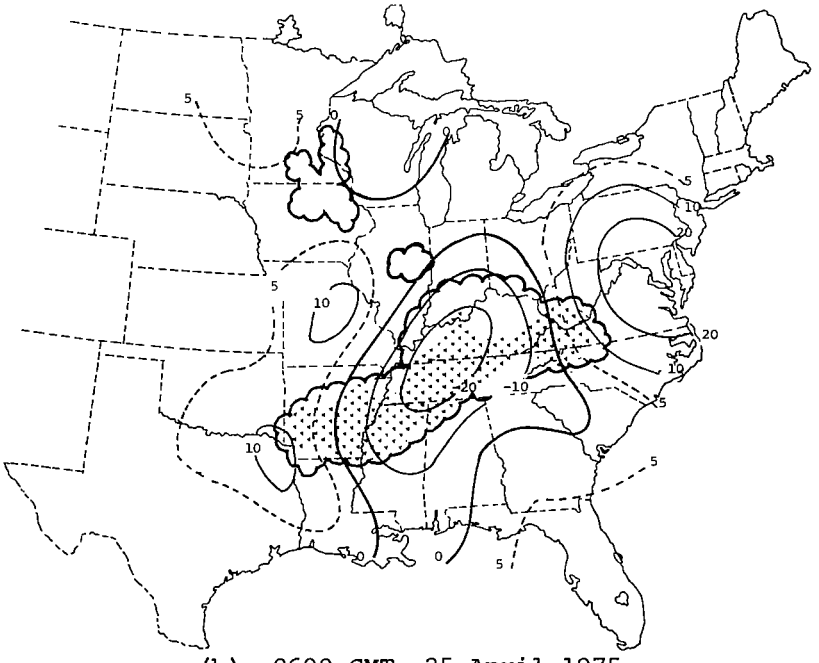

(b) 0600 GMT, 25 April 1975.

Fig. 43. Analyses of the net horizontal boundary flux of moisture in the layer from 750-500 mb. (Superimposed is radar-observed convection lagged by 3 h. Units: $x10^{-6}$g $cm^{-2}s^{-1}$).

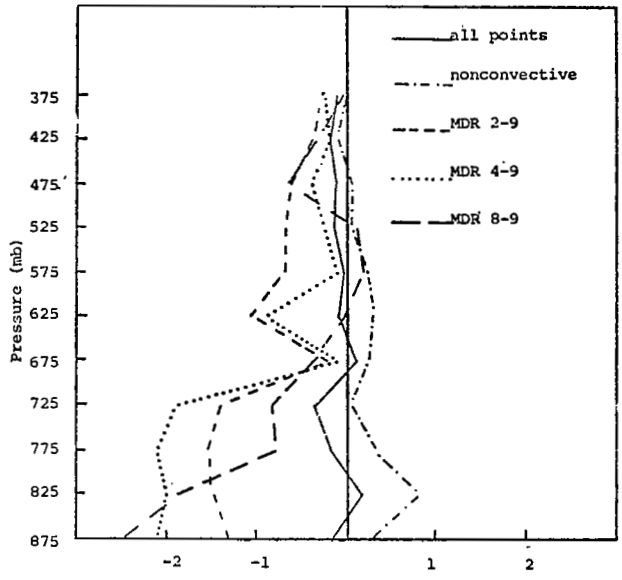

Fig. 44. Vertical profiles of the residual of moisture related to MDR lagged by 3 h. (Units: $x10^{-6}$g $cm^{-2}s^{-1}$).

lagged (Table II). However, sizes of the terms differed, especially in the regions of precipitation.

It was found from the vertical profiles that the net vertical and horizontal boundary fluxes indicated large reductions of moisture flow in the lower layers of the atmosphere around regions of strong convection. Table IIIe shows the averages of each term in these areas. A comparison of these values with those in Table IIe revealed that the decrease of negative net horizontal boundary flux in the 900-750-mb layer nearly balanced a corresponding decrease of positive vertical flux divergence in the same layer. Since these two terms are directly connected by the continuity equation, changes in one should be reflected by changes in the other. Therefore, the reduction of the imbalance of moisture in the lower layer by lagging the radar data was due to the large difference of the local rate-of-change of moisture.

Above the lowest layer, large reductions of moisture loss were caused by changes in all of the terms. Outside of the most intense

Table III. Averages of each term in the moisture budget equation in the layers indicated related to values of MDR lagged by 3 h. (Units: $x10^{-6}$g $cm^{-2}s^{-1}$).

a. All points

Layer	Local Change	Net Vertical Flux	Net Horizontal Flux	Horizontal Divergence	Horizontal Advection	Residual
500-350	-0.4	-0.7	0.6	0.1	0.5	-0.5
750-500	-0.9	-2.1	2.4	-0.3	2.7	-0.6
900-750	-0.4	1.6	-1.3	-2.9	1.5	-0.2

b. MDR 0-1

500-350	-0.5	-0.2	0.6	0.0	0.6	-0.1
750-500	-1.8	-0.6	3.2	0.4	2.9	0.8
900-750	-0.9	0.8	1.5	-0.8	2.3	1.4

c. MDR 2-9

500-350	0.1	-1.9	0.5	0.3	0.2	-1.3
750-500	1.3	-5.7	0.4	-2.2	2.4	-4.1
900-750	0.7	3.7	-8.7	-8.4	-0.5	-4.4

MDR 4-9

500-350	0.5	-1.9	0.7	0.3	0.3	-0.8
750-500	1.4	-7.1	2.4	-1.6	3.7	-3.3
900-750	0.1	4.0	-10.3	-10.0	-0.7	-6.2

MDR 8-9

500-350	0.8	-1.7	-0.1	0.6	-0.7	-1.1
750-500	2.7	-5.0	2.0	0.4	1.7	-0.3
900-750	-0.1	1.4	-8.2	-8.7	0.1	-6.9

convective regions, the residual of moisture was almost unchanged in each layer, although large changes occurred in some of the terms.

Analyses of the LHS of Eq. 7 at 0600 GMT on 24 April and 0600 GMT on 25 April appear in Figs. 45 through 47. MDR data lagged 3 h behind the computed fields have been superimposed. Empirically, it is seen that a better relation existed between the charts and radar data when it was lagged than when it was not. This again indicates that on the synoptic scale, moisture was found to be collecting in regions where heavy precipitation occurred 3 h later.

c. Interpretation of residual

The contribution of the terms on the LHS of Eq. 7 toward the total moisture balance of the atmosphere from 900-350 mb is presented in Fig. 48. The effect of each term is shown individually and combined into one for the residual of moisture. Each term was averaged for all times and categorized by MDR data to reveal changes of moisture with different storm intensity.

Considering the AVE grid as a whole (the "all points" column), the terms in the moisture budget were small. The net vertical and horizontal boundary fluxes nearly balanced each other while the local rate-of-change of moisture was negative. This resulted in a small negative residual in the total atmospheric moisture content. This means that over the eastern United States, the amount of precipitation and condensation during the AVE IV experiment exceeded the total evaporation of water vapor from clouds. This seems only logical since over a large area of this size, the liquid water content usually can be considered a constant (i.e. condensation equals evaporation) which would yield a residual of moisture near zero. However, in AVE IV two intense squall lines occurred in just 36 h, making the condensation and precipitation large in a section of the AVE IV area. Averaged over the entire grid, this would give a small negative residual of moisture as seen in Fig. 48.

In areas where MDR $\leq$ 1, the residual was slightly positive. That is, in locations where it was not raining or raining only very lightly, cloud evaporation was larger than the total effect of con-

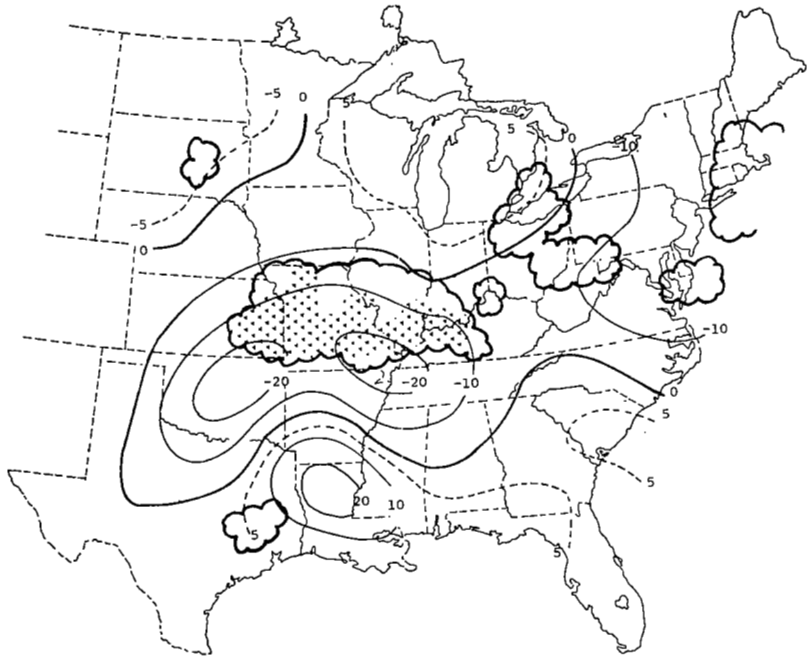

(a) 0600 GMT, 24 April 1975.

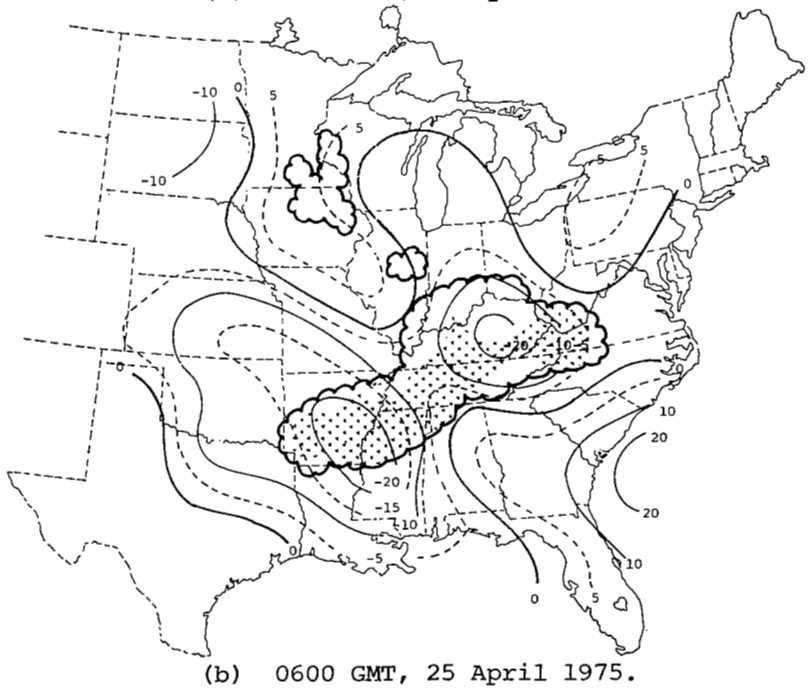

(b) 0600 GMT, 25 April 1975.

Fig. 45. Analyses of the residual of moisture in the layer from 900-750 mb. (Superimposed is radar-observed convection lagged by 3 h. Units: $x10^{-6}$g $cm^{-2}s^{-1}$).

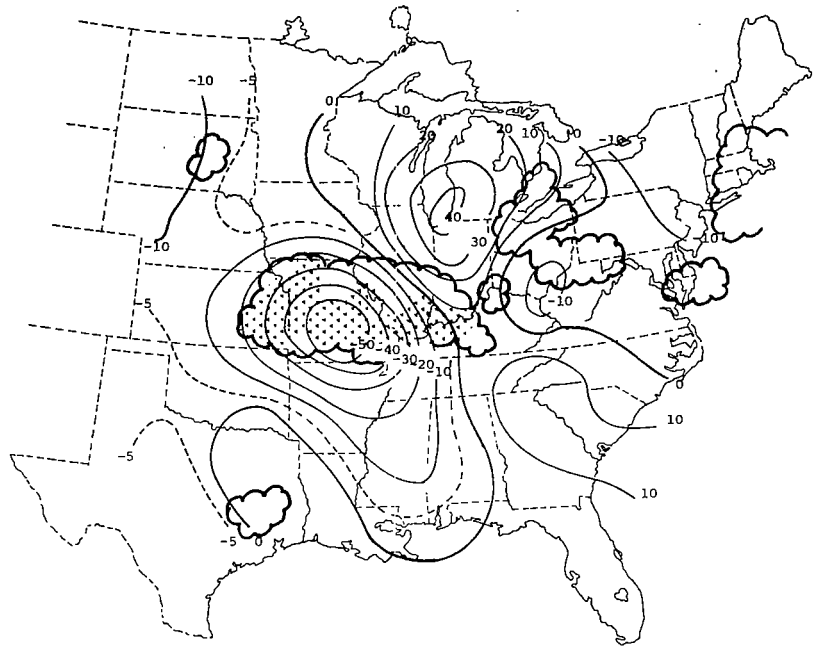

(a) 0600 GMT, 24 April 1975.

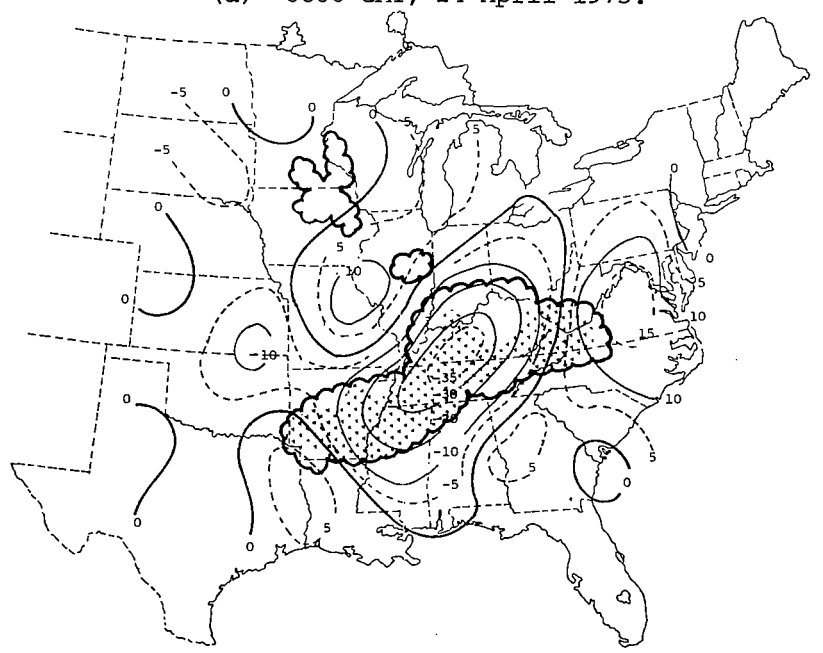

(b) 0600 GMT, 25 April 1975.

Fig. 46. Analyses of the residual of moisture in the layer from 750-500 mb. (Superimposed is radar-observed convection lagged by 3 h. Units: $x10^{-6}$g $cm^{-2}s^{-1}$).

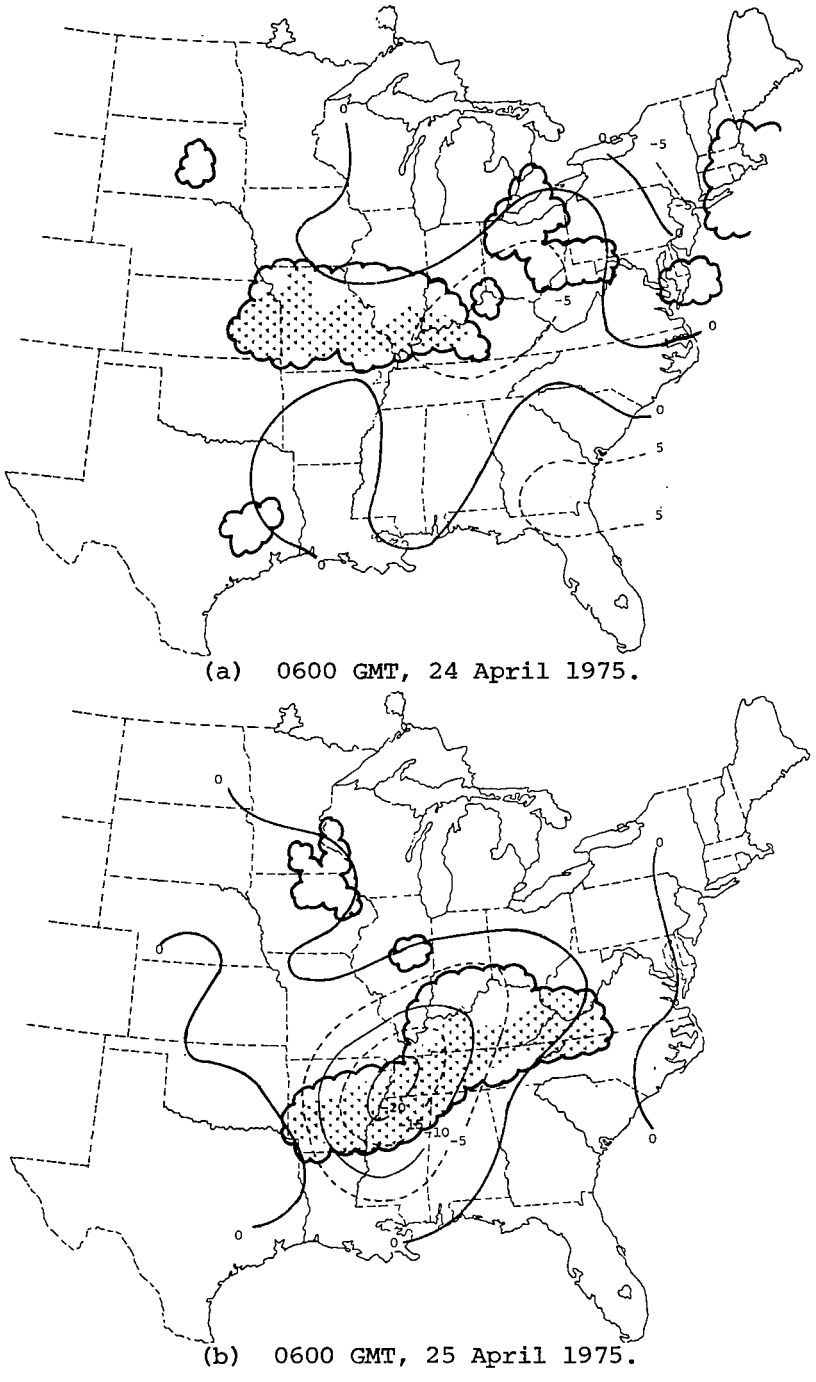

(a) 0600 GMT, 24 April 1975.

(b) 0600 GMT, 25 April 1975.

Fig. 47. Analyses of the residual of moisture in the layer from 500-350 mb. (Superimposed is radar-observed convection lagged by 3 h. Units: $x10^{-6}$g $cm^{-2}s^{-1}$).

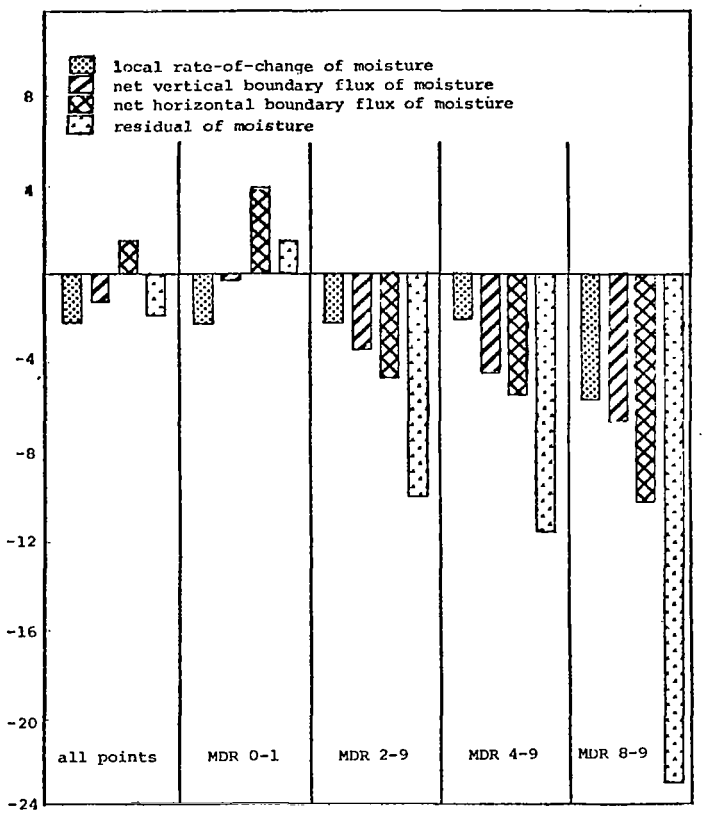

Fig. 48. Moisture budget from 900-350 mb related to MDR (Units: $x10^{-6}$ g $cm^{-2}s^{-1}$).

densation and precipitation. This, also, seems likely since one would expect to find large amounts of condensation close to and just shortly before the occurrence of precipitation. Therefore, the areas of maximum condensation would be associated with higher values of MDR. Conversely, the greatest amount of cloud evaporation would be expected well downstream from the area of storm development in the layers of the cirrus anvils where MDR values would be low.

The amount of residual averaged for all times was much larger when convective activity was strong. In all regions of precipitation, the atmosphere on the whole gained moisture from vertical and horizontal flux convergence but lost moisture locally. This resulted in a large negative residual, indicating an excess of precipitation

and condensation over evaporation. As the convection became more intense, shown by higher MDR values, the difference between the source and sink terms in the residual became even larger.

Analyses of the LHS of Eq. 7 at 0600 GMT on 24 April and 0600 GMT on 25 April appear in Fig. 49. Surface fronts and radar-observed precipitation have been superimposed. These charts confirm that a large negative residual of moisture existed in the convective areas of the two squall lines. This fact is shown very well at 0600 GMT on 25 April which best represents the findings of most of the observation times not shown. The relationship is also good over Missouri in Fig. 49a but at the same time, it is not good over southern Michigan. As previously stated, this was an area where downward motion encountered the leading edge of the first squall line. For a short while this indicated a positive residual (i.e. evaporation > precipitation + condensation) which is opposite of that found in all other convective regions of the experiment. Again, however, the situation did not last long as all precipitation had ended within 3 h. The area of the residual that had the largest absolute value was just downstream of the most intense convection. (See Appendix II for location of MDR $\geq$ 8.)

In an attempt to account for the negative region, analyses of hourly precipitation data were performed. Three-hour composites centered at 0600 GMT on both days are presented in Fig. 50. It should be remembered that these charts are not analyses of the rainfall as it actually fell but rather they are the result of averaging over the same area represented in the computed quantities. It is realized that the measurement of precipitation occurs outside the area where the LHS of Eq. 7 was evaluated. However, it is believed that this does not present a significant problem.

Comparing these analyses with Fig. 49, it was found that the centers of precipitation were located slightly west or northwest of the largest residual values. The magnitude of the precipitation was close enough to the values of the residual to suggest that rainfall could account for the largest portions of the residual. The relationship was especially good in Fig. 50b and was fair over cen-

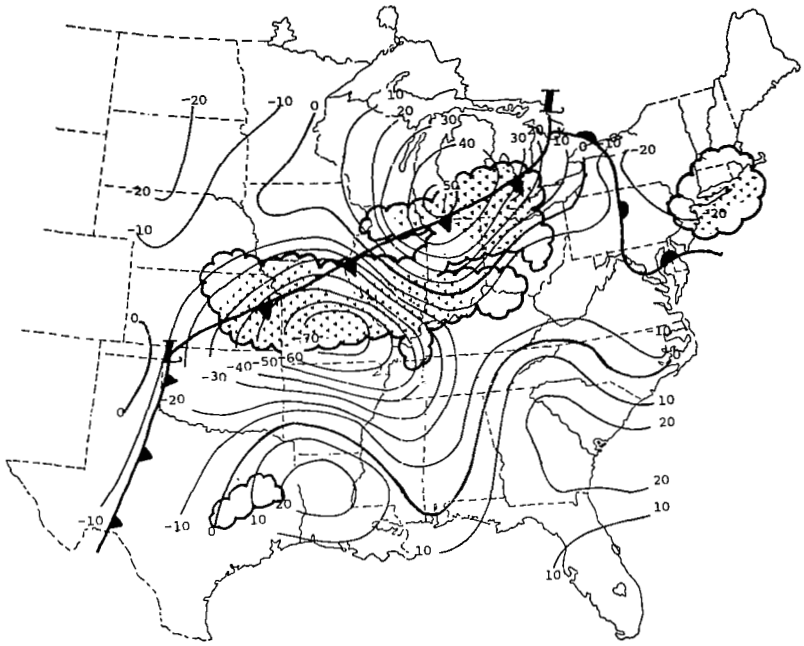

(a) 0600 GMT, 24 April 1975.

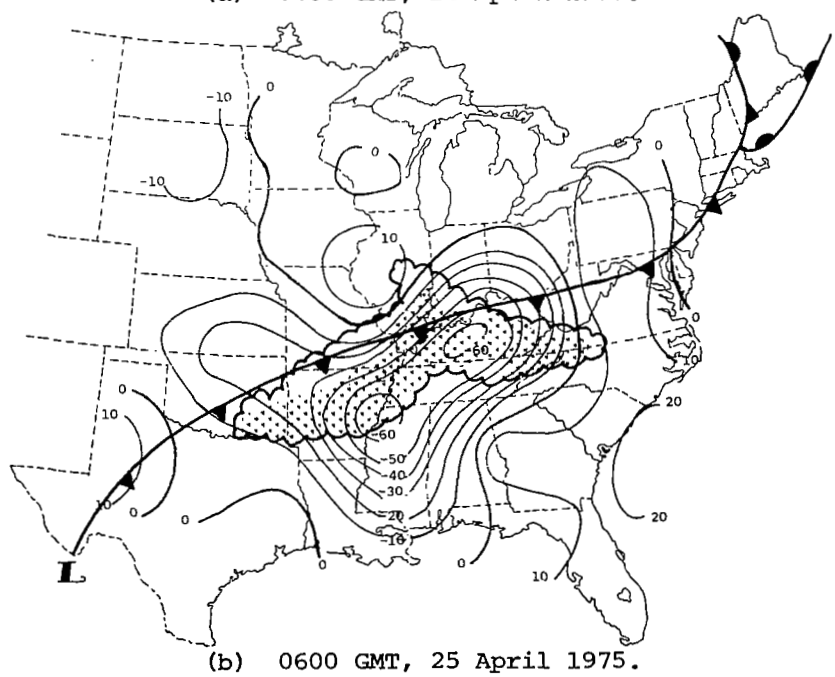

(b) 0600 GMT, 25 April 1975.

Fig. 49. Analyses of the residual of moisture in the layer from 900-350 mb. (Superimposed are surface frontal positions and radar-observed convection. Units: $x10^{-6}g\ cm^{-2}s^{-1}$).

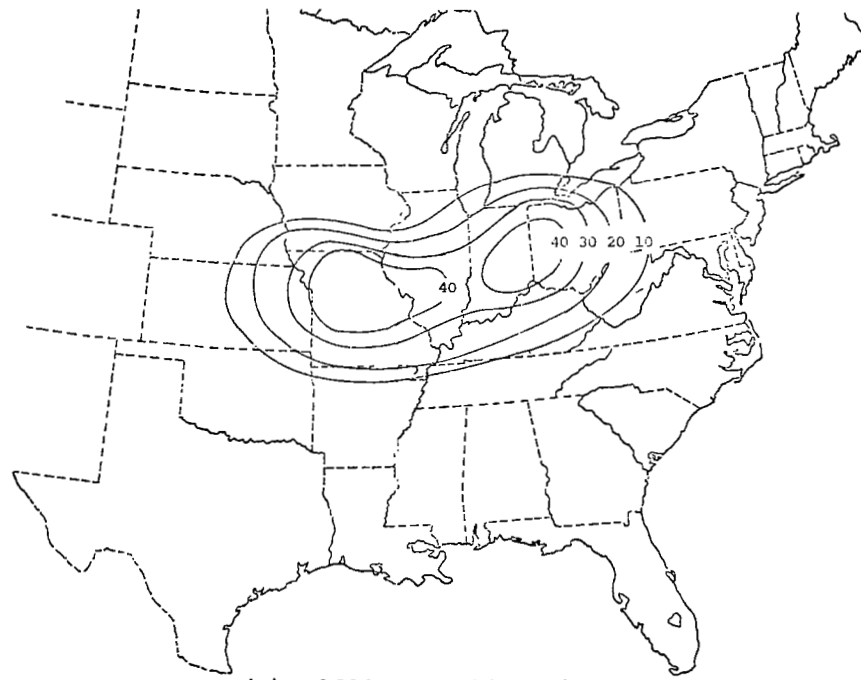

(a) 0600 GMT, 24 April 1975.

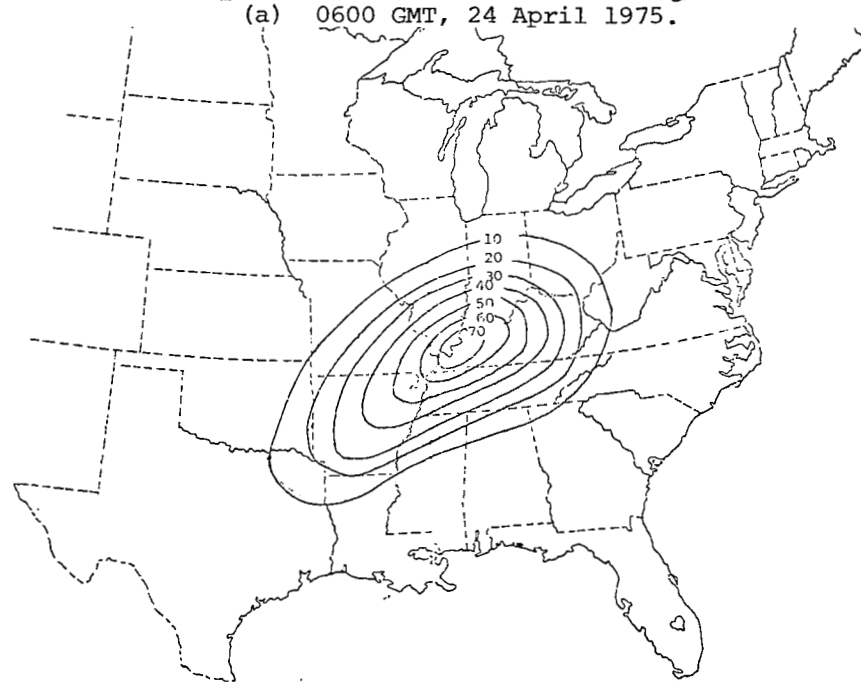

(b) 0600 GMT, 25 April 1975.

Fig. 50. Three-hour composites of precipitation flux obtained from rainfall rates. (Units: $x10^{-6}g\ cm^{-2}s^{-1}$).

tral Missouri at 0600 GMT on 24 April. Agreement was not good at this time from Michigan to Kentucky, as was indicated in previous discussions about this region of convection. The fact that the precipitation related fairly well to the residual areas was not expected since due to its small horizontal extent, convective rainfall often passes unmeasured between recording rain gage stations.

Most of the area of negative residual that the precipitation did not account for was located slightly to the east and southeast of the convective systems. These are regions where one would expect an increase in cumulus cloud activity (i.e. condensation) due to the general ambient conditions ahead of the approaching storms. Condensation would also be strong in the precipitation areas which are revealed the best by the MDR data.

Evaporation, on the other hand, made a positive contribution to the residual of moisture. In the convective regions, evaporation of falling precipitation slightly reduced the effects of precipitation and condensation. It was thought that the heavy cloud cover kept the surface evaporation low. However, in areas where the surface evaporation was large, its effect was an implicit part of the terms on the LHS of Eq. 7 since evaluations were not made below 900 mb. Some evaporation of cirrus anvils probably occurred downstream from the convective regions. However, since it occurred over such a wide area and generally in the upper layers, its effect was considered negligible.

7. SUMMARY

An evaluation of the moisture budget equation has been carried out using the 3- and 6-h AVE IV rawinsonde data, Manually Digitized Radar data, and hourly precipitation data. Computations were made for 50-mb layers of the atmosphere from 900-350 mb. Analyses of the local rate-of-change of moisture and net vertical and horizontal boundary flux were made using the unique rawinsonde data. Comparisons were then made with radar-observed convection to investigate interrelationships between synoptic-scale parameters and convective systems. Changes in these relationships were investigated by allowing the Manually Digitized Radar data to lag the analyses by 3 h. Precipitation data from recording rain gages were used to help explain the residual term of the moisture equation. The increased frequency of the rawinsonde launches was used to observe meteorological events on a time scale which are impossible to resolve from regular 12-h data.

8. CONCLUSIONS

It was determined by the evaluation of the moisture budget equation that during the AVE IV experiment the net horizontal and vertical boundary fluxes of moisture accounted for a large part of the moisture balance in the areas of convective storm activity. Strong horizontal convergence of the wind fluxed large amounts of moisture into the environment of the convective systems, mostly below 700 mb. Much of this moisture was transported vertically upward by synoptic-scale vertical motion to heights above 500 mb. Horizontal moisture advection showed importance only above 750 mb and the local rate-of-change of moisture was comparable to the other terms only near the ground.

Maximum values of moisture accumulation due to the net horizontal and vertical boundary fluxes were centered just downstream of the regions of strongest convection as reflected in Manually Digitized Radar data, indicating a favored position for future development or continued maintenance of storms. This result is supported by the fact that at most observation times during the experiment, a closer relationship existed between the computed moisture quantities and radar-observed convection when the MDR data were lagged by 3 h.

The evaluation of the moisture budget resulted in a large negative residual of moisture in the convective regions. It was found that precipitation accounted for a large part of the residual, even though measurements of these data are not always representative in convective rainfall areas.

REFERENCES

Barnes, S. L., 1964: A technique for maximizing detail in numerical weather map analysis. J. Appl. Meteor., 3, 396-409.

Barr, S. , W. K. Widger, Jr., I. A. Miller, and R. Stanton, 1971: Objective analysis. J. Appl. Meteor., 10, 410-417.

Bradbury, D. L., 1957: Moisture analysis and water budget in three different types of storms. J. Meteor., 14, 559-565.

Chang, Simon W. and Harold D. Orville, 1973: Large-scale convergence in a numerical cloud model. J. Atmos. Sci., 30, 947-950.

Fankhauser, J. C., 1965: Water budget considerations in an extensive squall-line development. Tech. Note 4-NSSL-25, U. S. Weather Bur., Washington D. C., 28pp.

Foster, D. S. and R. M. Reap, 1975: Thunderstorms and Severe Local Storm Frequency Distributions for 1974 derived from manually digitized radar data and severe local storms reports. Preprints of Papers, Ninth Conf. on Severe Local Storms, Norman 64-67.

Fritsch, J. M., 1975: Synoptic-meso scale budget relationships for a tornado producing squall line. Preprints of Papers, Ninth Conf. on Severe Local Storms, Norman 165-172.

Fucik, Nancy F. and Robert E. Turner, 1975: Data for NASA's AVE IV experiment: 25-mb sounding data and synoptic charts, NASA TM X-64952, Marshall Space Flight Center, Alabama, 458pp.

Fuelberg, H. E., 1974: Reduction and error analysis of the AVE II pilot experiment data. NASA Contractor Report CR-120496. Marshall Space Flight Center, Alabama, 140pp.

Haltiner, Goerge J., 1971: Numerical Weather Prediction, Wiley, 161-163.

Hudson, H. R., 1971: On the relationship between horizontal moisture convergence and convective cloud formation. J. Appl. Meteor., 10, 755-762.

Kreitzberg, Carl W. and H. Albert Brown, 1970: Mesoscale weather systems within an occlusion. J. Appl. Meteor., 9, 417-432.

Lenhard, Robert W., 1973: A revised assessment of rawinsonde accuracy. Bull. Amer. Meteor. Soc., 54, 691-693.

Lewis, J. M., Y. Ogura, and L. Gidel, 1974: Large-scale influences upon the generation of a mesoscale disturbance. Mon. Wea. Rev., 102, 545-560.

Ninomiya, K., 1968: Cumulus group activity over the Japan Sea in wintertime in relation to the water vapor convergence in sub-cloud layer. J. Meteor. Soc. Japan, 46 373-386.

_____, 1971: Mesoscale modification of synoptic situations from thunderstorm development as revealed by ATS III and aerological data. J. Appl. Meteor., 10, 1103-1121.

O'Brien, J. J., 1970: Alternate solution to the classical vertical velocity problem. J. Appl. Meteor. 9, 197-203.

Palmén, E. and E. O. Holopainen, 1962: Divergence, vertical velocity and conversion between potential and kinetic energy in an extra-tropical distrubance. Geophysica, 8, 89-113.

_____ and C. W. Newton, 1969: Atmospheric Circulation Systems, Academic Press, Chapters 12 and 13.

Shuman, F. G., 1957: Numerical methods in weather prediction: II Smoothing and Filtering. Mon. Wea. Rev., 85, 357-361.

Spar, J., 1953: A suggested technique for quantitative precipitation forecasting. Mon. Wea. Rev., 81, 217-221.

APPENDIX I

Rawinsonde Stations Participating in AVE IV Experiment.

Station Number	Location
208 (CHS)	Charleston, South Carolina
211 (TPA)	Tampa, Florida
213 (AYS)	Waycross, Georgia
220 (VPS)	Apalachicola, Florida
226 (CEN)	Centerville, Alabama
232 (BVE)	Boothville, Louisiana
235 (JAN)	Jackson, Mississippi
240 (LCH)	Lake Charles, Louisiana
248 (SHV)	Shreveport, Louisiana
255 (VCT)	Victoria, Texas
260 (SEP)	Stephenville, Texas
261 (DRT)	Del Rio, Texas
265 (MAF)	Midland, Texas
304 (HAT)	Hatteras, North Carolina
311 (AHN)	Athens, Georgia
317 (GSO)	Greensboro, North Carolina
327 (BNA)	Nashville, Tennessee
340 (LIT)	Little Rock, Arkansas
349 (UMN)	Monette, Missouri
363 (AMA)	Amarillo, Texas
402 (WAL)	Wallops Island, Virginia
405 (IAD)	Sterling, Virginia (Dulles Airport)
425 (HTS)	Huntington, West Virginia
429 (DAY)	Dayton, Ohio
433 (SLO)	Salem, Illinois
451 (DDC)	Dodge City, Kansas
456 (TOP)	Topeka, Kansas
486 (JFK)	Fort Totten, New York (Kennedy Airport)
518 (ALB)	Albany, New York
520 (PIT)	Pittsburg, Pennsylvania
528 (BUF)	Buffalo, New York
532 (PIA)	Peoria, Illinois
553 (OMA)	Omaha, Nebraska
562 (LBF)	North Platte, Nebraska
606 (PWM)	Portland, Maine
637 (FNT)	Flint, Michigan
645 (GRB)	Green Bay, Wisconsin
654 (HUR)	Huron, South Dakota
655 (STC)	St. Cloud, Minnesota
662 (RAP)	Rapid City, South Dakota
11001 (MFS)	Marshall Space Flight Center, Alabama
22002 (FSI)	Fort Sill, Oklahoma

APPENDIX II

Three-hour composites of Manually Digitized Radar Summary.

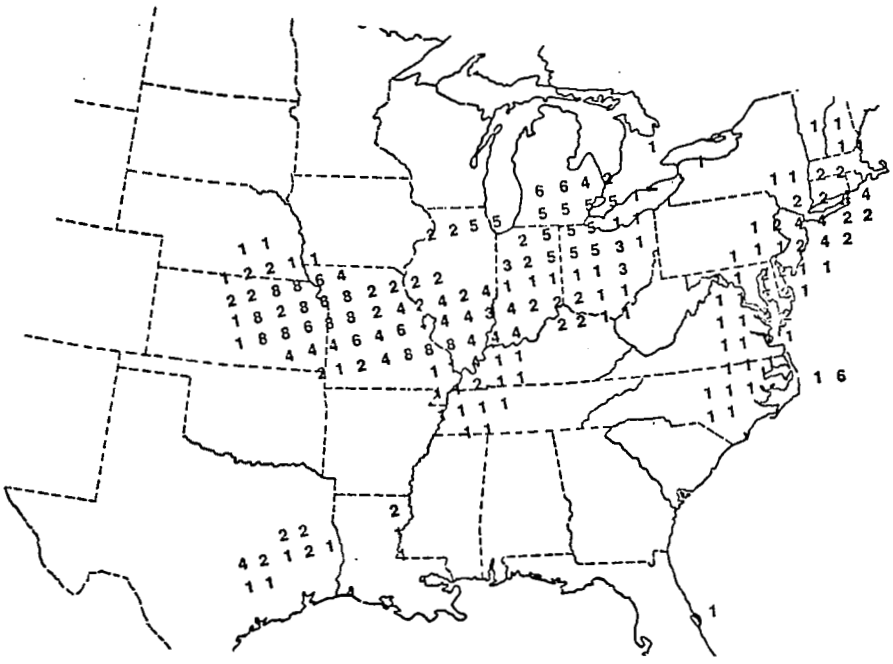

(a) 0600 GMT, 24 April 1975.

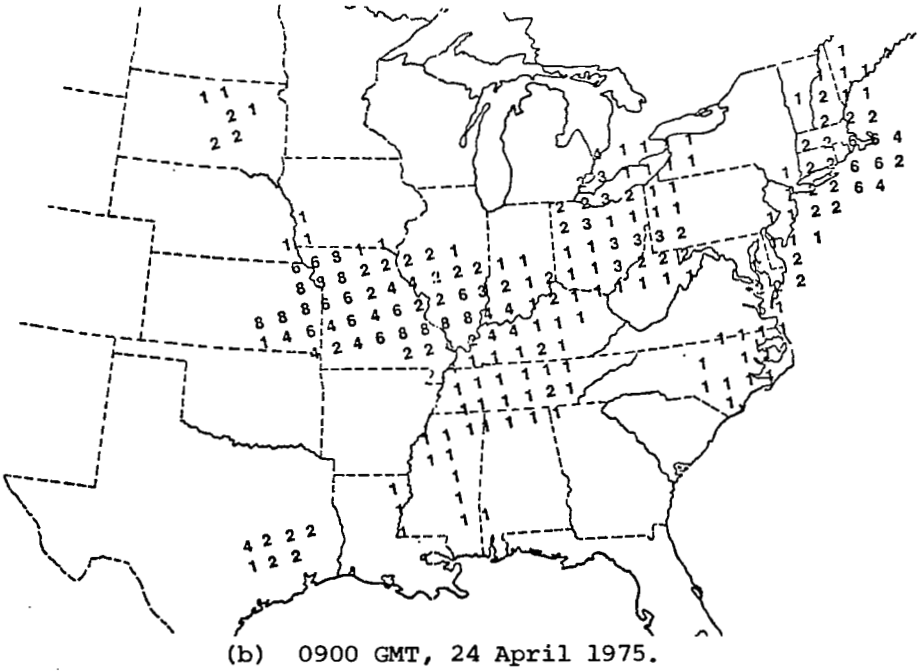

(b) 0900 GMT, 24 April 1975.

APPENDIX II (Continued)

Three-hour composites of Manually Digitized Radar Summary.

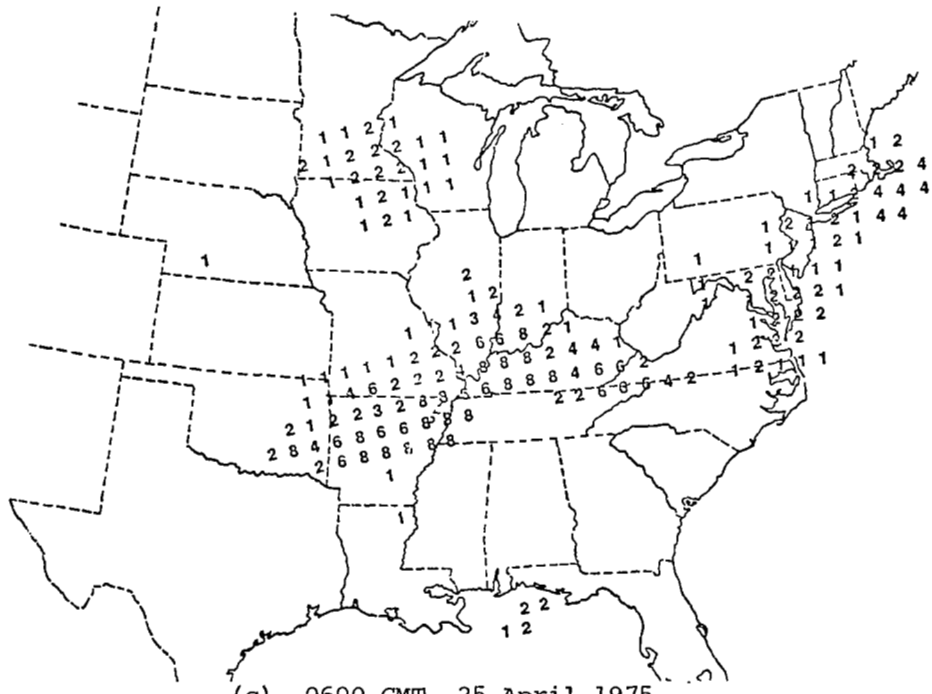

(c) 0600 GMT, 25 April 1975.

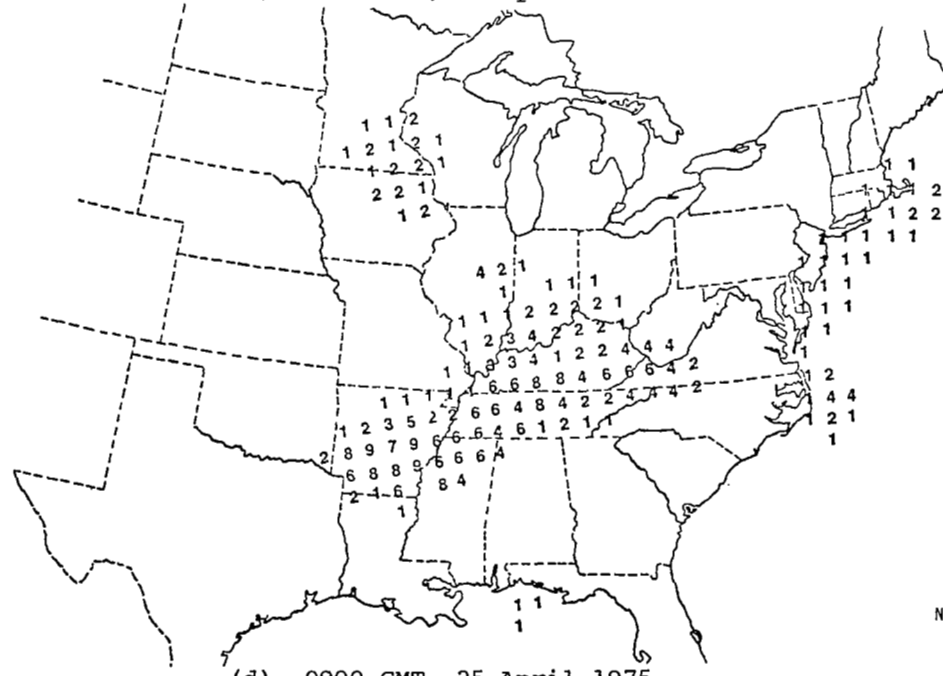

(d) 0900 GMT, 25 April 1975.

NASA-Langley, 1977